



**AN INVESTIGATION OF THE USEFULNESS OF 3-D
DIGITIZED FACIAL IMAGES FOR THE ISSUANCE
OF THE MCU - 2/P PROTECTIVE MASK (U)**

Yvette Kline

**ARKLINE RESEARCH
1020 ROBWill PASS
CHERRY HILL NJ 08034-3626**

Jennifer J. Whitestone

**CREW SYSTEMS DIRECTORATE
HUMAN ENGINEERING DIVISION
WRIGHT-PATTERSON AFB OH 45433-7022**

MARCH 1994

19960227 128

FINAL REPORT FOR THE PERIOD APRIL 1989 TO APRIL 1990

Approved for public release; distribution is unlimited

**AIR FORCE MATERIEL COMMAND
WRIGHT-PATTERSON AIR FORCE BASE, OHIO 45433-6573**

FORM QUALITY INSPECTED 1

**ARMSTRONG
LABORATORY**

NOTICES

When US Government drawings, specifications, or other data are used for any purpose other than a definitely related Government procurement operation, the Government thereby incurs no responsibility nor any obligation whatsoever, and the fact that the Government may have formulated, furnished, or in any way supplied the said drawings, specifications, or other data, is not to be regarded by implication or otherwise, as in any manner licensing the holder or any other person or corporation, or conveying any rights or permission to manufacture, use, or sell any patented invention that may in any way be related thereto.

Please do not request copies of this report from the Armstrong Laboratory. Additional copies may be purchased from:

National Technical Information Service
5285 Port Royal Road
Springfield, Virginia 22161

Federal Government agencies and their contractors registered with the Defense Technical Information Center should direct requests for copies of this report to:

Defense Technical Information Center
8725 John J. Kingman Road, Suite 0944
Ft. Belvoir, Virginia 22060-6218

DISCLAIMER

This Technical Report is published as received and has not been edited by the Technical Editing Staff of the Armstrong Laboratory.

TECHNICAL REVIEW AND APPROVAL

AL/CF-TR-1995-0162

This report has been reviewed by the Office of Public Affairs (PA) and is releasable to the National Technical Information Service (NTIS). At NTIS, it will be available to the general public, including foreign nations.

The voluntary informed consent of the subjects used in this research was obtained as required by Air Force Instruction 40-402.

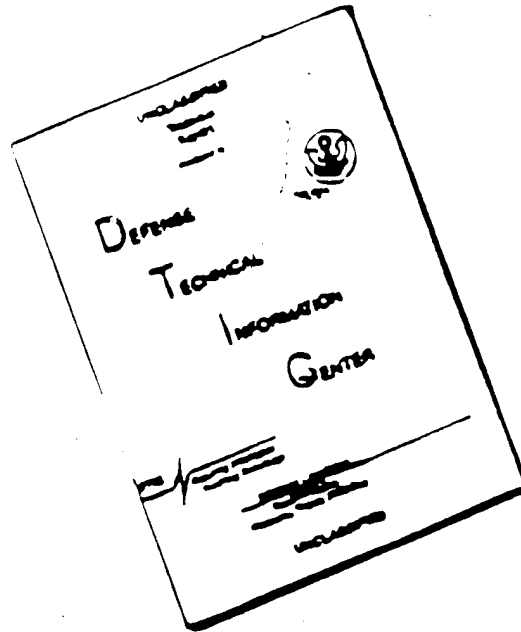
This technical report has been reviewed and is approved for publication.

FOR THE COMMANDER



KENNETH R. BOFF, Chief
Human Engineering Division
Armstrong Laboratory

DISCLAIMER NOTICE



THIS DOCUMENT IS BEST
QUALITY AVAILABLE. THE COPY
FURNISHED TO DTIC CONTAINED
A SIGNIFICANT NUMBER OF
PAGES WHICH DO NOT
REPRODUCE LEGIBLY.

REPORT DOCUMENTATION PAGE			Form Approved OMB No. 0704-0188	
Public reporting burden for this collection of information is estimated to average 1 hour per response, including the time for reviewing instructions, searching existing data sources, gathering and maintaining the data needed, and completing and reviewing the collection of information. Send comments regarding this burden estimate or any other aspect of this collection of information, including suggestions for reducing this burden, to Washington Headquarters Services, Directorate for Information Operations and Reports, 1215 Jefferson Davis Highway, Suite 1204, Arlington, VA 22202-4302, and to the Office of Management and Budget, Paperwork Reduction Project (0704-0188), Washington, DC 20503.				
1. AGENCY USE ONLY (Leave blank)		2. REPORT DATE March 1994		3. REPORT TYPE AND DATES COVERED Final - April 1989 - April 1990
4. TITLE AND SUBTITLE An investigation of the usefulness of 3-D digitized facial images for the issuance of the MCU-2/P protective mask			5. FUNDING NUMBERS C: F33615-88-C-0552 PE: 62202F PR: 7184 TA: 08 WU: 51	
6. AUTHOR(S) * Yvette M. Kline Jennifer J. Whitestone				
7. PERFORMING ORGANIZATION NAME(S) AND ADDRESS(ES) * Arkline Research 1020 Robwill Pass Cherry Hill NJ 08034-3626			8. PERFORMING ORGANIZATION REPORT NUMBER	
9. SPONSORING / MONITORING AGENCY NAME(S) AND ADDRESS(ES) Armstrong Laboratory, Crew Systems Directorate Human Engineering Division Human Systems Center Air Force Materiel Command Wright-Patterson AFB OH 45433-7022			10. SPONSORING / MONITORING AGENCY REPORT NUMBER AL/CF-TR-1995-0162	
11. SUPPLEMENTARY NOTES				
12a. DISTRIBUTION / AVAILABILITY STATEMENT Approved for public release; distribution is unlimited.			12b. DISTRIBUTION CODE	
13. ABSTRACT (Maximum 200 words) This report presents a new issuance method (called "Bestfit") for the MCU-2/P protective mask. The authors formulated a new issuance method based on the discovery of the exact location on the face where the mask provides the most efficient protection. Three-dimensional (3-D) digitized measurements of this location can be compared to mask-size measurements to provide the best possible fit. This report includes comparisons of the Bestfit method to the existing caliper, mentonsellion length, and Slate fit methods. Benefits of the new issuance method include: the method provides wearers the maximum protection afforded by the mask's design; the method identifies wearers the mask will not fit; and the method establishes a half-face database for the wearer population. Drawbacks of the new method include: 3-D measurement techniques could be foiled by irregular skin surfaces, requiring additional image processing; and results indicate that the new method is not reliable at predicting wearability.				
14. SUBJECT TERMS Anthropometry Personal protective equipment Full-face masks Issuance methods Fit tests			15. NUMBER OF PAGES 169	
			16. PRICE CODE	
17. SECURITY CLASSIFICATION OF REPORT UNCLASSIFIED	18. SECURITY CLASSIFICATION OF THIS PAGE UNCLASSIFIED	19. SECURITY CLASSIFICATION OF ABSTRACT UNCLASSIFIED	20. LIMITATION OF ABSTRACT UNLIMITED	

THIS PAGE INTENTIONALLY LEFT BLANK

PREFACE

The research described in this report was conducted as a Phase 1 SBIR (contract number F33615-88-C-0552), issued by the Air Force Systems Command, Aeronautical Systems Division to Arkline Research, Cherry Hill, NJ. The period of performance was April 1989 to April 1990. Data for the effort was obtained and preprocessed at Wright-Patterson Air Force Base, Dayton, OH in cooperation with the effort's sponsor, the Human Engineering Group of the Armstrong Aerospace Medical Research Laboratory.

TABLE OF CONTENTS

	PAGE
INTRODUCTION	1
Objectives.....	2
Result Highlights	2
TECHNICAL DISCUSSION.....	3
Research Strategy and the Role of Statistics.....	3
The Research Strategy.....	3
The Role of Statistics in this Research	4
Data Description.....	4
Sample and Subsample Population.....	4
Equipment.....	6
Description of Raw Data.....	7
Preliminary Data Analyses	9
Dependent Variable Analyses.....	10
Distributions	10
Trends.....	10
Characterization of Standard Exercises.....	11
Characterization of Alternate Exercises.....	11
Characterization of Overall Fit Factor.....	12
Independent Variable Analyses	13
Lateral Skin Displacement Analysis.....	13
Analysis of Anatomical and Mask Coordinates	14
Sequential Delta ρ Analysis.....	15
Polygonal Perimeter Analysis.....	15
Datasheet and Scan Data Analysis.....	16
Mask Deformation Analysis.....	17
Description of Bestfit Method	18
Constraint	18
The Point6 Line.....	19
The Zygon Locus and its Relation to Point6.....	19
Relationships and Algorithms	21
Final Data Analyses	22
Comparison of Sizing Methods.....	22
Dependent Variable Analyses for the Bestfit Subsample	23
CONCLUSION AND RECOMMENDATIONS	24
Conclusion	24
Recommendations	25
REFERENCES	26
APPENDIX A: Figures.....	27
APPENDIX B: Tables.....	151
APPENDIX C: Distance Data	160

AN INVESTIGATION OF THE USEFULNESS OF 3-D DIGITIZED FACIAL IMAGES FOR THE ISSUANCE OF THE MCU-2/P PROTECTIVE MASK (U)

INTRODUCTION

The MCU-2/P protective mask protects a wearer's face, eyes and respiratory tract from airborne toxic contaminants which could be encountered in warfare. The mask contacts the face via a facial seal located at the mask's periphery, and the protection afforded by the mask is directly (although not uniquely) related to the quality and integrity of the face to mask seal. Fit factor testing is used to quantify the face to seal relationship in a controlled environment: A high fit factor indicates a good seal and a low fit factor indicates a poor one. Based on models of toxic attack and user activity, an acceptable fit factor has been defined as equal to or greater than 10,000.

The mask comes in three sizes (small, medium and large) in order to accommodate size and shape variations between faces. The determination of who should get what size mask is herein referred to as "issuance," and has been a topic of some study in masks bearing the MCU-2/P type of seal. Historically, these masks have been issued on the basis of one or two linear measurements. Because these measurements were made manually, they had to be taken between points that were easy to locate. This increased the reliability of the measure when taken by different measurers, i.e., it reduced the interobserver error. Menton-sellion length and bizygomatic breadth are two dimensions that were thought to meet this requirement; but when tested, menton-sellion length demonstrated considerable interobserver error (Case et al., 1988). Testing of the protection provided by the menton-sellion method and the combined menton-sellion and bizygomatic method of issuance shows the methods to be helpful (Naval Surface Warfare Center, 1988) but non-optimum. In fact, efforts to correlate protection level with any standard length/width measures (and combinations thereof) have failed (Naval Surface Warfare Center, 1988).

An optimum method of issuance would provide each wearer with the size mask that will afford him/her the greatest protection. Assuming the mask's other features are properly proportioned, the issued mask would impose minimum encumbrance on the user. Advances in the collection and processing of size and shape data have eased the constraint that facial measurements must be made between easy to locate points. Highly accurate digitized three

dimensional images permit computerized access to almost any conceivable measurement, and provide the motivation to take another look at methods of issuance.¹

Objectives

The primary objective of this effort was to explore the usefulness of measurements extracted from digitized images in producing an issuance method which will afford each user the greatest protection in the MCU-2/P. The primary co-objectives were:

- to quantify the expected greatest protection and establish that value as the nominal fit factor of a correctly issued mask,
- to explore the mean changes in fit factor if one or more mask sizes are eliminated,
- to identify testing pitfalls and use that information to determine how to design a verification test of a new issuance method, and
- to identify users who are unable to get an acceptable fit in any size of the MCU-2/P.

The secondary objective of this effort was to characterize where the seal of a best fit mask sits on the face, and how that location changes during facial movement.

Result Highlights

A new issuance method was formulated which shows promise of identifying the best fit mask for each user. The method is based on having found a means to predict where the best fit mask sits on the face. Key dimensions are taken from this area and compared to dimensions of the small, medium and large mask to determine the best fit size. The method does not identify users who are unable to get an acceptable fit in any size mask, but unique facial characteristics of such people were identified and are measurable by the same techniques which would be needed to execute the issuance method. Details of the method are presented in the description of bestfit method on page 18. It should be noted that the best fit size does not provide minimum encumbrance to the small user, many of whom commented on nose cup related discomforts.

The nominal fit factor of a correctly issued mask was indicated to be 310,000. This was determined by a subsample (n=37), and would have to be verified on a larger, more representative sample prior to adoption. The caliper measured menton-sellion method provided

¹ The method of issuance will also provide the method of tariffing. Consequently, the method must be applicable to the type of data available for each activity.

the next closest mean fit factor of approximately 240,000 (on the same subsample). At a 95% confidence level, the fit factor difference is significant.

The nominal fit factor of a correctly issued mask is the grand average fit factor of the small subjects in the small mask, the medium subjects in the medium mask, and the large subjects in the large mask. Comparing the small, medium and large group averages to those that were obtained when subjects were tested in a non-optimum size mask revealed the following:

- testing large subjects (n=5) in medium masks depressed their mean fit factor from 330,000 to 120,000, and
- testing small subjects (n=23) in medium masks depressed their mean fit factor from 340,000 to 120,000.

The mean fit factor of the medium mask (n=10) is 230,000. Based on the subsample population, elimination of the small and the large masks would yield a nominal fit factor less than 230,000 but greater than 120,000.

TECHNICAL DISCUSSION

This section describes the research performed during the effort. Applicable analyses are contained within the body of the text for ease of reference. Figures are contained in Appendix A.

Research Strategy and the Role of Statistics

This section describes the research strategy and the role of statistics in the effort.

The Research Strategy

As described in the Objectives section, this was exploratory research. Consequently, the research strategy could well be termed "prospecting." The testing was structured to gather as much information on as many subjects as was feasible such that the data could be inspected for trends or patterns. Observation and physical interpretation were the primary research methods and statistical analyses were used to reinforce observations and interpretations.

The Role of Statistics in this Research

The testing was not structured in the classic statistical inquiry sense, in which a specific null hypothesis had been stated and a suitable test design selected to check the veracity of the hypothesis to a predetermined confidence level. An objective of this effort was to identify testable null hypotheses and to learn how to test them.

This is not to imply that statistical procedures were not employed in the effort. Elementary procedures were employed during the data analyses and are identified in the data analysis sections of this report, beginning on page 9.

Data Description

This section describes the data used in the effort. It includes paragraphs on the sample populations, equipment, raw data and analyses performed to check the reliability of the raw data. The collected data consists of datasheets, which contain the subjects' fit factor scores and anthropometrics, and datafiles, which list labeled sets of points. Copies can be requested from the sponsoring agency.

Sample and Subsample Population

Due to the exploratory nature of this effort and the desire for a large sample, the sample population was recruited from a local college. A small monetary sum was paid to each collegian volunteer as an incentive. Some Air Force personnel volunteered as gratis subjects. All subjects were screened for health and safety concerns prior to testing. The screening questions and test protocol bore the approval of the Human Use Committee at Wright-Patterson.

A total of 115 subjects were tested. Of these, the first three had outlying fit factor scores which seemed to be due to external environment conditions; consequently, they were eliminated from further study. The remaining sample of 112 was used in the preliminary dependent variable (fit factor scores) analyses. A quantitative characterization was not tallied for this report, but qualitatively the group is described as young (mostly 18 to 25) and white.

Of the 112 subjects, 37 were selected for inclusion in the preliminary independent variable (facial dimensions) analyses and the final analyses. The subsample selection method is outlined below:

- Does the subject have a complete and ostensibly accurate facial dimension data set? 47 subjects were eliminated for this reason.
- Of the remaining subjects, does the subject's fit factor score clearly place him or her in a unique best fit size? A score of approximately 50,000 greater than the next closest score was used as the criterion in this selection. (The cutoff came from the analyses described on pages 8 and 9). 28 subjects were eliminated for this reason, leaving the selected subsample of 37.

Elimination by the fit factor score criterion was not as definitive as described, and some judgment was employed during that final round of elimination. The objective, however, was to eliminate the "gray" cases, and use only uncontested small, medium and large subjects to define their respective unique characteristics. The fact that there were a considerable number of gray cases should be considered when interpreting the results of the analyses conducted on the subsample.

A quantitative characterization of the subsample was tallied (Figure A1) and is summarized below:

SIZE:	SEX:	AGE: 18 - 34	
23 SMALL	16 FEMALE	7 MALE	18 - 20: 20
9 MEDIUM	3 FEMALE	6 MALE	21 - 25: 14
5 LARGE	1 FEMALE	4 MALE	26 - 34: 3

N = 37	20 FEMALE	17 MALES	HEIGHT: 62 - 80 IN
	RACE: (ALL WHITE)	(1 BLACK)	WEIGHT: 105 - 210 #

In addition to the subsample population, the sample population also yielded a misfit population. Misfits are subjects who were unable to achieve an acceptable fit factor in any size mask, i.e. they are the people whom the MCU-2/P (as currently sized) does not accommodate. Confirmed misfits are subjects 14, 40 and 100 (a male and two females, respectively). Suspected misfits are subjects 13 and 92 (a male and a female, respectively). Four of the five candidate misfits are white, and one (misfit 13) is Asian. Complete data sets do not exist for each misfit; however, the existing data was compared to the results of many of the analyses as a means to identify divergences.

The sample and subsample are not representative of the user population: There are too many whites and too many females, and presumably too many smalls and not enough mediums and larges. The sexual and racial deviations are known to be significant for facial dimensions (Case et al., 1988). The presumption itself is based on the following point of reference: The Navy permits male aviators to have a maximum weight of 235 pounds (Department of the Navy, 1989), and the subsample has only one subject greater than or equal to 200 pounds.

For this effort a truly representative sample would have been desirable, but was not necessary. The reader is reminded that the research conducted was exploratory, and that its results cannot be generalized to another population without first passing a validation test.

Equipment

Other than calipers and tape measures, two principal equipment systems were used in this study. Fit factor data was collected using a quantitative fit test instrument (QFTI) built by TSI. Corn oil was the challenge, and a condensation nucleus counter measured its concentration. The QFTI was preprogrammed for testing the standard (Air Standardization Coordinating Committee, AIR STD 61/14A) six exercises listed in the Description of Raw Data on page 7. Facial dimension data was collected by a low power helium-neon laser scanner and was digitized by an echo digitizer built by Cyberware, Inc. Dimensions were extracted from the three-dimensional data via a Silicon Graphics workstation with interactive software.

Data analysis was performed on a PC, using GB-STAT's not-yet-released Version 2.

Description of Raw Data

Data collected and data used during the effort are identified below. Appendix C contains complete breakdowns of distance data from head scans and data sheets.

FIT FACTOR (FF) DATA

OVERALL FIT FACTOR

STANDARD EXERCISES:

BREATHE NORMALLY (BN)
BREATHE DEEPLY (BD)
HEAD SIDE TO SIDE (SS)
HEAD UP AND DOWN (UD)
READ RAINBOW PASSAGE (RP)
FACIAL EXPRESSIONS (FE)

ALTERNATE EXERCISES:

BREATHE NORMALLY (BN)
YAWN (YA)
SMILE (SM)
FROWN (FR)
ROTATE CHIN (RC)
HEAD UP (HU)

DATA SHEET DATA

AGE
SEX
HEIGHT
WEIGHT
X TRAGION TO TOP OF HEAD
X HEAD CIRCUMFERENCE
X CORONAL ARC
X MINIMUM FRONTAL ARC
X SUBNASALE ARC
MENTON ARC (MNARC)
SUBMANDIBULAR ARC (SBMARC)
X HEAD LENGTH
X HEAD BREADTH
BIZYGOMATIC BREADTH (BIZYBR)
BIGONIAL BREADTH (BIGOBR)
MENTON SELLION LENGTH (MENSEL)
X NOSE BREADTH

NOTE: AN X INDICATES THAT THE DATA WAS COLLECTED BUT NOT USED IN THE ANALYSES.

SCAN DATA (RAW)

LEFT AND RIGHT TRAGION
LEFT AND RIGHT ZYGION
LEFT AND RIGHT GONION
LEFT AND RIGHT ZYGOFRONTALE
LEFT AND RIGHT INFRAORBITALE
GLABELLA
SELLION
PRONASALE
MENTON
MASKPOINTS 1 TO 20

SCAN DATA (DERIVED)

POLYGONAL PERIMETER
DELTA ρ
MENTON SELLION LENGTH (MNSSELL)
MENTON GLABELLA LENGTH (MNGLAB)
SELLION GONION LENGTH (SELGON)
L ZYGION TO R GONION LENGTH (XZYGON)
L ZYGION TO L GONION LENGTH (ZYGON)
MENTON MASKPOINT 1 LENGTH (MNPT1)
MENTON MASKPOINT 11 LENGTH (MNPT11)
MENTON MASKPOINT 6 LENGTH (MNPT6)
BIZYGOMATIC BREADTH (ZYGZYG)
BIGONIAL BREADTH (GONGON)
BIZYGOMATIC + BIGONIAL (BZG+BG)
MASKPOINT 6 TO 16 BREADTH (6+16)
MASKPOINT 1 TO 11 LENGTH (P1P11)
MNPT1 - MNGLAB (GLBPT1)

VISUAL OBSERVATION (OF FACE IN MASK) DATA

YAWN
SMILE
FROWN
ROTATE CHIN LEFT
ROTATE CHIN RIGHT
HEAD UP

Anthropometric descriptions are not included in this report, as a number of sources exist. Descriptions of maskpoints and mask and anatomical coordinate systems follow.

Maskpoints are a set of 20 points equispaced around the perimeter of the mask's seal. Each is approximately centered on the width of the seal. The points were located on one each small, medium and large mask with dividers, and a 3/16 inch diameter hole was punched through the seal at each point. The mask then served as a template to transfer the points to the subject's face via a makeup pencil (Figure A2). During the visual observation, the mark's movement relative to the hole was observed and recorded during specific facial exercises. After the mask was removed, each mark's location was extracted from the scanned data in the scanner's coordinate system. The coordinates were subsequently transferred to a mask coordinate system and an anatomical coordinate system.

Sketches of the mask and anatomical coordinate systems are shown in Figure A3. Both cartesian (x, y and z) and spherical (ρ, θ and ϕ) coordinates were used in the effort. It should be noted that due to a programming glitch the measurement of ϕ was incorrect between points 7 and 15. The correct measure is 270 degrees minus the listed measure. The corrected value has been used in any analysis for which the difference mattered. Use of the raw or corrected value of ϕ will be identified as applicable in discussions of specific analyses.

Two analyses were performed on the data. The first analysis checked the reliability of the fit factor data, and the second analysis compared hand measurements to machine measurements. Each is described below.

Twenty-six subjects from the sample population performed both standard and alternate exercises in each of the three masks. Both the standard and alternate exercise sets began with the breathe normally exercise. The difference between the standard breathe normally exercise and the alternate breathe normally exercise should be zero. The value $s - a$ was computed three times, once for each mask size. The resulting three distributions appeared approximately normal (Figure A4), so the means and their confidence intervals were determined (Figure A5). The means are all positive, ranging from 26,000 to 96,000, yet zero is within the 95% confidence interval for each mean. The standard error of measurement for all three measures ($s - a$ for small, medium and large) was 38,000 (Figure A6). (For a general discussion of reliability analysis, see Winer, 1971.) This means that if a subject's "true" fit factor was 38,000, the value measured via the employed procedure and equipment is expected to be in the range of zero to 76,000. This is a larger than desired spread, and it might have an explanation in the test procedure itself. In all cases the alternate exercise was performed after the standard exercise; consequently the alternate scores may have been depressed by residual contamination on the

equipment or the face itself. This is something that will have to be protected against in future testing.

Three measurements which were made by hand (using calipers) were also computed from the scanned data: These were bizygomatic breadth, bigonial breadth and menton-sellion length. A comparison was made between the hand-made and machine-made measurements for the combined subsample population and the three misfits for whom scanned data existed (total $n = 40$). The distributions resulting from subtracting the hand-made values from the machine-made values appeared approximately normal (Figure A7) so each was subjected to a t-test to determine if significant differences were present (Figure A8) between the hand-made values and machine-made values. At a 95% confidence level, the test revealed that significant differences exist for all three measures. The mean difference for bizygomatic breadth is 9 mm, for bigonial breadth it is 7 mm, and for menton-sellion length it is -3 mm. The negative mean difference for the latter was a surprise: Positive means were anticipated because hand-made measurements are smaller due to tissue compression. The explanation is that the sellion was not marked on the subjects' faces prior to scanning, so its location was determined by eye from the image of the face on the computer monitor. (The reader will recall that the processing software was interactive.) Because of the position in which the head was scanned, data in the vicinity of the sellion was sometimes missing (i.e. in a shadow), thereby confounding the best efforts to locate it.

The means of the differences for the bizygomatic data and the bigonial data were expected to be approximately equal (based on the assumption that tissue compression in those two areas are similar). An F-test revealed equal variances, thereby allowing the use of a t-test which indicated the means were not equal at a 95% confidence level (Figure A9.)

Preliminary Data Analyses

Both a preliminary and a final data analysis were conducted during the effort. In the preliminary analysis the dependent and independent variables were studied in order to find trends or patterns. Once found, they were formulated into a method for issuing the MCU-2/P. The method was studied in the final data analysis. The method is presented in the Description of Bestfit Method on page 18, and the final analysis is presented in Final Data Analyses on page 21. The preliminary analyses are presented below.

Dependent Variable Analyses

Fit factor was the dependent variable in this effort. Several fit factor scores were collected. The overall fit factor is derived from the standard exercise set. Past testing has revealed that facial exercises resulted in relatively low protection factors. In order to determine which of the exercises were to blame, fit factor scores for the alternate exercises were also collected. Distributions, trends and characteristics of the fit factor data are presented in the remainder of this section.

Distributions: Standardized overall fit factor distributions are presented along with their logarithmic and exponential transforms in Figure A10. The scores used were from the main sample population ($n = 112$) plus 10 repeated measures (total $n = 122$). The small histogram represents all subjects who were tested in the small mask ($n = 110$); the medium histogram represents all subjects who were tested in the medium mask ($n = 117$); and the large histogram represents all subjects who were tested in the large mask ($n = 80$). The raw and transformed distributions deviate enough from a normal distribution so as to prohibit analysis by the elementary statistical methods employed in this effort. Quantitative descriptions of the raw distributions are presented in Figure A11.

It was noticed, however, that the distributions of the differences between scores were approximately normal. Therefore, subsequent statistical analyses of the dependent variables were performed on difference data rather than raw data. The difference histograms are presented in Figure A12. They are followed by a comparison of all distributions discussed in this paragraph (Figure A13).

Trends: The overall fit factor scores and the fit factor scores of each alternate exercise were examined to see if subjects who scored relatively well in one size mask scored relatively poorly in another. The method of analysis was to sort a table of fit factor scores on the basis of one of the three mask sizes. These were the x values. Each x value had two corresponding y values, i.e. the subject's score in the other two mask sizes. When plotted, least squared lines were drawn to indicate trends. The sample size was not recorded for this analysis but are approximately $n = 100$ for the overall plots and $n = 26$ for the alternate exercise plots.

Figures A14 to A21 show the trend lines for each subject's fit factor score compared to the other two mask sizes. As evidence by the data, there is a significant amount of data scatter (variability) which hinders the ability to draw conclusions regarding correlation of fit factor scores

between mask types. There is some indication that subjects who score relatively well in one mask size will also score relatively well in the other sizes. A notable exception is manifest in the breathe normally exercise in which the medium mask exhibits the expected trend with the small and the large masks (Figure A16). Curiously, a positive correlation always existed between the small and the large mask. This surfaced many times throughout the dependent variable analyses, and a candidate explanation for it is contained in the Mask Deformation Analysis on page 17.

Characterization of Standard Exercises: In this analysis the main sample population (n = 112) was tested in each mask size for which a visually obvious gross sizing problem did not exist. This crude method of issuance yielded the following sample sizes:

small	medium	large
n = 103	n = 111	n = 76
misfits = 9	misfits = 1	misfits = 36

A comparison of the standard exercise scores is shown in overview in Figure A22, and in more detail in Figures A23 through A26. Distributions of some of the scores are shown in Figures A27 through A30, and deviations from normality are evident. Nevertheless, three noteworthy patterns emerge from the charts of the confidence intervals:

- Rainbow passage and facial expressions yield the lowest fit factors in every mask,
- Rainbow passage and facial expressions are approximately equal for each mask, and
- The (relatively) depressed means and tight confidence intervals for these exercises indicates that (relatively) gross leakage is common during their performance.

The effect of the rainbow passage and facial expressions exercises on the overall fit factor is shown in Figures A23 through A25, and is seen to be large. Individual facial expressions were isolated and tested in an attempt to identify the most insidious of them. A discussion of that analysis follows.

Characterization of Alternate Exercises: In this analysis 26 subjects from the main sample population performed the alternate exercises in each size of mask. Subjects were instructed to breathe while holding each pose to assure that it was rigorously challenged. As

shown in Figures A39 through A44, the distributions deviate from normality, so only general observations were made from the computed confidence intervals.

Figure A31 reveals that yawn and smile yielded the lowest fit factors, and that they were approximately equal for each mask. The combination of a (relatively) depressed mean and tight confidence interval appeared for yawn and smile in the small mask, thereby indicating that (relatively) gross leakage was common for those exercises in that size. Tabulated data is presented in Figure A32.

Comparisons between the three sizes for each exercise is shown in Figures A33 through A38. In general, the medium mask showed a higher mean with a larger confidence interval than did the small or the large mask.

Characterization of Overall Fit Factor: Two sets of overall fit factor scores were compared in this analysis. The first set was derived from the standard exercises discussed in Characterization of Alternate Exercises on page 11. The second set is a subset of the first, and consists of the highest overall fit factor attained by each subject. Review of the first set of scores reveals that the crude sizing method explained in Characterization of Alternate Exercises yields the following results.

Of the sample population of 112:

- If only the small mask existed, 103 users could expect a nominal overall fit factor of 190,000, and there would be 9 identified misfits.*
- If only the medium mask existed, 111 users could expect a nominal overall fit factor of 120,000, and there would be 1 identified misfit.*
- If only the large mask existed, 76 users could expect a nominal overall fit factor of 93,000, and there would be 36 identified misfits.*

* The actual number of misfits is expected to be up to 5 higher because the misfit population described in Sample and Subsample Population on page 4 is included in the sample of 112.

Descriptive statistics for the first set of scores are contained in Figures A45 through A48. Subtracting the scores of the larger size from the smaller size helped normalize the distributions, and permitted the performance of an F-test to check the equality of the means of the differences (Figures A49 through A52). Those means range from 45,000 to 82,000, and the F-test failed to

reject the null hypothesis that they were all equal. (A formal check on the homogeneity of the variances is needed to substantiate this result, but it was not performed in this analysis.)

If the sample population represented the user population, this result would have practical application to the crude issuance method. Specifically, of those sizes for which a visually obvious gross sizing problem does not exist, issuance of the smallest of the sizes can be expected to provide a fit factor which on average is between 45,000 and 82,000 greater than issuance of any larger mask. The mean result however is not expected to exceed 190,000 which is the mean of all subjects tested in the small mask (by the crude issuance method).

The second set of data contains only the highest overall fit factor score for each subject. Descriptive statistics for this data are shown in Figures A53 through A55, and deviations from normality are observed. In this data set, however, the size ($n = 9$) and distribution of the large data are questionably represented by the mean and confidence intervals of the normal distribution and should be viewed with skepticism. Ignoring this caveat, the data is interpreted as follows.

Employment of an issuance method which provides the best fit factor mask, but would not be able to weed out misfits, would be expected to yield a nominal fit factor somewhere within the range of 180,000 to 280,000. Hidden within the sample of 112 subjects are up to 5 misfits.

Comparing the results of the two sets of data analyzed in this paragraph it can be claimed that a single size medium mask system would yield a nominal fit factor at least 60,000 less than that provided by a correctly issued mask in a three size system, with about the same number of misfits.

Independent Variable Analyses

The independent variables discussed in this section are not all independent, and the label merely serves to distinguish fit factor scores from the many measures taken to try to predict them. Those measures and their analyses are the topic of this section.

Lateral Skin Displacement Analysis: This analysis was conducted on data obtained from the visual observation of subjects wearing their bestfit mask. The maskpoints were transferred to the subject's face via a makeup pencil, and the each mark's movement (magnitude and direction) relative to the hole was observed and recorded while the subject held the following

poses: yawn, smile, frown, rotate chin left, rotate chin right, and head up. Eleven of the 37 subjects in the subsample were so observed, as well as 4 of the 5 misfits. The occurrence of relative lateral movement for these subjects is tallied in Figure A56. The figure reveals that maskpoints 4 through 7, their counterpoints 15 through 18, and 10 through 12 were common sites of movement. These points are in the temple to cheek and submandibular regions. No obvious differences were evident between the lowest fit factor exercises, yawn and smile, and the rest of the exercises. Generally, a greater percentage of misfits than bestfits were represented for any given point/exercise combination, except in the submandibular region, where it was noted that some marks could not be observed for 3 of the 4 participating misfits. Of all the misfits analyses performed in this effort, the test conductors' noted mask/face anomalies in the submandibular region could provide the best discriminator.

Analysis of Anatomical and Mask Coordinates: These analyses commenced by plotting ρ , θ and ϕ for the maskpoints of several subjects in both anatomical and mask coordinates. Figures A57 and A58 show some of the output, which was used merely to provide a first look at the nature of the data. Of the subjects reviewed, no gross deviations from symmetry were observed, and it was decided to study only maskpoints 1 through 11 (the left side of the face) for the rest of the effort.

The ranges of the mask coordinate data for maskpoints 1 through 11 are contained in Figure A59, and it is seen that the angular ranges between the mask size are almost identical for each point. Assuming the midpoint of each range represents the angles' true values², the three mask sizes can be visualized as being nested on a set of radiating spokes; the first spoke passing through maskpoint1 of all three masks, the second through maskpoint2, etc. If the hub of the spokes is coincident with the origin of the mask coordinate system, then the length of each spoke is ρ . Viewed in this manner, ρ provides an approximate measure of the ranges of distortion and accommodation of the bestfit seal, regardless of where the seal fits on the face relative to the anatomical system. A comparison between the ranges of the anatomical ρ and the mask ρ for maskpoints 1 through 4 reveal that the mask ρ ranges for the small and medium groups do not overlap, while the corresponding anatomical ρ ranges demonstrate considerable overlap. Although interesting, the usefulness of this information for issue/tariff purposes is questionable because no data was gathered on other than bestfit sizes.

² This assumption is somewhat specious, and it should be recognized that the angular ranges introduce error which challenges the validity of the mask ρ variable.

More useful information comes from a comparison of the misfits' mask ρ to the ranges of the bestfits' mask ρ . On the two subjects for whom this data was collected, it is seen that misfit40, wearing small maskpoints³, shares the low ρ of the range for maskpoints 10 and 11; and misfit13, wearing medium maskpoints, falls below low ρ for maskpoints 1 and 2, and is 1 mm greater than low ρ for maskpoint 11.

A second analysis was performed to determine how the misfits compare to the confidence intervals about the means for both anatomical and maskpoints. This analysis used mask ρ values. Because the validity of the confidence intervals depends upon how well a normal distribution represents the data, frequency histograms were plotted for the small subjects ($n = 23$). These are shown in Figure A60, and reveal a mixed bag of distributions, some of which appear normal. It must therefore be recognized that the resulting confidence intervals will bear some error.

Deviations from the 99% confidence intervals are plotted for misfits 13 and 40 in Figures A61 through A64, yet a review of the raw mask ρ data (Figures A65 through A67) for bestfits reveals that falling beyond this interval is very common. Therefore it was concluded that only range data should be used in subsequent analyses.

Sequential Delta ρ Analysis: Mask ρ is a useful measure to check the "waviness" of a face under the seal. This is important because a sudden rise or dip under the seal might create a leak path into the mask. This analysis was performed to determine the ranges of the differences between sequential ρ . The results are tabulated in Figure A68. Sequential delta ρ ranges are very similar for the three size groupings. Misfits 13 and 92 fall out of range in the submandibular region: For misfit13, the difference between maskpoints 10 and 11 is greater than the range, and for misfit92 the difference between maskpoints 9 and 10 is greater than the range.

Polygonal Perimeter Analysis: The polygonal perimeter is the sum of the linear distances between maskpoints. An analysis of the perimeter as it lengthened from maskpoint1 to maskpoint11 was performed for the small bestfit group. The results are shown in Figure A69. The figure reveals that the perimeter of the undeformed small mask lies within each identified range. Values in excess of the mask's perimeter suggest that the mask perimeter was stretched and or the facial tissue was compressed when the mask was on the face. Values less than the

³ Misfits were scanned in their bestfit mask.

mask's perimeter do not imply an absence of either. To understand why that is, it is helpful to review what happens as the mask meets the face and is tightened on it.

By the expert fit method employed in this effort, the mask was always donned in the following manner. The chin was first placed in the chincup, then the mask was rotated up to the forehead. Once in position, the headharness was flipped from the front of the mask to the back of the head and was tightened. Deformations of the mask and skin begin upon their contact with each other, and should be evident around both the nose cup and the mask seal. Quite likely deformations that took place as the mask points were coming in contact with the face inflated the perimeter of the skin while the mask was worn. A good view of this is provided in Figure A70, which shows a series of magnetic resonance images of a face's deformation in a mask bearing an MCU-2/P type of seal⁴.

It was speculated that the short perimetered subjects would have less tissue compression under the seal than would the long perimetered subjects, and as a consequence would experience more leakage. A check of fit factor values for long and short perimetered subjects did not substantiate this speculation.

A review of the polygonal perimeters for the three undeformed masks revealed that the perimeters of the medium and large mask are very similar⁵.

Datasheet and Scan Data Analyses: Recorded distances from the datasheet data and computed distances from the scan data were analyzed to determine discriminators between the three size groups and between the size groups and the misfits. Figures A71 through A76 show plots of the distances and a graphic comparison of their ranges. Considerable range overlap exists for all of the variables except for menton to point 6 length, point 1 to point 11 length, and menton to point 1 length. Some amount of range overlap was always evident between the medium and large groups.

Misfits fell out of range on a number of variables when compared to their bestfit size group, but in order to determine the most revealing variables, an out of range score was only recorded if it was outside of the combined small and medium range. By this criterion, misfit40 fell at the low end of the bigonial breadth range; misfit92 fell below the left zygion to left gonion

⁴ This work was conducted by the principal investigator, and was independent of the subject contract.

⁵ This may have been due to the crude method used to determine them. The method is explained in Mask Deformation Analysis on page 17.

range; and misfit 13 fell above bigonial, bizygomatic, bigonial plus bizygomatic, and left zygion to right gonion ranges. Data on misfits 13 and 40 is included in Figures A124 and A125.

Frequency histograms were plotted for the smalls ($n = 23$) for all variables (Figures A77 and A78), and demonstrate varying degrees of normality. The histograms do not show a common skew direction, thereby indicating that the group of smalls are true smalls. Descriptive statistics for the variables are contained in Figures A79 through A87.

Mask Deformation Analysis: The purpose of the mask deformation analysis was to identify the range of deformation demonstrated by the small mask on bestfit small faces, by the medium mask on bestfit medium faces and by the large mask on bestfit large faces. The size and shape of the undeformed mask was approximated by transferring the maskpoints to the mask's plastic packaging holder, and then scanning the holder. The results of this exercise are shown in Figure A88; the maskpoints are tabulated in Figure A89. The plots reveal that ρ differs between the three masks, while angles θ and ϕ are virtually identical, with one notable exception: ϕ for the large mask deviates from the small and medium between maskpoints 6 and 16. The uncorrected ϕ is shown on the plot. When corrected, ϕ for the large mask is greater in these areas, with the greatest difference occurring at maskpoint11. When viewed in the x-z plane the angle between the lines emanating from maskpoint6 (origin) to maskpoint1 and maskpoint11 (ρ_1 and ρ_{11} , respectively) is greater for the large mask than it is for the small and medium mask.

To obtain a more complete picture of this observation, ρ_1 , ρ_{11} and the angle between them (ϕ_{11}) were drawn to scale, and will henceforth be called the mask triangles. They are shown overlaid in Figure A90. The figure depicts the large mask with a longer seal than either the small or medium mask, and it also reveals that the medium mask has a deeper seal than either the small or the large mask. The commonality of the seal depth between the small and large mask may help explain why subjects tend to obtain higher fit factor scores in these two sizes than they do in the medium mask. If a one size (medium) mask is adopted and it is desirable to increase the protection it provides, mask designers should take a closer look at the speculated seal depth-fit factor score relationship.

In order to determine the range of deformation, ρ_1 , ρ_{11} and ϕ_{11} were drawn to scale for a number of small, medium and large subjects. (Included in each group were subjects with the longest and the shortest mask length, P1P11, in each size.) The resulting figures will henceforth be called the deformed triangles. The tragion (projected onto the midsagittal plane) and menton were added to the figures yielding a triangle that will henceforth be called the face triangle. An

example of the resulting drawing is shown to scale in Figure A91. Figure A92 compares the set of drawings that were made. The comparison revealed that within sizes the length between the tragon and point6 as measured in the midsagittal plane differs greatly, and for the small and medium subjects, a relatively long distance between those points corresponded to a relatively short mask length.

The deformed triangles for each size are shown superimposed in Figure A93. The figure reveals that with the exception of large subject62⁶, there are distinct differences between the sizes, and that these differences mirror the differences between the undeformed masks: The small is distinguished from the medium and large in length, and the medium is distinguished from the small and large in depth. These distinctions suggest that the triangles may be of use for issuance and tariffing. This is the topic of the following section.

Description of Bestfit Method

The bestfit method makes use of each mask's range of deformation and where each user's bestfit mask sits on his/her face. Knowing, for example, the location of the bestfit mask's point6, devices such as the deformation triangles could be indexed to it. The deformation triangle that places point1 in an appropriate place on the forehead and point11 in an appropriate place under the chin would indicate the size of the bestfit mask. Appropriate locations for points 1 and 11 relative to the glabella and menton, respectively were determined in the scan data analysis (Datasheet and Scan Data Analyses). Figure A94 shows the general idea, including the glabella-point1 relationship. The points shown either occur in or are orthogonally projected onto the midsagittal plane. The figure also shows that the location of point6 is critical to the success of the method.

This section provides more detail about the method.

Constraint: In order for the bestfit method to be of most value it had to be applicable to both tariffing and issuing; and both jobs would require appropriate tools for their performance.

The laser scanner is an appropriate tool for establishing an accurate and comprehensive

⁶ Subject62 was the only black subject in the subsample, and his deviation highlights the need for increased racial diversity in the sample. That notwithstanding, subject62's inclusion in the large population is questionable. He clearly scored higher in the large mask (overall ff = 570,000 as compared to 230,000 in the medium mask), yet a review of the maskpoints on his face revealed that the forehead portion of the seal was in his hairline. Subject87 had the same problem (and had an overall ff = 670,000 in the large, as compared to 200,000 in the medium mask). The seal touched the hairline in the temple region for all 5 of the large subjects, prompting speculation that the hair itself is blocking a leak path in that area and filtering out the corn oil challenge.

database of heads, and when used in conjunction with software to automatically locate facial landmarks, the system will support any (landmark based) tariffing algorithm. The same system could be used for issuing the mask, but a simpler and more rugged data collection tool is more suitable for the issuing environment. The data collection tool would be much more simple if it could gather all pertinent information in one view. Specifically, it would eliminate the need for scanning (with its associated moving parts), and it would avoid the drawbacks of the common scanning alternative, taking and merging multiple views. For this reason, the following constraint was employed during the development of the bestfit method.

All pertinent data for the method must be obtainable from one view of the face.

The Point6 Line: The profile was the logical view to consider in light of the aforementioned constraint. Profiles were generated for eight members of the subsample population who demonstrated at least one dimensional extreme. Upon examination of their left profiles, it was found that maskpoint 6 (point6) lies along the line traversing the center of the lips and tangent to the top of the ear (Figures A95 through A102). The top of the ear could prove unreliable, and so an arc with approximately a 16 mm radius from the tragon is proposed as a substitute.

It should be noted that the profiles used were not orthogonal projections; rather they bore a distortion which in two dimensions had the effect of stretching the face from the profile toward the back of the head. Whether or not the relationship holds in a true orthogonal projection has yet to be demonstrated, and may be of little consequence because the distortion used is repeatable. It should also be noted that point16, the mirror image of point6, showed greater deviation from the corresponding line on the right side of the face.

Fixing point6 along the point6 line is the topic of the next paragraph.

The Zygion Locus and its Relation on Point6: The left zygion lies in proximity to point6 and could be used to determine the approximate location of point6. From that approximate location, point6 could be allowed to slide up or down the point6 line within defined boundaries. The means by which the zygion determines the approximate point6 location, and the boundaries within which the point could be adjusted are discussed below.

A plot of the left zygion projected onto the midsagittal (x-z) plane is shown to scale in Figure A103. (The values for each subject are tabulated in Figure A104.) Point6 is at the origin

of the x and z axes. The plot reveals that the zygion locus is roughly contained in a band around the z axis.

A point6 line is also shown on the plot. It should be recognized, however, that the slope of the point6 line will vary somewhat between wearers. When the zygion is orthogonally projected onto the point6 line, it is readily seen that it provides a poor point6 approximation. Consequently, a correction factor was needed. Accepting that the length of the projection of the zygion onto the z axis (i.e., the z component of the zygion) is approximately equal to the length of its projection onto the point6 line, a method was sought to determine if the zygion's component could be predicted based on facial characteristics.

Recognizing that the mask's headharness would tend to pull the mask in the positive z direction, it was speculated that the zygion of wearers who had some "slack" in the lower part of the mask would tend to be plotted toward the left, while the zygion of wearers lacking slack would tend to be plotted toward the right. Mask slack was expected to be related to bizygomatic and bigonial breadths and the length of the chin. A linear multiple regression analysis was conducted to determine if bizygomatic breadth (ZYGZYG), bigonial breadth (GONGON) and anatomical p menton (ANARHM) could be used to determine the z component of the zygion. A separate analysis was conducted for each size group. The analyses are shown in Figures A105 through A107, and the results are promising. The multiple correlation coefficients range from 0.73 for the small group (n = 23) to 1.0 for the large group (n = 5). Consequently, the approximate point6 location could be found by projecting the zygion onto the point6 line and then subtracting out the predicted z value. Neglecting the error due to the substitution of the point6 line for the z axis, this method located point6 within (+ or -) 7mm of its true value for 34 of the 37 subjects in the subsample. It is possible that further regression analyses could accommodate all subjects within this, or tighter, boundaries. Such should be the goal.

It should be noted that during the issuance procedure point6 will be located by the small regression equation for the small mask triangle, by the medium regression equation for the medium mask triangle, and by the large regression equation for the large mask triangle. Because the equations differ, point6 will be relocated for each size trial. The effect of the relocations has not been fully determined; however, a check of the first 4 medium subjects in the small equation yielded the following values:

ACTUAL Z (MM)	Z PREDICTED FROM S EQ'N	Z PREDICTED FROM M EQ'N	DELTA PREDICTED
9.8	21.2	6.9	14.3
-13.5	2.1	-11.3	13.4
4.0	20.2	5.3	14.9
-2.8	10.6	-4.8	15.4

For these subjects point6 for the small mask trial is located an average 14.5 mm closer to the center of the lips than it is for the medium trial.

The analyses discussed in this section provide hope that point6 can be reasonably well located given the tragion, zygion, gonion, menton (ANARHM is the distance between the tragion and the menton in the midsagittal plane), and the center of the lips. The single view constraint is upheld if bizygomatic breadth and bigonial breadth are approximated by twice the distance from their respective landmark to the midsagittal plane.

Relationships and Algorithms: Although size discriminators were identified on the deformed mask triangles, it is still likely that additional algorithms will be needed for guidance in the grey areas. The algorithms would be based on relationships. For example, the menton-point11 relationship would produce an algorithm that restricts searching for point11 within a specified range for each mask. Similarly, the glabella-point1 relationship would provide search ranges for point1 referenced to the glabella. (The glabella thereby becomes the sixth landmark required by the method.)

Another helpful relationship appeared between the bizygomatic breadth and the mask length (point1 to point11) for medium subjects. A strong positive correlation was demonstrated between them (Figure A108 through A110), and a different, weak correlation was demonstrated among the larges. The ability to predict medium mask length from bizygomatic breadth would help distinguish a medium user from a large user, as this length forms one of the legs of the distortion triangle.

It is likely that other relationships exist and could be used to create algorithms. The type of algorithms desired will be determined as the deficiencies of the method itself become known.

Final Data Analyses

Having found a method which may provide the bestfit mask to each user, it is worthwhile to compare it to existing methods. The comparison is contained in the Dependent Variable Analyses section on page 9. It is followed by a detailed look at the fit factor scores of the bestfit subsample.

Comparison of Sizing Methods: The bestfit method was compared to three other sizing methods to determine if it produced superior results. The methods are summarized as follows:

The caliper method assigns mask size based on menton sellion length as measured by sliding calipers,

The MSL method assigns mask size based on menton sellion length as measured by a caliper with a modified scale, and

The Slate method assigns mask size based on caliper-measured menton sellion length and bizygomatic breadth.

A summary of the comparison between the methods is shown in Figure A111⁷. Of note in the figure is the tally of the subjects' complaints about the three mask sizes. Small and medium subjects frequently preferred a larger than bestfit mask, commenting that the bestfit mask was tight, pinched the nose, and most commonly, restricted breathing. Although the subjects were not experienced mask wearers their comments should not be taken lightly. A mask must be comfortable enough to promote long term wear, as the risk exists that a user will remove an unbearable mask.

While most of the complaints are noseclip related, some are not: A comment about tightness or speech interference may have to do with the size or stiffness of the facial seal, and should be more fully investigated prior to adoption of a bestfit method based on fit factor alone.

Chi-square goodness of fit tests were performed to determine if one sizing method was significantly better than another. Results of the chi-square goodness of fit tests are shown in Figure A112. The test was based on the number of correct mask size matches for each sizing method. The first goodness of fit test evaluated all four methods and revealed that there are significant differences between the four groups at $\alpha=0.5$. However, there is an inherent bias in that the correct mask size for each subject is specified by the best fit method. This magnifies the

⁷ The designated caliper, MSL and Slate size were provided by AAMRL.

differences between the bestfit method as compared to the other sizing methods. A second more appropriate goodness of fit test was performed to evaluate the differences between the caliper, MSL, and slate method compared to the standard set by the bestfit method. This test indicates that there are no significant differences between the caliper, MSL, and slate sizing methods. However, a review of the descriptive statistics indicate there may be non-significant tendencies. The caliper and MSL method are fairly equal with each method prescribing the correct mask size about 50 - 60 percent of the time. The slate method was the worst performer identifying the correct mask size only 30% of the time.

Dependent Variable Analyses for the Bestfit Subsample: In these analyses, overall and standard exercise fit factor scores were reviewed for the bestfit subsample⁸ to determine if any additional information could be extracted from them. Histograms for the overall fit factor scores are shown in Figure A115. Also included in the figure are plots of the trend lines (described in the Trends section on page 10) which reveal that high scoring subjects within a size group tend to be high scoring subjects (relative to their own group) when their size group is tested in another size mask.

Figure A116 through A118 present descriptive statistics for the overall and standard exercises for the three size groups. Upon comparing the means of the overall and standard exercise scores for the crudely sized small (Figure A23) to the 95% confidence intervals for the bestfit smalls it was observed that the means of the crudely sized smalls always fell below the range of the means for the bestfit smalls. This exercise was not performed for the medium and larges because each had too few members for a meaningful comparison.

It is also of interest that even among the bestfit subjects, the rainbow passage and facial expressions exercises bore the (relatively) depressed mean and tight confidence interval characteristics of (relatively) gross leakage.

Figure A119 shows the descriptive statistics for the overall and standard exercises which resulted from the large subjects wearing the medium mask. It should be noted that the mean for the rainbow passage exercise was 94,000 and the mean for the facial expressions exercise was 88,000. Confidence intervals for this n = 5 group are meaningless, and therefore cannot be used to indicate the low end of the mean.

⁸ An extra (unidentified) medium subject was inadvertently included in the medium group, yielding n = 10 for these analyses.

Further comparisons of bestfit subjects tested in other than bestfit sizes are presented in Figures A120 through A123.

CONCLUSION AND RECOMMENDATIONS

Having identified a candidate method that would provide each user with his/her bestfit mask size, it is necessary to decide what, if any, action should be taken. The purpose of this section is to discuss what courses of action should be considered.

Conclusion

It is not necessarily surprising that issuing and tariffing methods can be fine tuned by incorporating more dimensions. For the subsample, the bestfit method required taking several measurements relating to 6 landmarks (menton, gonion, tracion, zygion, glabella and the center of the lips), in order to provide a 29% increase $[(310,000 - 240,000)/240,000]$ in nominal fit factor over the current caliper method, which required taking one measurement between two landmarks (menton and sellion). Clearly, the bestfit method would require non-contact measurement, image processing and data processing to be feasible for issuance and tariffing. Assuming that the method only uses data from one side of the face, the technical challenge in realizing the method is automating the identification of the needed landmarks. That's the good news. The bad news is that non-contact measurement techniques could be foiled by facial blemishes, and may require additional image processing to smooth irregular skin surfaces.

More bad news is that the bestfit size did not impose minimum encumbrance on the user. The nose cup of the small mask did not accommodate the group of bestfit smalls, and there is some suspicion that the seal itself may be too tight for some bestfit smalls.

The question of whether or not the benefits of the bestfit method are worth the added complexity and implied design changes can only be answered by those cognizant of both the perceived threat environments and the bestfit method benefits. The benefits of the method are:

- Providing each user with the maximum protection afforded by the mask's design,
- Identifying misfits,⁹ and

⁹ Identified misfits pose a design problem. Assuming that their major leakage problem has to do with their fit in a particular region of the mask (the submandibular region was implicated in this effort), a

- Permitting the establishment of a half face database for the true user population.

Also worthy of consideration are the benefits of pursuing the method. These benefits are:

- To increase the understanding of the mask-face relationship, which is of use in the design of masks, as well as in computer modeling efforts.
- To promote the development of algorithms to accurately locate landmarks on a three-dimensional image.
- To demonstrate an application for a database of three-dimensional size and shape data, which makes use of the flexibility it offers over standard anthropometric data and which yields an objective measure of success, i.e. the fit factor score.

Recommendations

If it is decided that the benefits outweigh the costs of pursuing the bestfit method, then the following course of action is recommended for the data already collected:

- Determine whether or not the point6 line is identifiable on distortion free orthogonal projections of the left profile for the subsample.
- Determine if there is a difference between the left and the right profile projections for the subsample.
- Determine if the method holds for the entire sample population.

If a decision to abort the effort has not arisen as a result of the aforementioned activities, then a formal test should be devised to check the method on a representative population. The test should also identify any significant discomfort caused by the bestfit mask, and if identified, efforts should commence to correct it. Supporting hardware and software for the method will also need to be developed.

design effort can be undertaken to either modify the mask's design or to provide the misfits with a protection enhancement modification device. The device would likely be anchored to the mask's straps by the user.

References

Air Standardization Coordinating Committee. *The Measurement of Protection Provided to the Respiratory Tract and Eyes Against NBC Agents in Particulate Aerosol and Vapour Form* (p. 8) (Document No. ASCC AIR STD 61/14A).

Case, Henry, Ervin, Cay, and Robinette, Kathleen M. (1989). *Anthropometry of a Fit Test Sample Used in Evaluating the Current and Improved MCU-2/P Masks (U)* (Technical Rep. No. AAMRL-TR-89-009). Armstrong Aerospace Medical Research laboratory, Wright-Patterson Air Force Base, Ohio.

Department of the Navy (1989). *Naval Aviation Entrance Physical Evaluation (NAEPE) Program* (Document No. OPNAV 6120.2).

Naval Surface Warfare Center (1988). *Summary Report of MCU-2/P CBR Mask Protection Factor Testing* (p. 9).

Winer, B.J. (1971). *Statistical Principles in Experimental Design* (2nd ed.) (p. 283). New York: McGraw-Hill.

APPENDIX A: FIGURES

FIGURE A1

		SEX	RACE	AGE	HEIGHT	WEIGHT
<u>SUMMARY</u>	41	F	W	18	65	119
<u>SEX</u> 20 FEMALES:	63	M	W	26	65	145
16/23 SMALL	64	F	W	21	64	132
3/9 MED	68	M	W	19	68	150
1/5 LARGE	70	F	W	19	64	120
	72	M	W	19	71	175
17 MALES:	73	M	W	18	73	160
7/23 SMALL	74	F	W	23	64	130
6/9 MED	88	F	W	18	62	120
4/5 LARGE	89	F	W	25	62	105
<u>RACE</u>	90	M	W	23	68	176
36 WHITES	93	F	W	34	65	140
1 BLACK	94	F	W	22	63	125
	96	F	W	19	63	125
<u>AGE</u>	101	M	W	19	71	195
18-34	103	M	W	23	80	210
18-20: 20	105	F	W	19	71	145
21-25: 14	106	F	W	20	71	155
26-34: 3	107	F	W	20	68	135
	108	F	W	20	62	140
<u>HEIGHT</u> 62"-80"	109	F	W	20	66	132
	112	F	W	20	66	130
<u>WEIGHT</u> 105# - 210#	113	F	W	21	65	125
	10	M	W	22	69	155
	22	F	W	21	65	135
	23	M	W	22	69	150
	51	F	W	22	69	130
	53	M	W	20	73	175
	56	F	W	18	66	140
	60	M	W	18	74	165
	81	M	W	21	67	145
	91	M	W	18	73	137
	5	M	W	19	75	192
	50	F	W	30	68	155
	62	M	W	25	68	165
	76	M	B	21	73	155
	87	M	W	19	69	140

FIGURE A2

MASKPOINTS & THE X-Z AXES ON THE
MIDSAGITTAL PLANE

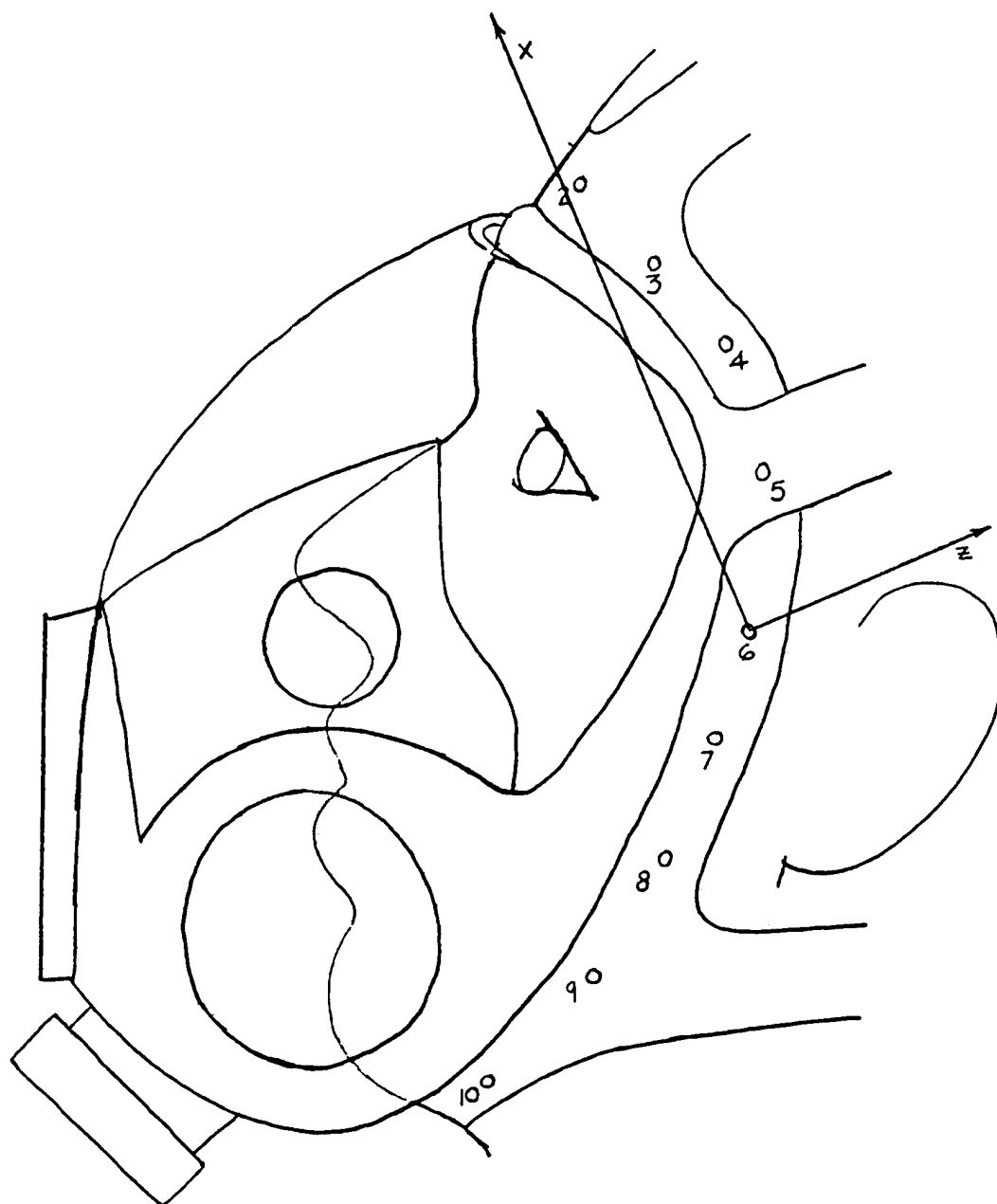


FIGURE A3

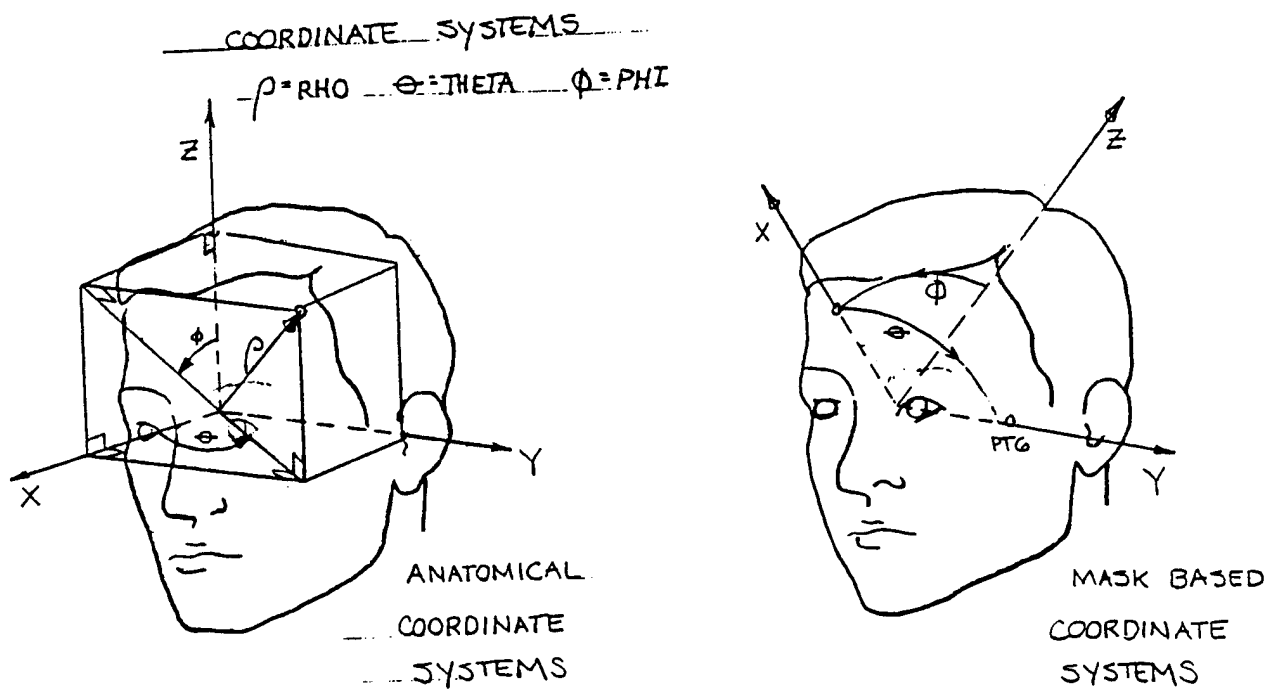
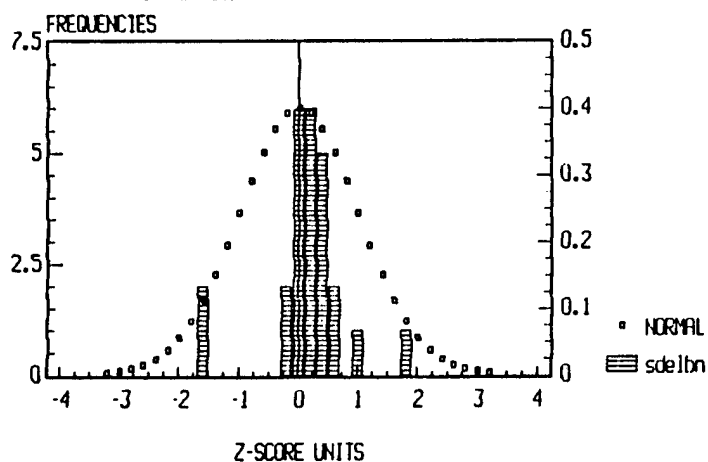
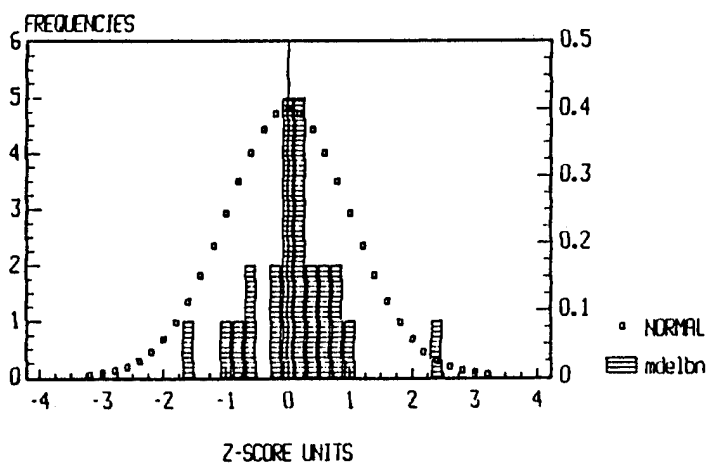


FIGURE A4

DISTRIBUTIONS OF DIFFERENCES BETWEEN
REPEATED TRIALS OF BREATHE NORMALLY
STANDARDIZED HISTOGRAM OF sdelbn



STANDARDIZED HISTOGRAM OF mdelbn



STANDARDIZED HISTOGRAM OF ldelbn

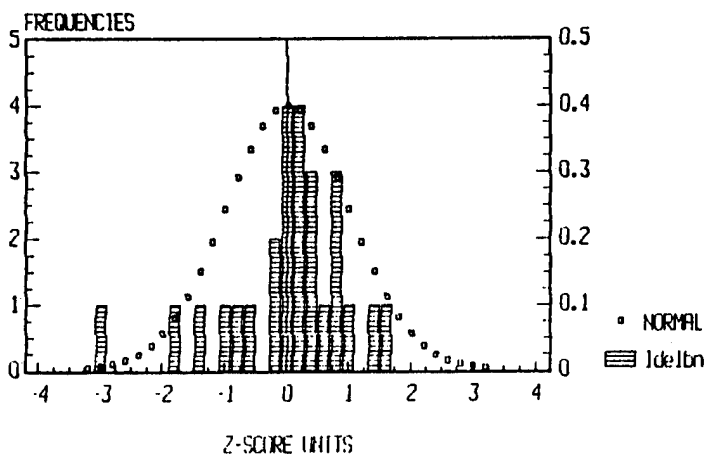
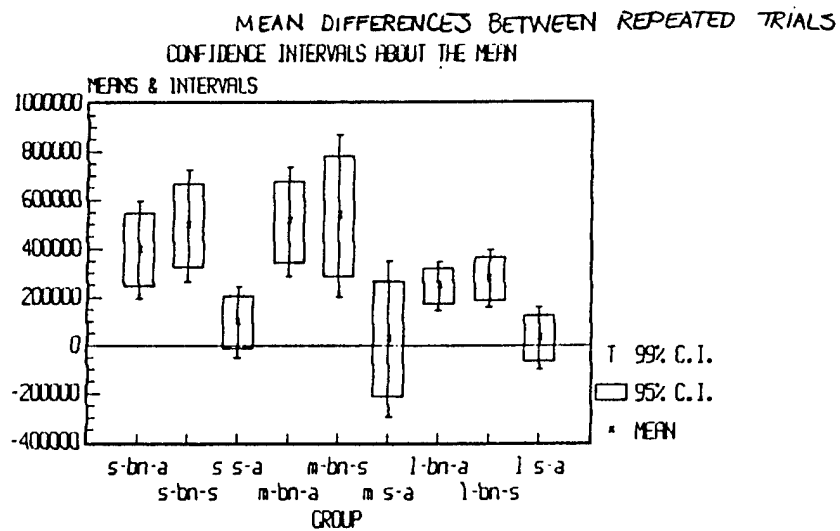


FIGURE A5



VAR NAME	MEAN	STD ERR	LOWER 95%	UPPER 95%	LOWER 99%	UPPER 99%
s s-a	96453.85	53223.97	-13187.52	206095.2	-51881.34	244789
m s-a	25561.54	115914.4	-213222.2	264345.2	-297491.9	348615
l s-a	29921.54	46523.31	-65916.48	125759.6	-99738.92	159582

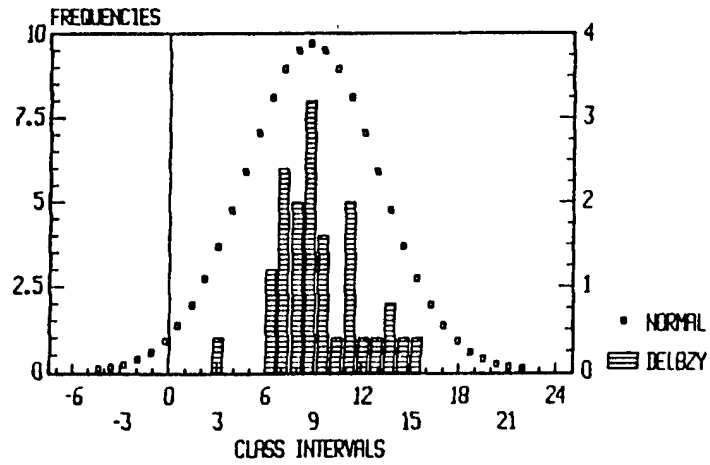
FIGURE A6

RELIABILITY ANALYSIS

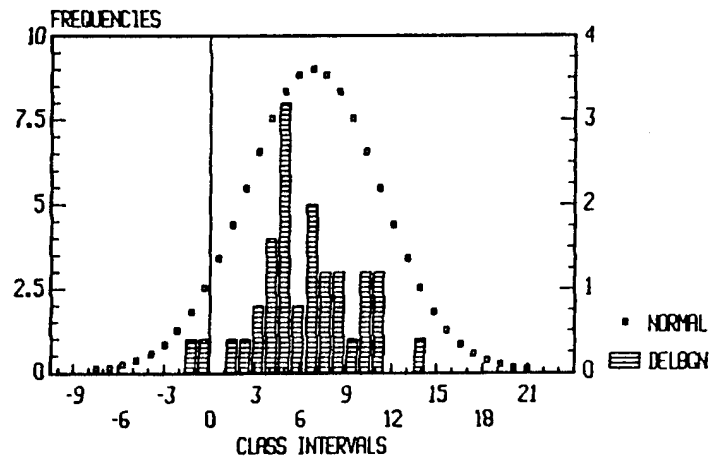
NUMBER OF MEASURES:	3
NUMBER OF CASES:	26
VARIANCE AMONG MEASURES:	4.104221E+10
VARIANCE AMONG CASES:	1.851072E+11
RELIABILITY COEFF R(XX):	.20543
STAND. ERROR OF MEASUREMENT:	383510.3

FIGURE A7

DISTRIBUTIONS OF DIFFERENCES
BETWEEN HAND AND MACHINE MADE MEASURES
HISTOGRAM OF DELBZY



HISTOGRAM OF DELBGN



HISTOGRAM OF DELMNS

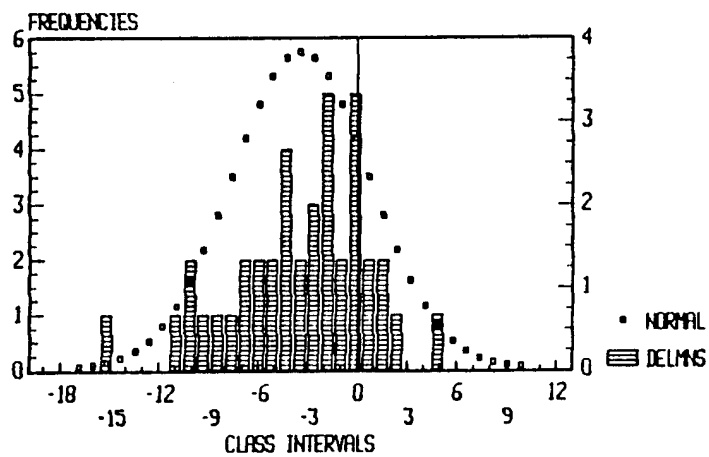


FIGURE A8

TEST FOR EQUAL MEANS

2-SAMPLE T-TEST

GROUP:	DELBZY	DELBGN
SIZE:	40	40
MEAN:	8.752	6.71975
SD:	4.119977	4.437638
F-RATIO (VAR):	1.18015	$H_0: \sigma_1^2 = \sigma_2^2$ Reject if $F > F_{\alpha/2, DF1, DF2}$ For $\alpha = .05$, $F_{.025, 39, 39} \approx 1.9$ Is $1.2 > 1.9$? No, so accept $\sigma_1^2 = \sigma_2^2$
DF:	39, 39	
2-TAIL PROB:	.6444	
T-VALUE:	2.122611	$H_0: \mu_1 = \mu_2$ $t_{\alpha/2, 78} \approx 2.0$ $H_a: \mu_1 \neq \mu_2$ Is $2.1 > 2.0$? Yes, so reject H_0 . Accept $\mu_1 \neq \mu_2$
DF:	78	
2-TAIL PROB:	.037	
OMEGA SQUARED:	.041979	
ETA SQUARED:	.054608	

FIGURE A9

1-SAMPLE T-TEST -----		
SAMPLE NAME:	DELBGN	
SAMPLE SIZE:	40	$H_0: \mu = 0\text{mm}$
SAMPLE MEAN:	6.71975	$H_a: \neq 0\text{mm}$
STANDARD DEVIATION:	4.437638	Reject H_0 if:
STANDARD ERROR:	.701652	$ t > t_{\alpha/2, n-1}$
COMPARISON VALUE:	5	$\alpha = .05$ $n-1 = 39$
T-VALUE:	2.451	$t_{\alpha/2, n-1} = 2.0$
DEGREES OF FREEDOM:	39	Is $9.6 > 2.0$
2-TAIL PROB:	.0188	Yes, so reject H_0
		Accept $\mu \neq 0\text{mm}$
1-SAMPLE T-TEST -----		
SAMPLE NAME:	DELBZY	
SAMPLE SIZE:	40	$H_0: \mu = 0\text{mm}$
SAMPLE MEAN:	8.752	$H_a: \neq 0\text{mm}$
STANDARD DEVIATION:	4.119977	Reject H_0 if:
STANDARD ERROR:	.651426	$ t > t_{\alpha/2, n-1}$
COMPARISON VALUE:	5	$\alpha = .05$ $n-1 = 39$
T-VALUE:	5.759674	Is $13.4 > 2.0?$
DEGREES OF FREEDOM:	39	Yes, so reject H_0
2-TAIL PROB:	<.0001	Accept $\mu \neq 0\text{mm}$
1-SAMPLE T-TEST -----		
SAMPLE NAME:	DELNNS	
SAMPLE SIZE:	40	$H_0: \mu = 0\text{mm}$
SAMPLE MEAN:	-3.492249	$H_a: \neq 0\text{mm}$
STANDARD DEVIATION:	4.171076	Reject H_0 if:
STANDARD ERROR:	.659505	$ t > t_{\alpha/2, n-1}$
COMPARISON VALUE:	-5	$\alpha = .05$ $n-1 = 39$
T-VALUE:	2.286185	Is $5.3 > 2.0?$
DEGREES OF FREEDOM:	39	Yes, so reject H_0
2-TAIL PROB:	.0278	Accept $\mu \neq 0\text{mm}$

FIGURE A10

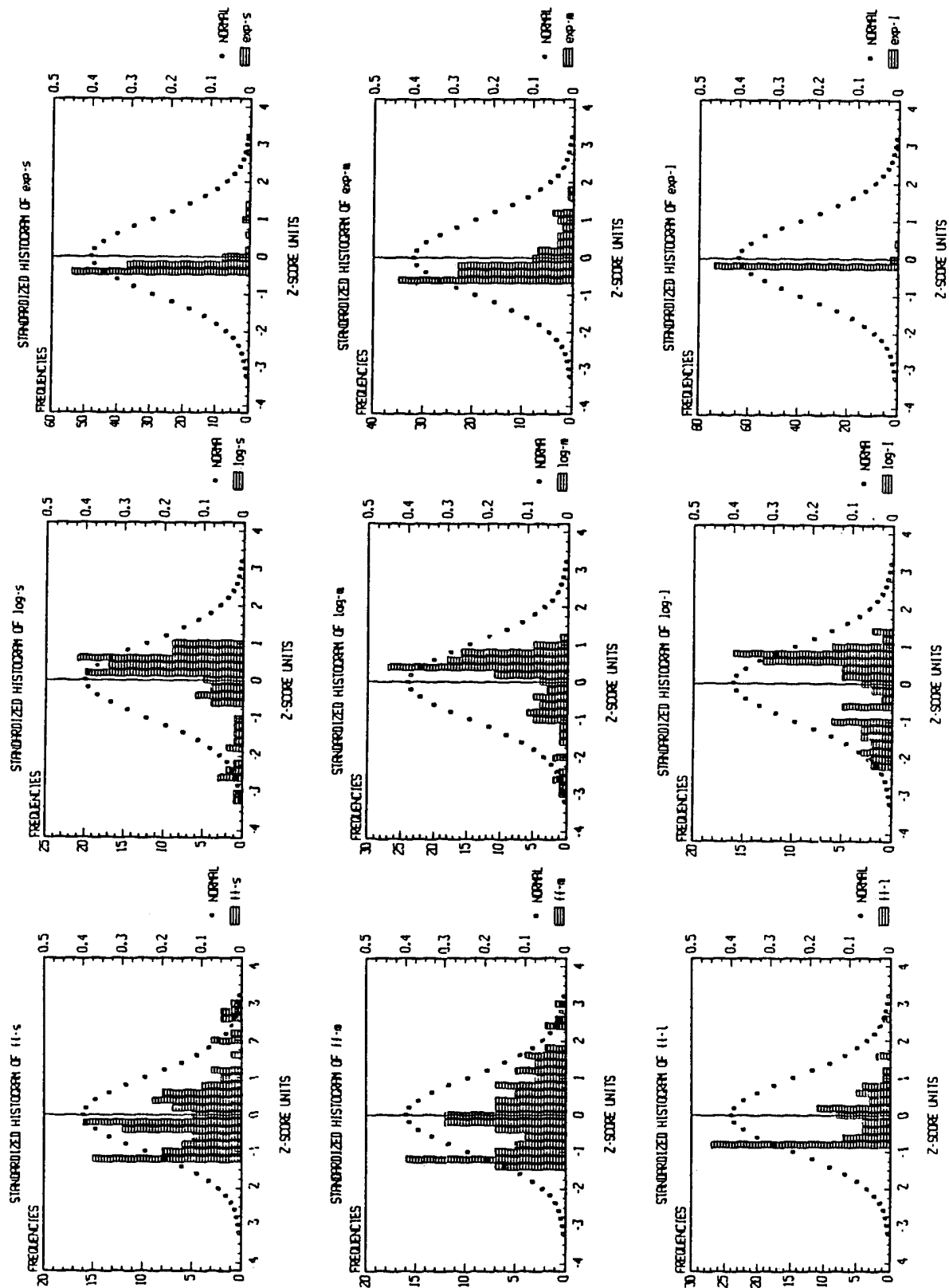


FIGURE A11

QUANTITATIVE DESCRIPTIONS OF RAW DISTRIBUTIONS
DESCRIPTIVE ESTIMATES FOR... ff-a

SAMPLE SIZE	110
NUMBER MISSING	12
MEAN	179579.6
HARMONIC MEAN	5655.941
MEDIAN	150000
VARIANCE	2.175401E+10
STANDARD DEVIATION	147492.4
MEAN ABS. DEVIATION	113996.7
STANDARD ERROR	14062.85
SKEWNESS	1.0744
KURTOSIS	.95798
MINIMUM	190
MAXIMUM	620000
RANGE	619810
SUM	1.975375E+07
SUM OF SQUARES	5.918558E+12

DESCRIPTIVE ESTIMATES FOR... ff-b

SAMPLE SIZE	117
NUMBER MISSING	5
MEAN	121669.1
HARMONIC MEAN	6099.633
MEDIAN	120000
VARIANCE	8.508124E+09
STANDARD DEVIATION	92239.49
MEAN ABS. DEVIATION	73502.06
STANDARD ERROR	8527.544
SKEWNESS	.61226
KURTOSIS	-.10259
MINIMUM	180
MAXIMUM	390000
RANGE	389820
SUM	1.423528E+07
SUM OF SQUARES	2.718936E+12

DESCRIPTIVE ESTIMATES FOR... ff-1

SAMPLE SIZE	80
NUMBER MISSING	42
MEAN	90170.67
HARMONIC MEAN	1248.707
MEDIAN	58000
VARIANCE	1.391734E+10
STANDARD DEVIATION	117971.8
MEAN ABS. DEVIATION	79821.33
STANDARD ERROR	13189.65
SKEWNESS	2.65781
KURTOSIS	9.57361
MINIMUM	84
MAXIMUM	670000
RANGE	669916
SUM	7213655
SUM OF SQUARES	1.74993E+12

FIGURE A12

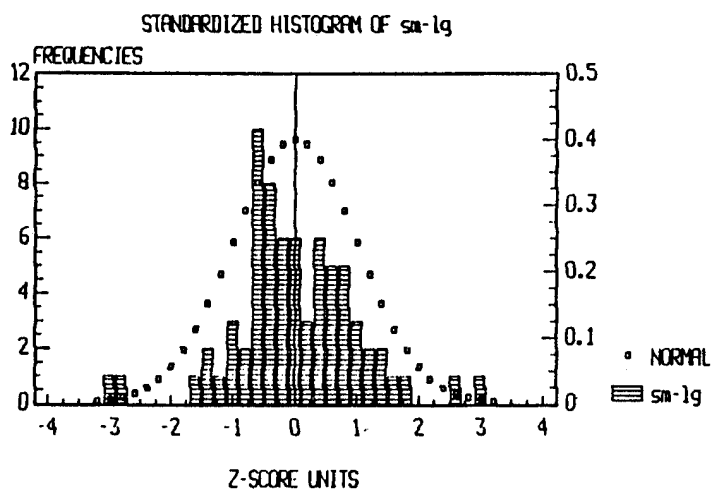
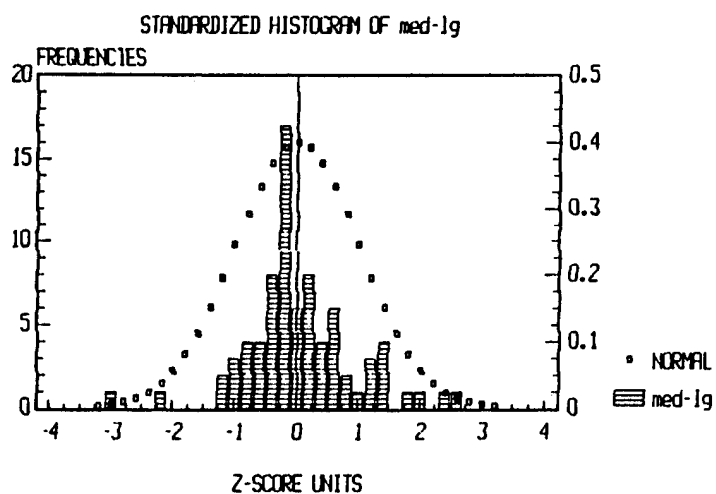
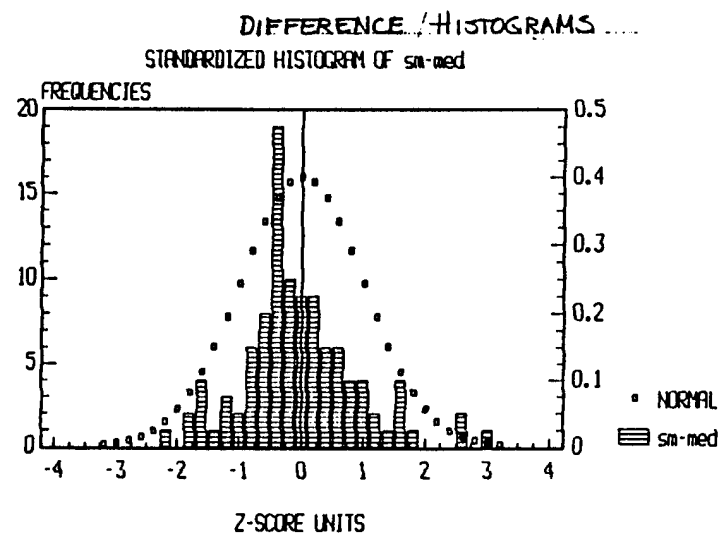


FIGURE A13

COMPARISON OF DISTRIBUTIONS					
VAR NAME	SIZE	MEAN	SAMPLE STD DEV	SAMPLE VARIANCE	COEF. OF VARIATION
ff-s	110	179579.6	147492.4	2.175401E+10	.82132
ff-m	117	121669.1	92239.49	8.508124E+09	.75812
ff-l	80	90170.67	117971.8	1.391734E+10	1.30832
sm-med	106	65478.1	151334.5	2.290212E+10	2.31122
med-lg	79	44040.59	126240.6	1.59367E+10	2.86646
sm-lg	71	79694.03	136020.3	1.850153E+10	1.70678
exp-s	110	27.49622	77.81652	6055.411	2.83008
exp-m	117	5.4905	7.27751	52.96216	1.32547
exp-l	80	17.25984	96.07948	9231.267	5.56665
log-s	110	-.05979	.77914	.60706	-13.03194
log-m	117	-.19446	.70588	.49827	-3.62996
log-l	80	-.68644	1.05193	1.10656	-1.53246

FIGURE A14

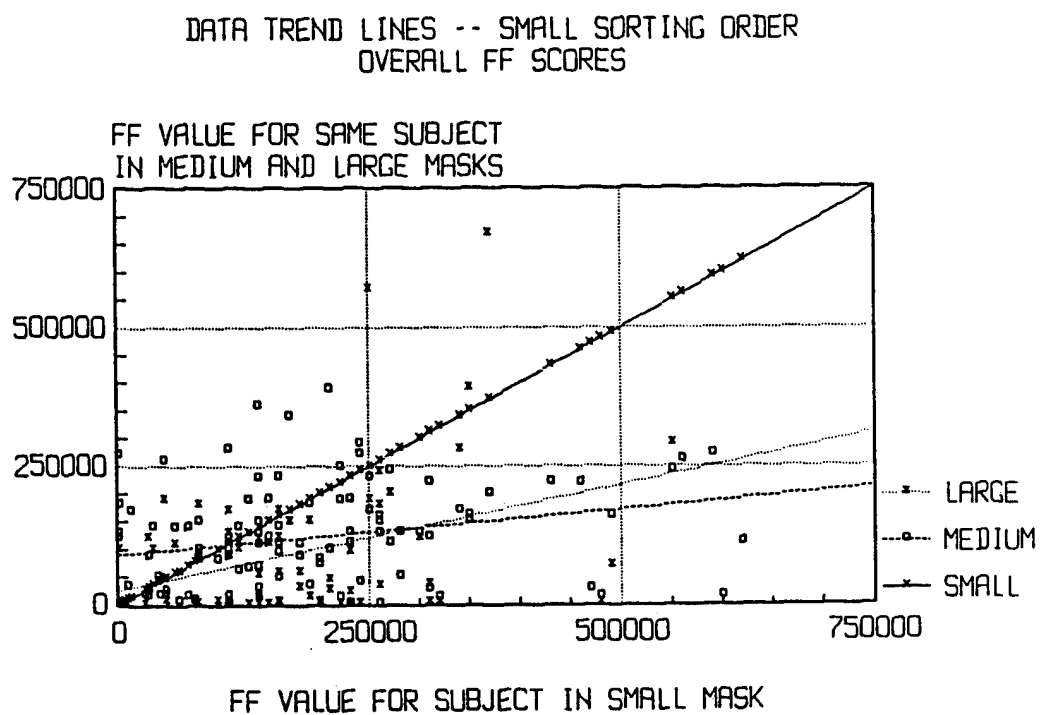


FIGURE A15

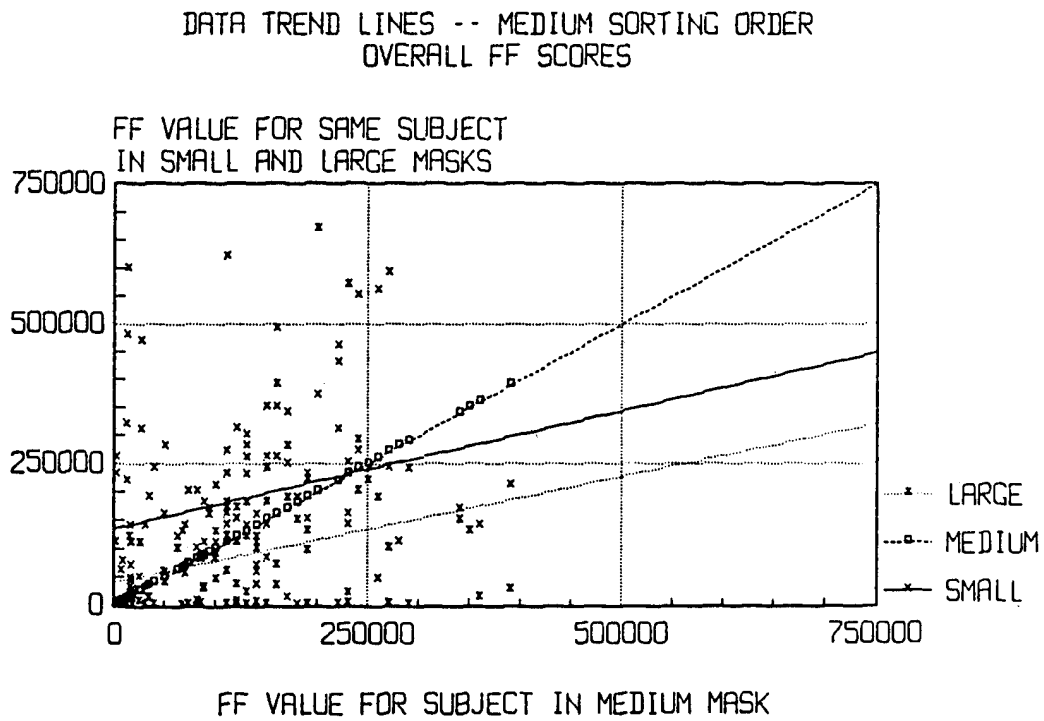
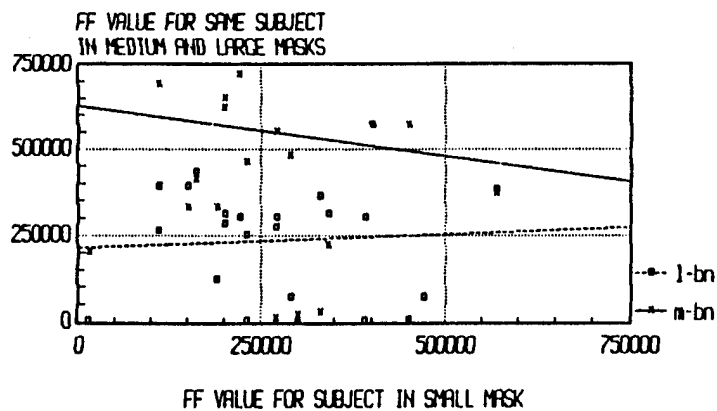
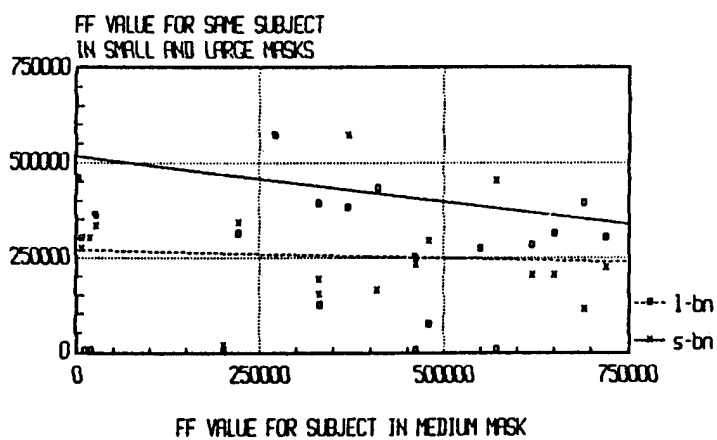


FIGURE A16

DATA TREND LINES -- SMALL SORTING ORDER
ALTERNATE EXERCISES -- BREATHE NORMALLY



DATA TREND LINES -- MEDIUM SORTING ORDER



DATA TREND LINES -- LARGE SORTING ORDER

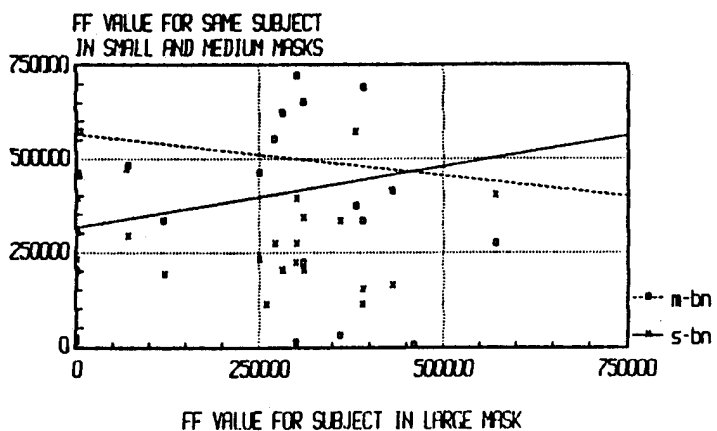
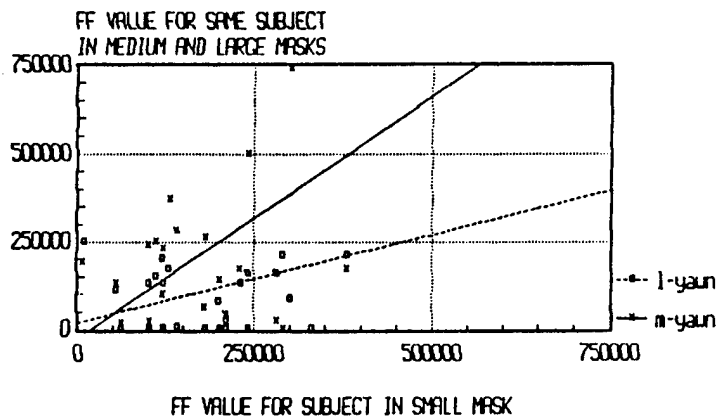
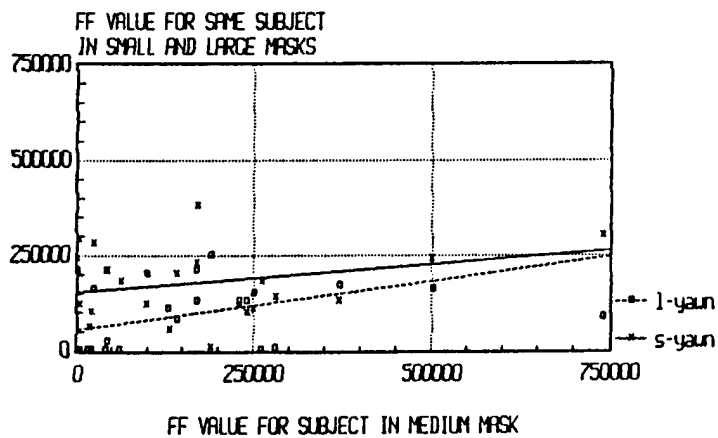


FIGURE A17

DATA TREND LINES -- SMALL SORTING ORDER
ALTERNATE EXERCISES -- YAWN



DATA TREND LINES -- MEDIUM SORTING ORDER



DATA TREND LINES -- LARGE SORTING ORDER

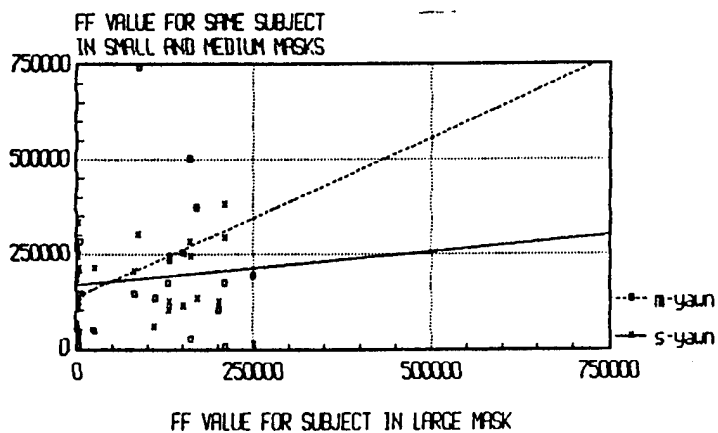
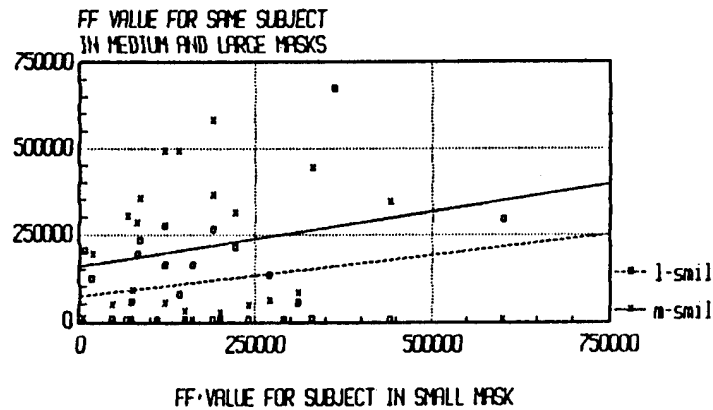
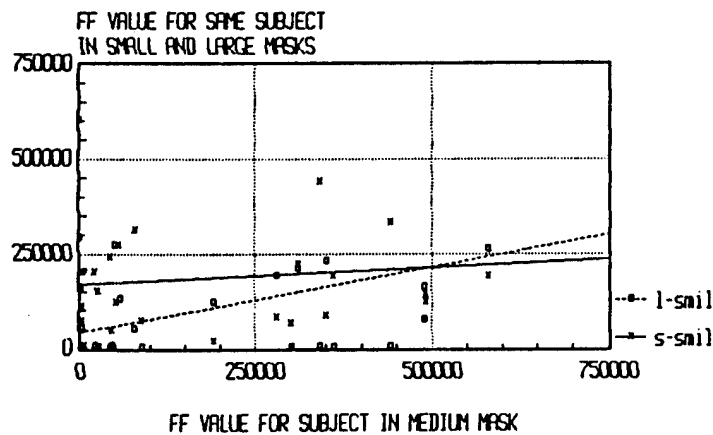


FIGURE A18

DATA TREND LINES -- SMALL SORTING ORDER
ALTERNATE EXERCISES - SMILE



DATA TREND LINES -- MEDIUM SORTING ORDER



DATA TREND LINES -- LARGE SORTING ORDER

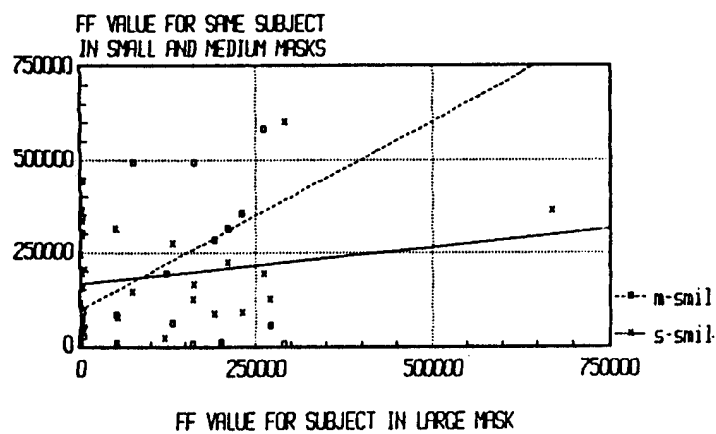


FIGURE A19

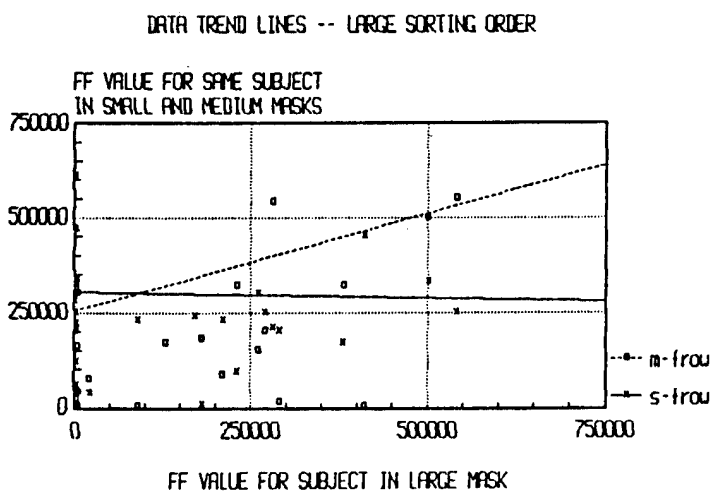
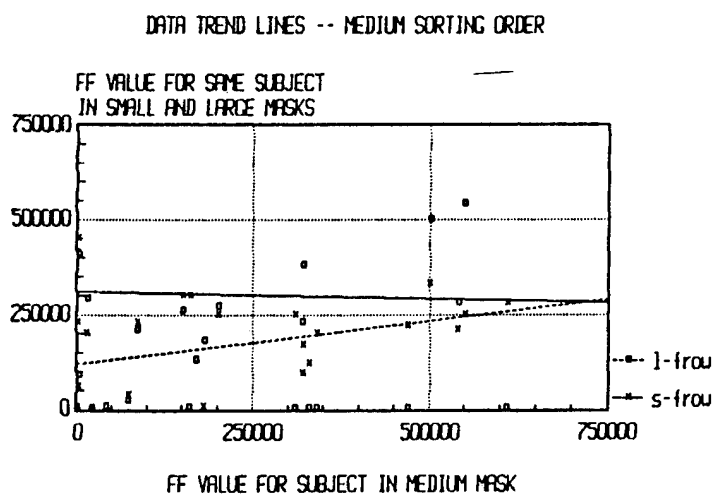
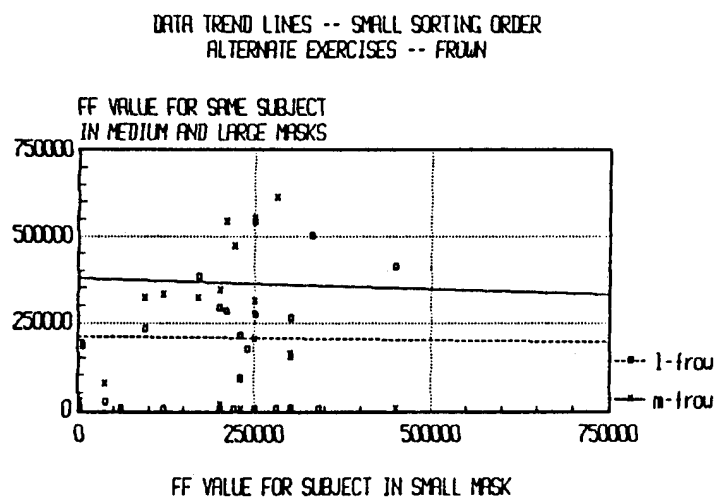


FIGURE A20

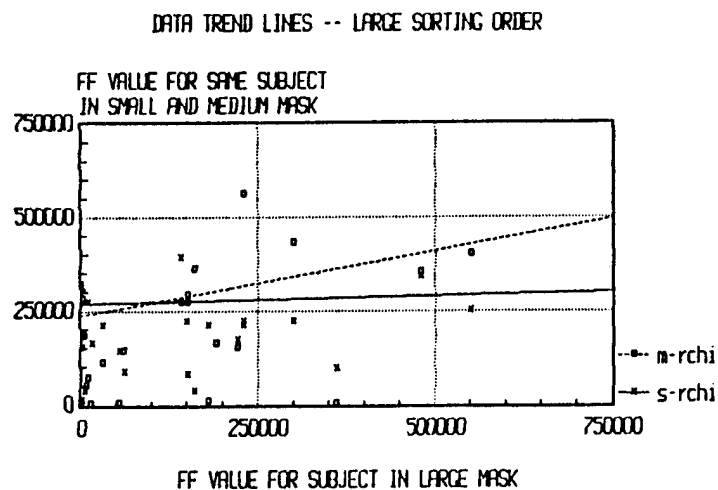
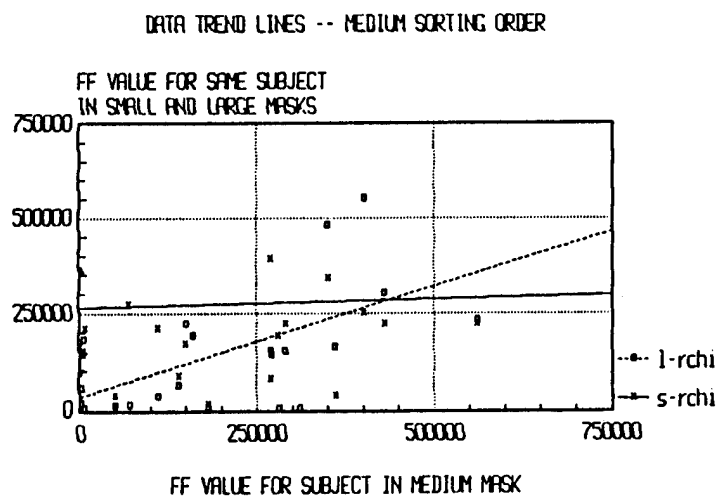
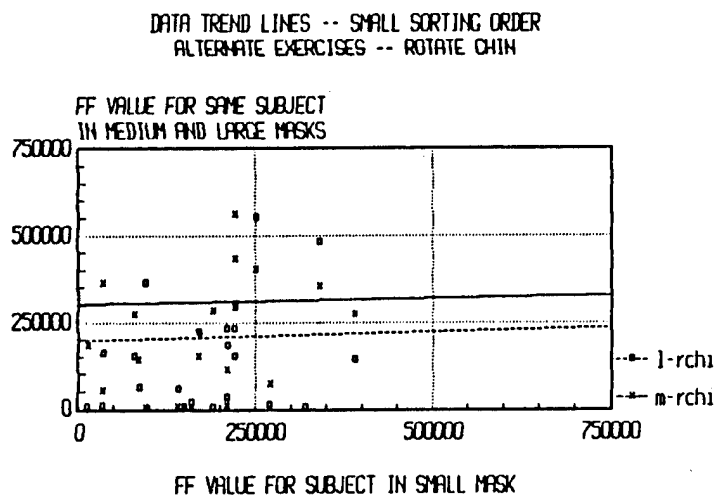


FIGURE A21

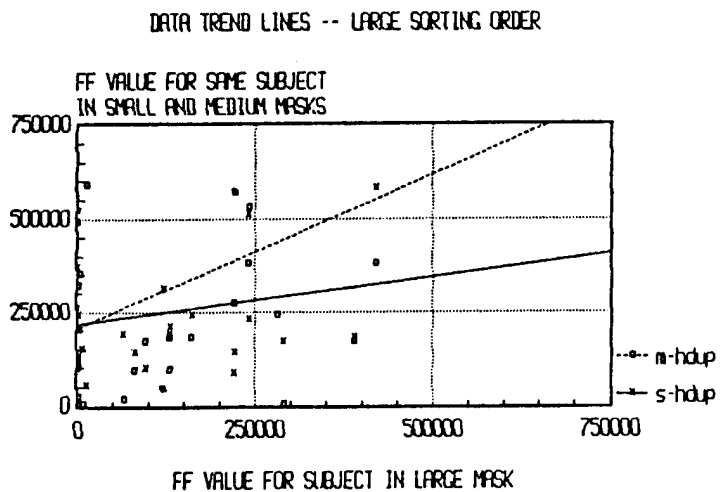
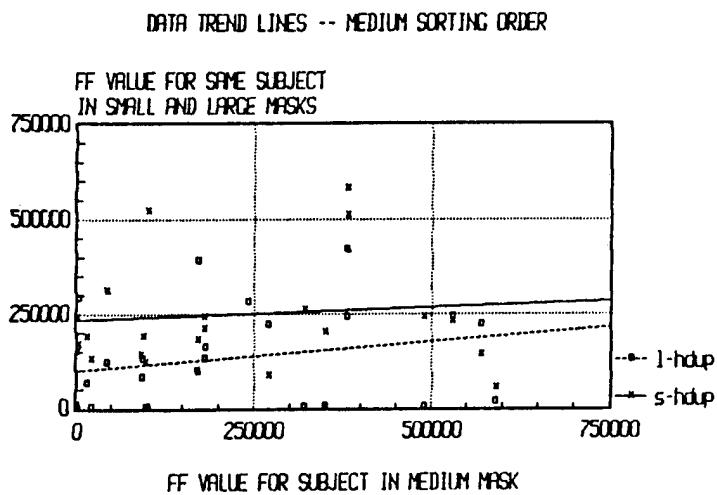
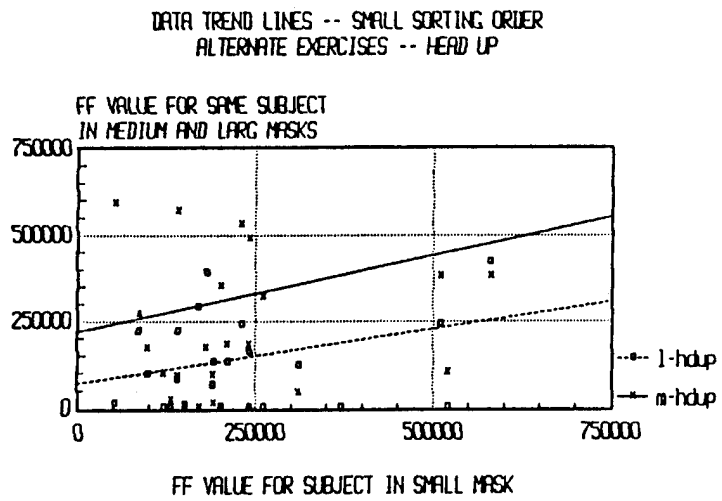


FIGURE A22

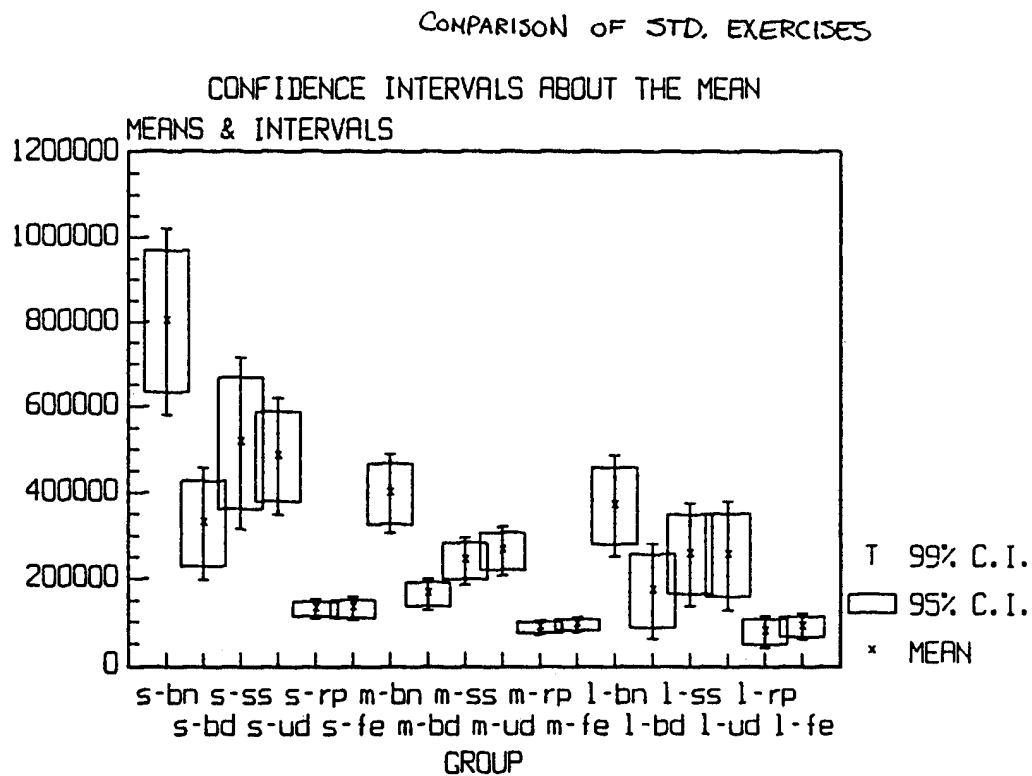


FIGURE A23

VAR NAME	MEAN	STD ERR	LOWER 95%	UPPER 95%	LOWER 99%	UPPER 99%
s-ff	190876.6	14346.57	162370	219383.2	153331.6	228421.6
m-ff	124123	8777.822	106681.4	141564.5	101151.4	147094.5
l-ff	92799.52	13777.38	65244.75	120354.3	56537.45	129061.6
s-bn	801095.1	84554.63	633085	969105.1	579815.6	1022375
s-bd	327874.1	49701.7	229116.8	426631.3	197804.7	457943.4
s-ss	515269.3	76737.09	362792.7	667745.9	314448.3	716090.3
s-ud	483888.9	52124.04	380318.4	587459.4	347480.3	620297.5
s-rp	130662.9	8235.931	114298.1	147027.7	109109.5	152216.3
s-fe	131240.7	10274.81	110824.6	151656.7	104351.5	158129.8

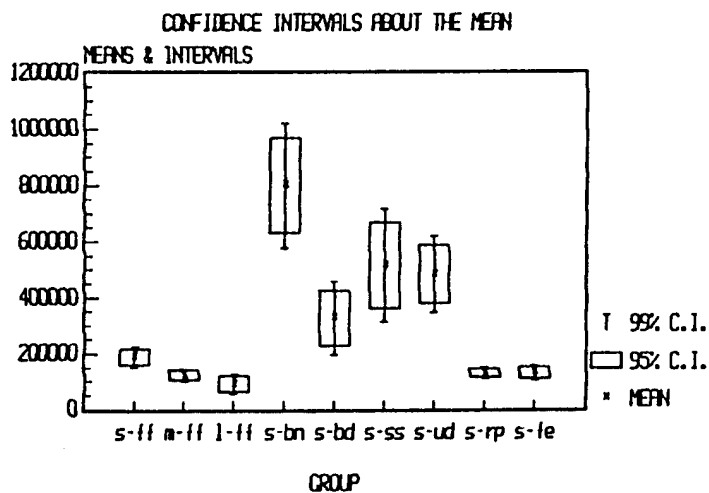


FIGURE A24

VAR NAME	MEAN	STD ERR	LOWER 95%	UPPER 95%	LOWER 99%	UPPER 99%
s-ff	190876.6	14346.57	162370	219383.2	153331.6	228421.6
m-ff	124123	8777.822	106681.4	141564.5	101151.4	147094.5
l-ff	92799.52	13777.38	65244.75	120354.3	56537.45	129061.6
m-bn	397303.8	35007.23	327744.4	466863.1	305689.8	488917.7
m-bd	164438.8	13638.79	137338.5	191539.1	128746.1	200131.5
m-ss	241469.6	20907.8	199925.8	283013.4	186753.8	296185.3
m-ud	264325.3	21574.04	221457.7	307192.9	207866.1	320784.6
m-rp	87375.38	6529.831	74400.61	100350.2	70286.61	104464
m-fe	94123.56	6542.922	81122.77	107124.4	77000.73	111246.4

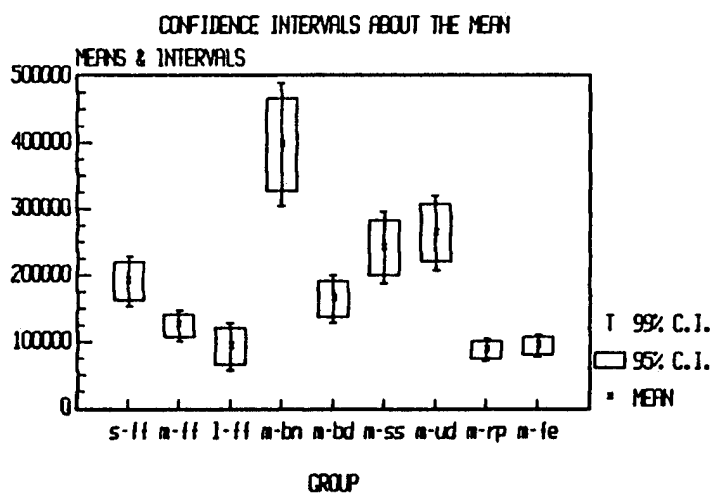


FIGURE A25

VAR NAME	MEAN	STD ERR	LOWER 95%	UPPER 95%	LOWER 99%	UPPER 99%
s-ff	190876.6	14346.57	162370	219383.2	153331.6	228421.6
m-ff	124123	8777.822	106681.4	141564.5	101151.4	147094.5
l-ff	92799.52	13777.38	65244.75	120354.3	56537.45	129061.6
l-bn	369497.5	44494.65	280508.2	458486.8	252387.6	486607.4
l-bd	171789.9	42184.57	87420.73	256159	60760.08	282819.7
l-ss	256651.9	45509.65	165632.6	347671.2	136870.5	376433.3
l-ud	254276	47746.54	158782.9	349769.1	128607.1	379944.9
l-rp	76941.35	14293.82	48353.71	105529	39320.02	114562.7
l-fe	89470.16	11740.35	65989.47	112950.8	58569.57	120370.7

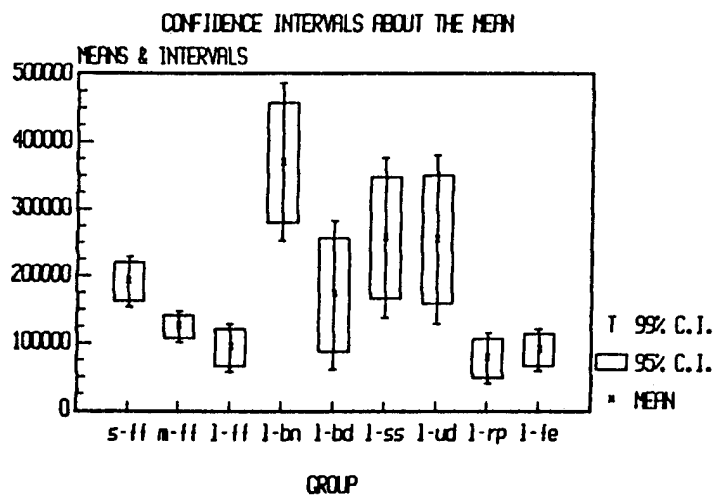


FIGURE A26

VAR NAME ----	SIZE -----	MEAN -----	SAMPLE STD DEV -----	SAMPLE VARIANCE -----	COEF. OF VARIATION -----	STD ERR -----
s-bn	103	801095	858135.7	7.363968E+11	1.0712	84554.63
s-bd	103	327874.1	504417.1	2.544366E+11	1.53845	49701.7
s-ss	102	515269.3	775006.6	6.006352E+11	1.50408	76737.09
s-ud	103	483888.9	529001.2	2.798423E+11	1.09323	52124.04
s-rp	103	130662.9	83585.56	6.986546E+09	.6397	8235.931
s-fe	103	131240.7	104277.9	1.087389E+10	.79456	10274.81
m-bn	111	397303.8	368824.1	1.360312E+11	.92832	35007.23
m-bd	111	164438.8	143693.6	2.064784E+10	.87384	13638.79
m-ss	111	241469.6	220277.4	4.852213E+10	.91224	20907.8
m-ud	111	264325.3	227296.6	5.166373E+10	.85991	21574.03
m-rp	111	87375.38	68796.04	4.732895E+09	.78736	6529.831
m-fe	111	94123.56	68933.96	4.751891E+09	.73238	6542.921
l-bn	76	369497.5	387895.3	1.504628E+11	1.04979	44494.65
l-bd	76	171789.9	367756.6	1.352449E+11	2.14073	42184.57
l-ss	75	256651.9	394125.2	1.553346E+11	1.53564	45509.65
l-ud	75	254276	413497.2	1.7098E+11	1.62617	47746.54
l-rp	76	76941.35	124610.6	1.552781E+10	1.61955	14293.82
l-fe	76	89470.16	102350	1.047551E+10	1.14396	11740.34

FIGURE A27

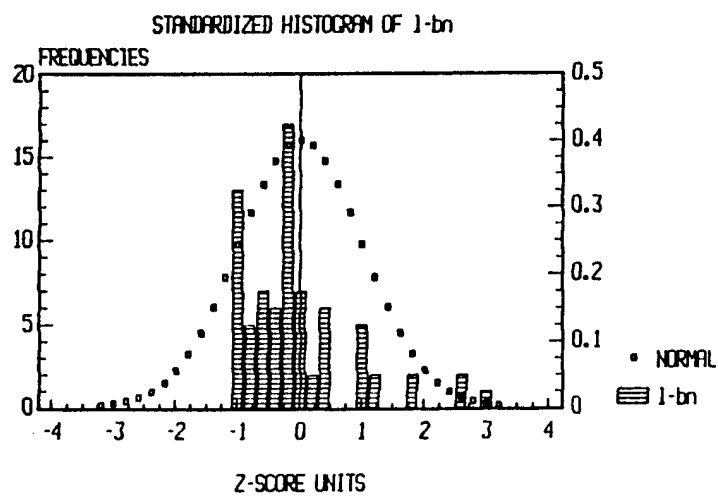
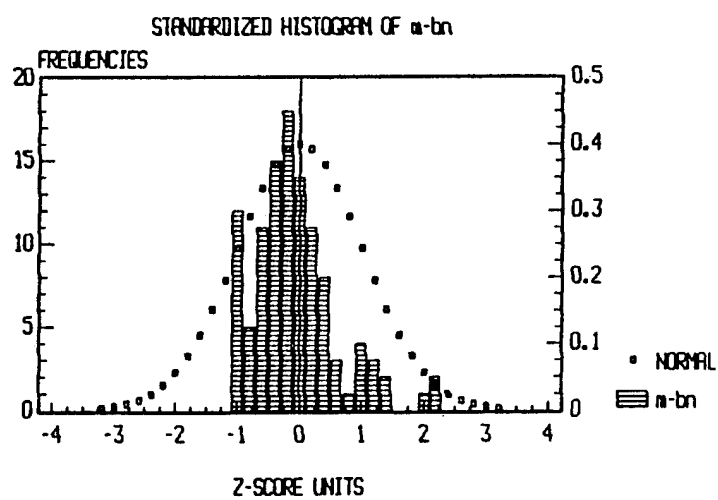
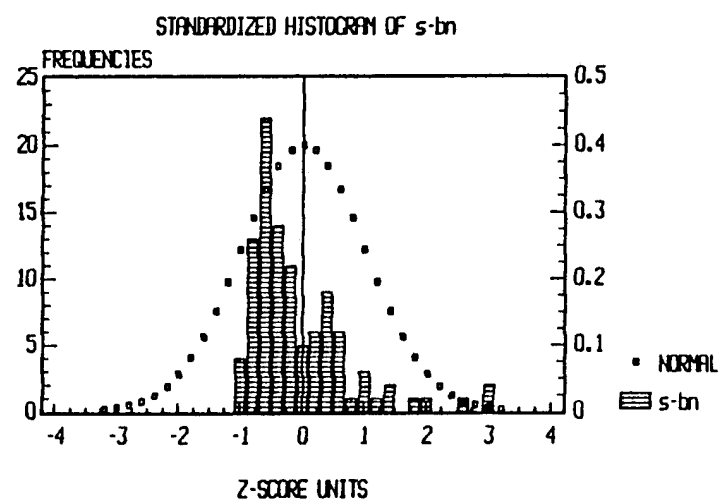


FIGURE A28

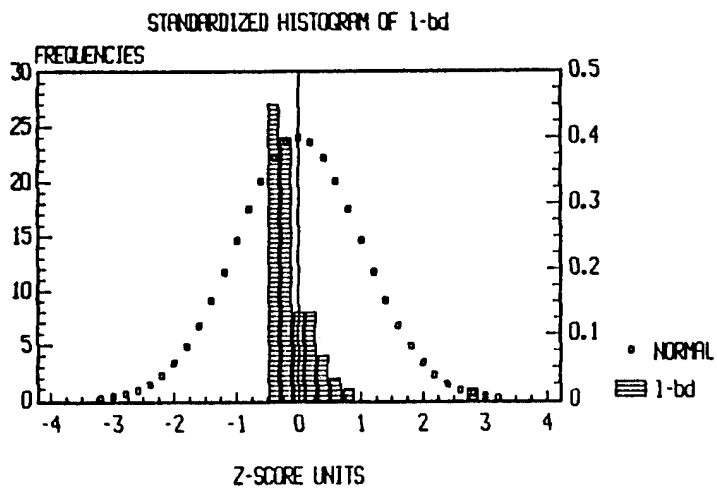
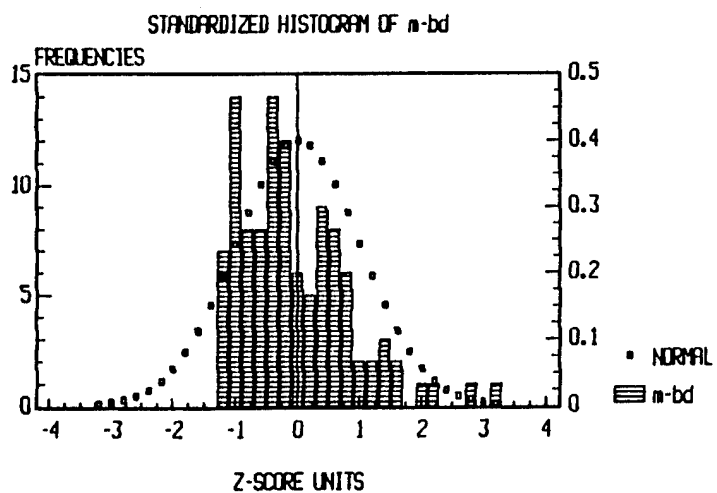
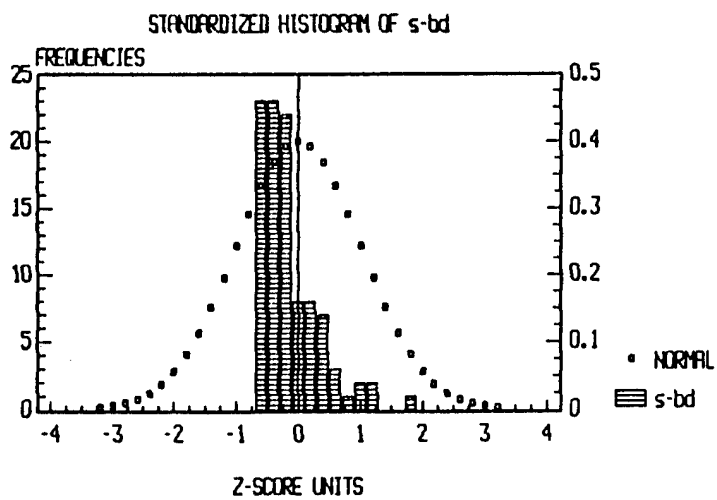


FIGURE A29

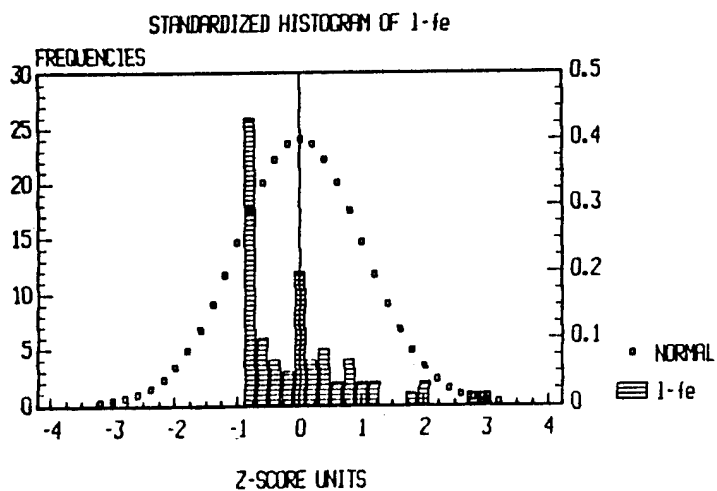
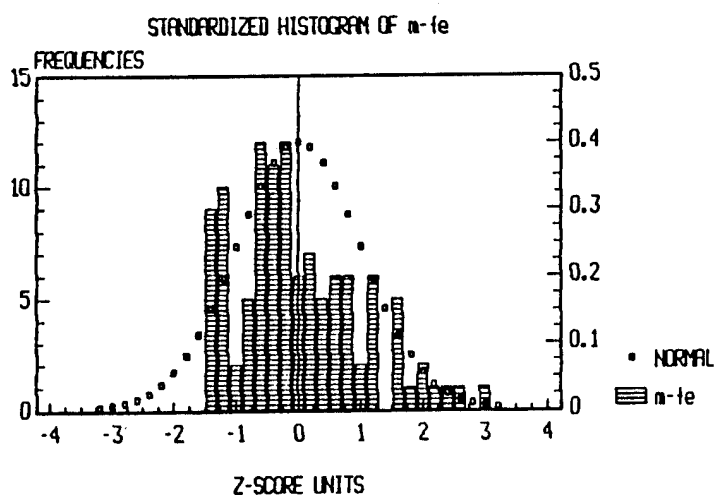
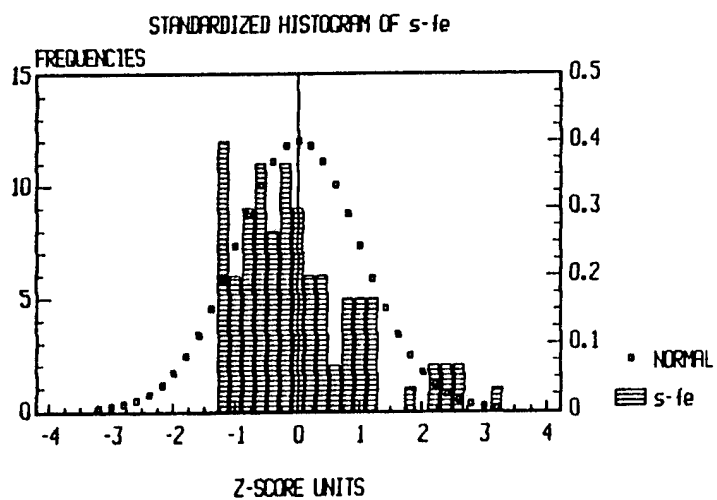


FIGURE A30

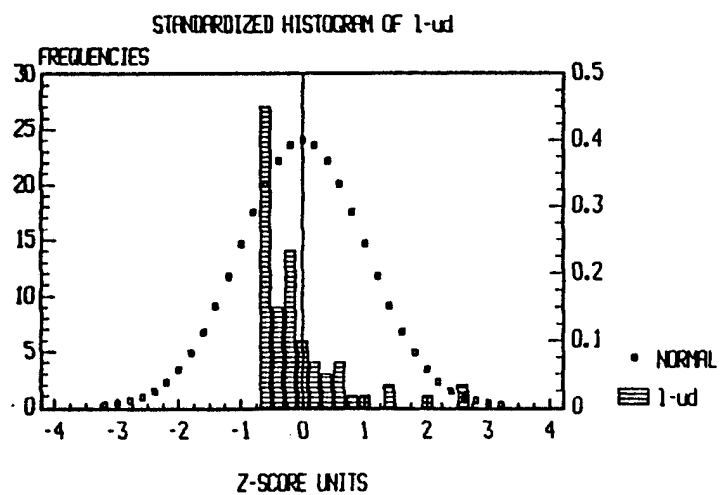
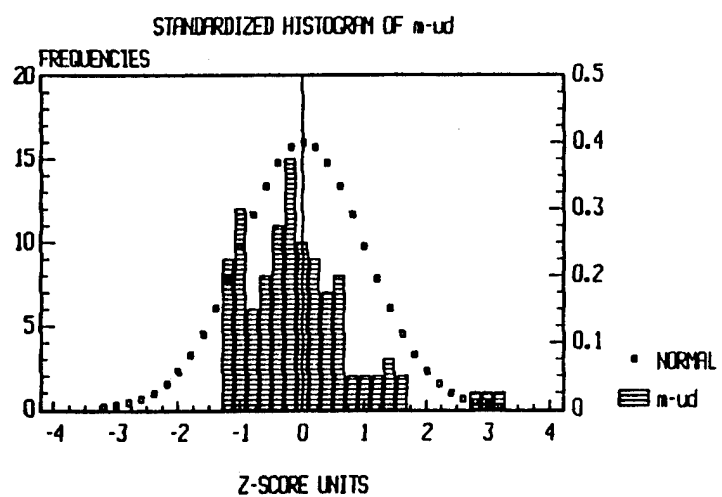
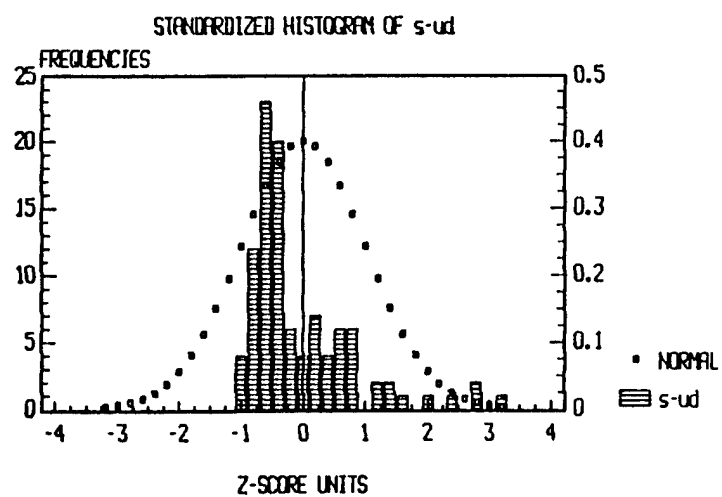


FIGURE A31

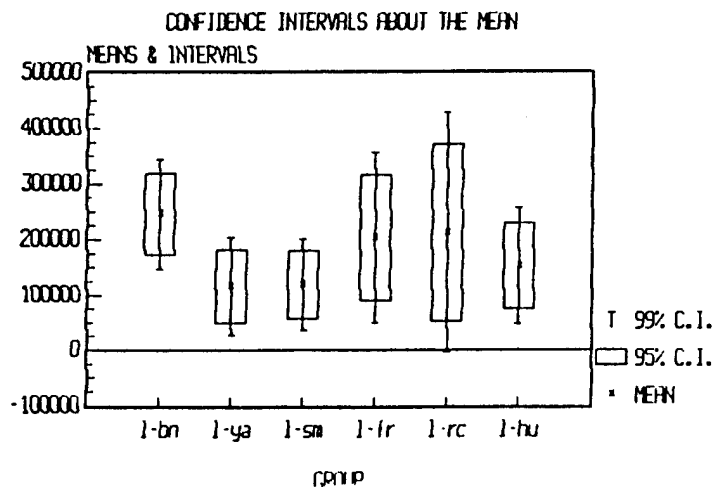
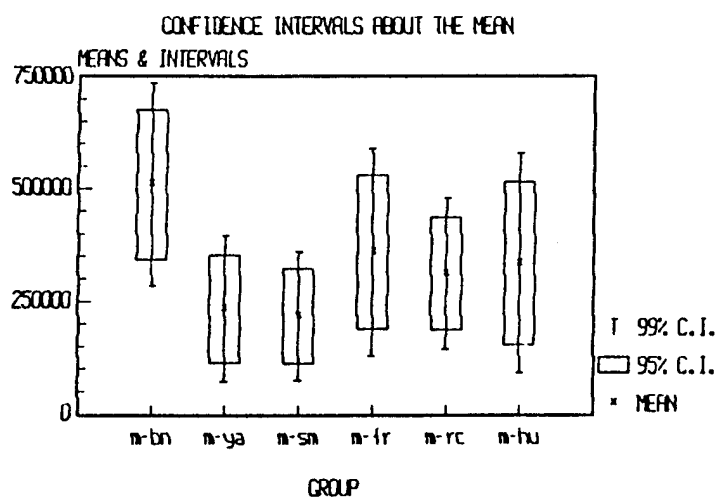
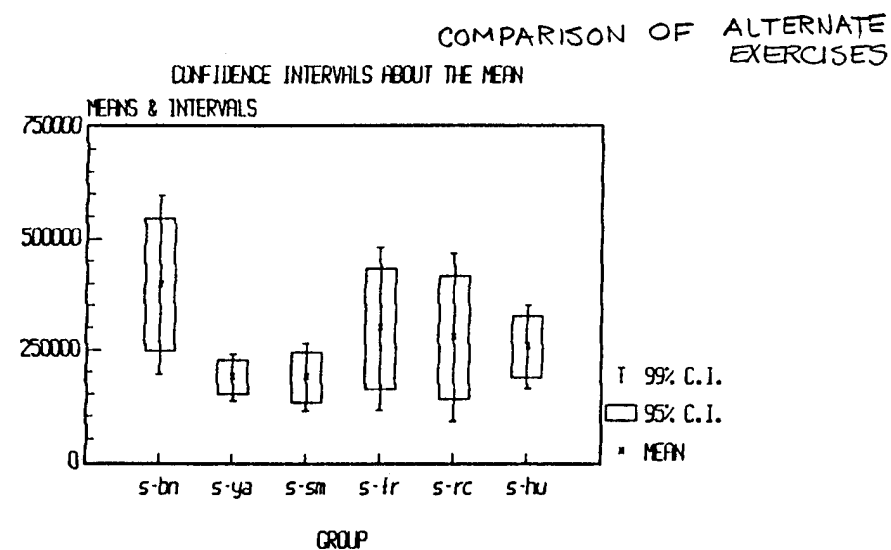


FIGURE A32

VAR NAME	MEAN	STD ERR	LOWER 95%	UPPER 95%	LOWER 99%	UPPER 99%
s-bn	395538.4	72025.41	247166.1	543910.8	194803.6	596273.2
s-ya	187757.7	18856.56	148913.2	226602.3	135204.5	240311
s-sm	187803.9	27338.47	131486.6	244121.1	111611.6	263996.2
s-fr	297160.8	66024.76	161149.8	433171.8	113149.8	481171.8
s-rc	278076.9	67541.66	138941.1	417212.8	89838.34	466315.5
s-hu	256307.7	33779.73	186721.4	325893.9	162163.6	350451.8
m-bn	509706.6	80884.1	343085.4	676327.9	284282.6	735130.6
m-ya	233766.9	58059.54	114164.3	353369.6	71954.98	395578.9
m-sm	217110.4	50944.98	112163.7	322057	75126.7	359094
m-fr	359624.7	82594.62	189479.8	529769.6	129433.5	589815.9
m-rc	310637.3	60085.95	186860.3	434414.4	143177.8	478096.8
m-hu	334047.7	87341.81	154123.5	513971.8	90626.03	577469.3
l-bn	245992.3	35493.43	172875.8	319108.8	147072.1	344912.5
l-ya	115797	31910.29	50061.77	181532.2	26862.99	204730.9
l-sm	118558.2	29721.5	57331.95	179784.5	35724.42	201392
l-fr	202822.5	54928.04	89670.75	315974.3	49738.06	355907
l-rc	212400.3	77463.64	52825.17	371975.4	-3490.89	428291.4
l-hu	152210.6	37564.36	74828.01	229593.2	47518.72	256902.4

FIGURE A33

VAR NAME	MEAN	STD ERR	LOWER 95%	UPPER 95%	LOWER 99%	UPPER 99%
s-bn	395538.4	72025.41	247166.1	543910.8	194803.6	596273.2
m-bn	509706.6	80884.1	343085.4	676327.9	284282.6	735130.6
l-bn	245992.3	35493.43	172875.8	319108.8	147072.1	344912.5

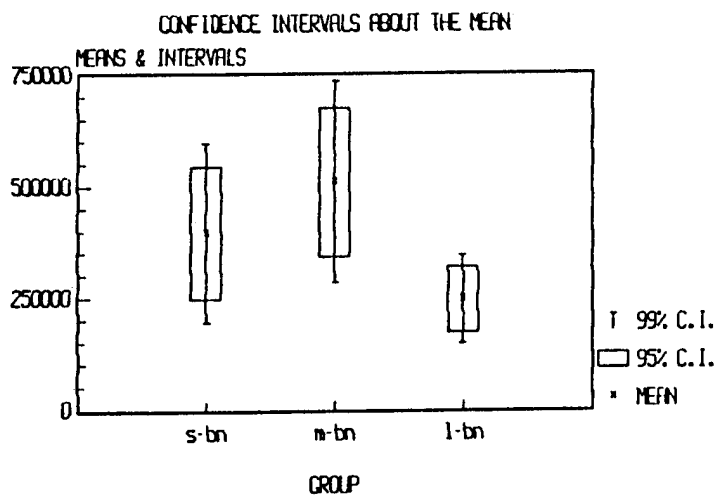


FIGURE A34

VAR NAME	MEAN	STD ERR	LOWER 95%	UPPER 95%	LOWER 99%	UPPER 99%
s-sm	187803.9	27338.47	131486.6	244121.1	111611.6	263996.2
n-sm	217110.4	50944.98	112163.7	322057	75126.7	359094
l-sm	118558.2	29721.5	57331.95	179784.5	35724.42	201392

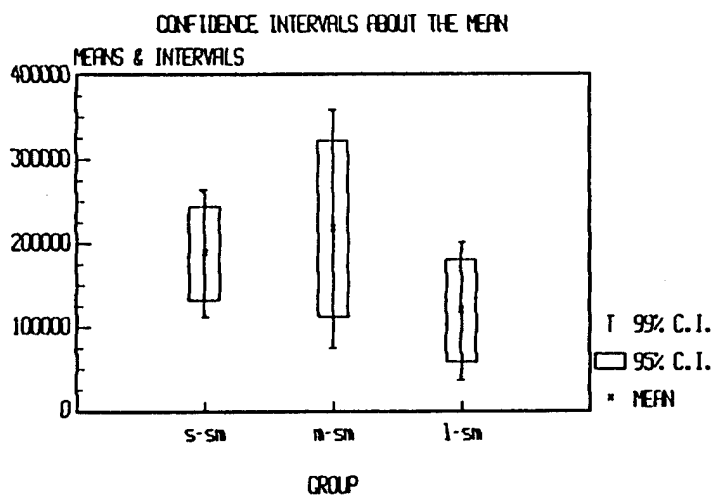


FIGURE A36

VAR NAME	MEAN	STD ERR	LOWER 95%	UPPER 95%	LOWER 99%	UPPER 99%
s-fr	297160.8	66024.76	161149.8	433171.8	113149.8	481171.8
m-fr	359624.7	82594.62	189479.8	529769.6	129433.5	589815.9
l-fr	202822.5	54928.04	89670.75	315974.3	49738.06	355907

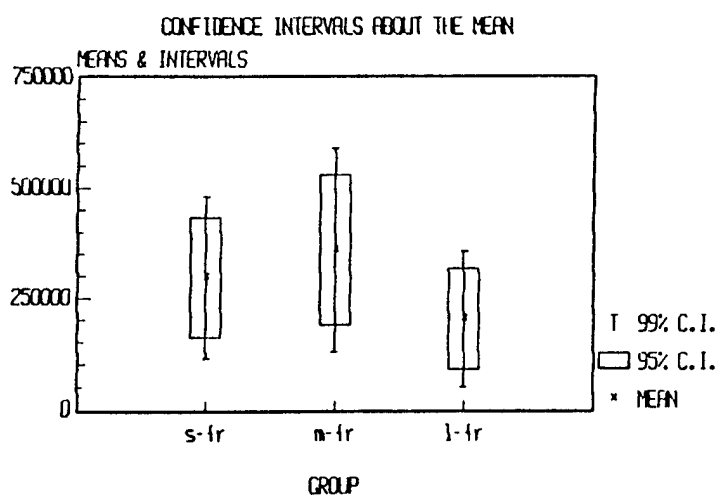


FIGURE A37

VAR NAME	MEAN	STD ERR	LOWER 95%	UPPER 95%	LOWER 99%	UPPER 99%
s-rc	278076.9	67541.66	138941.1	417212.8	89838.34	466315.5
m-rc	310637.3	60085.95	186860.3	434414.4	143177.8	478096.8
l-rc	212400.3	77463.64	52825.17	371975.4	-3490.89	428291.4

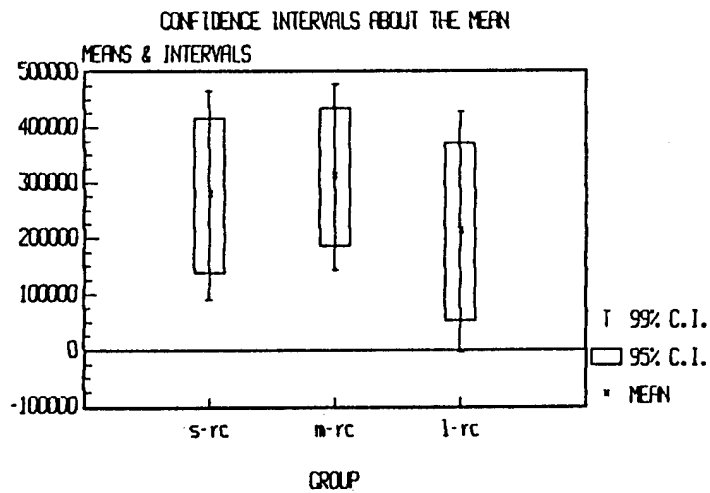


FIGURE A38

VAR NAME	MEAN	STD ERR	LOWER 95%	UPPER 95%	LOWER 99%	UPPER 99%
s-hu	256307.7	33779.73	186721.4	325893.9	162163.6	350451.8
m-hu	334047.7	87341.81	154123.5	513971.8	90626.03	577469.3
l-hu	152210.6	37564.36	74828.01	229593.2	47518.72	256902.4

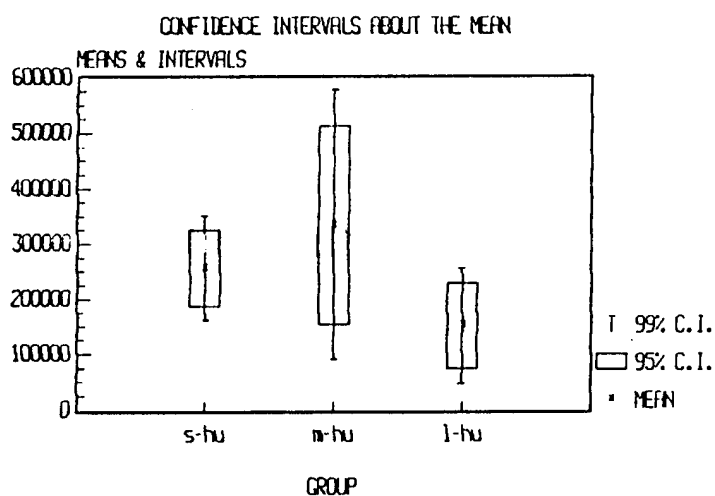


FIGURE A39

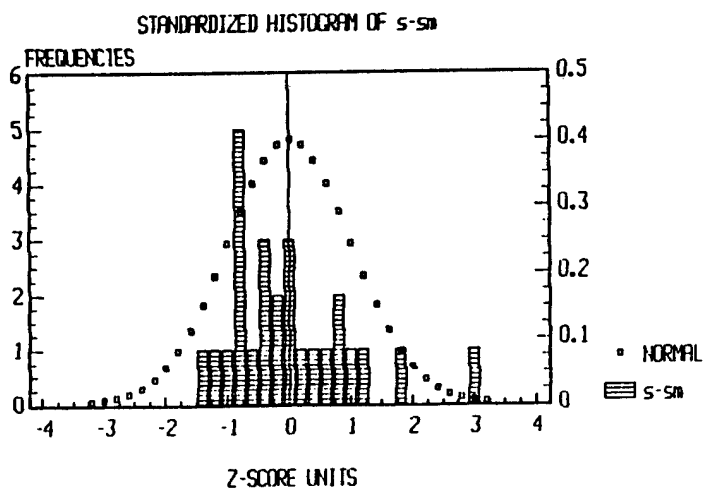
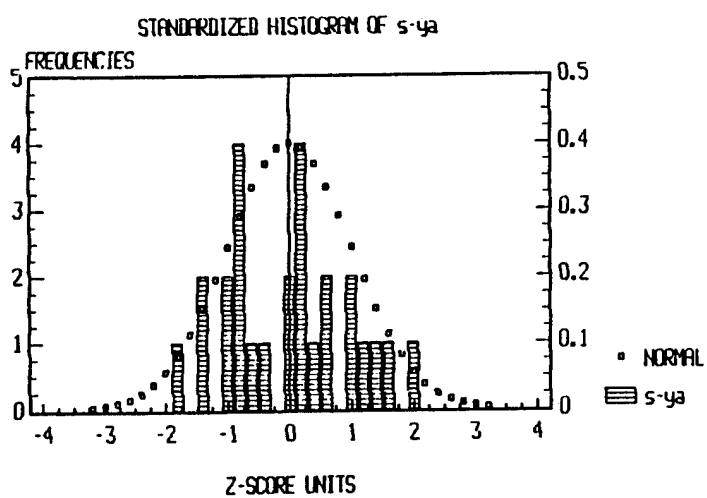
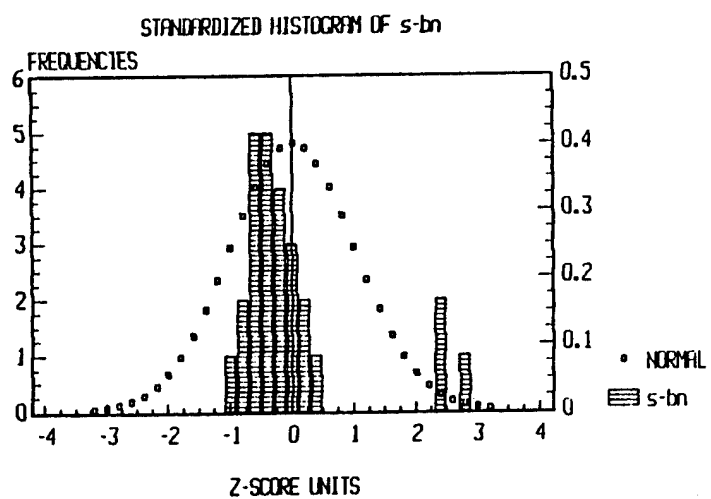


FIGURE A40

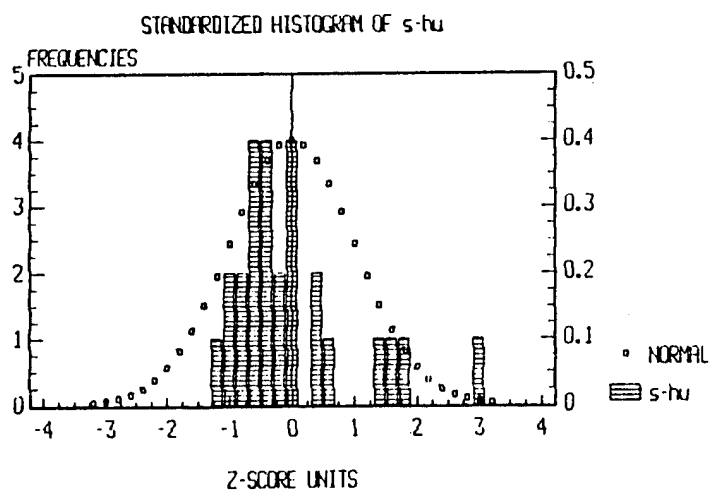
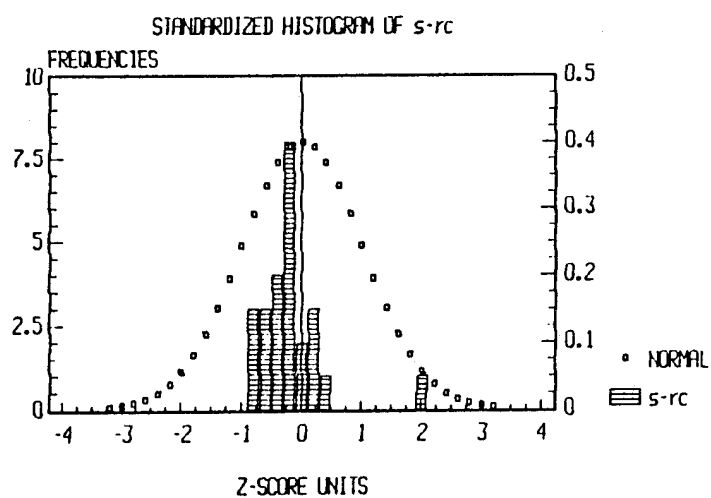
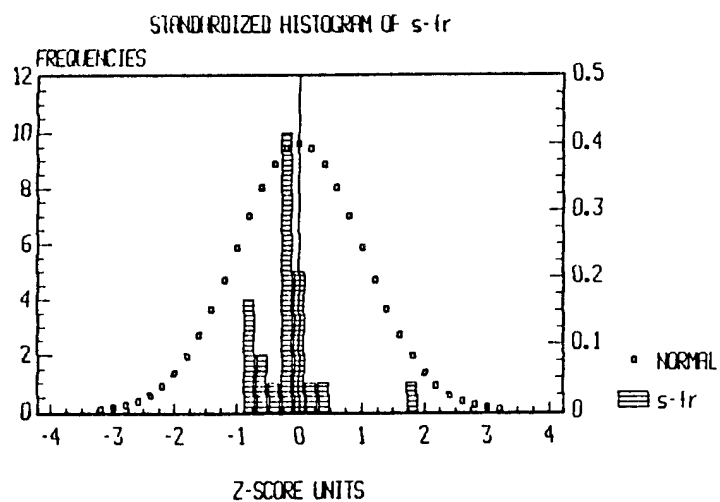


FIGURE A41

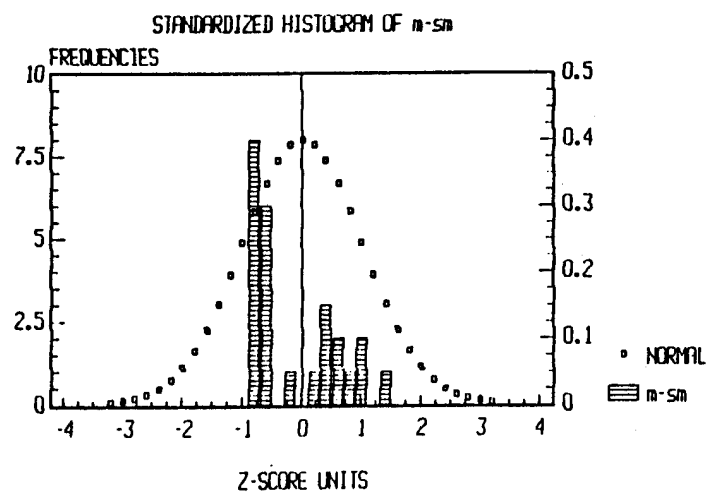
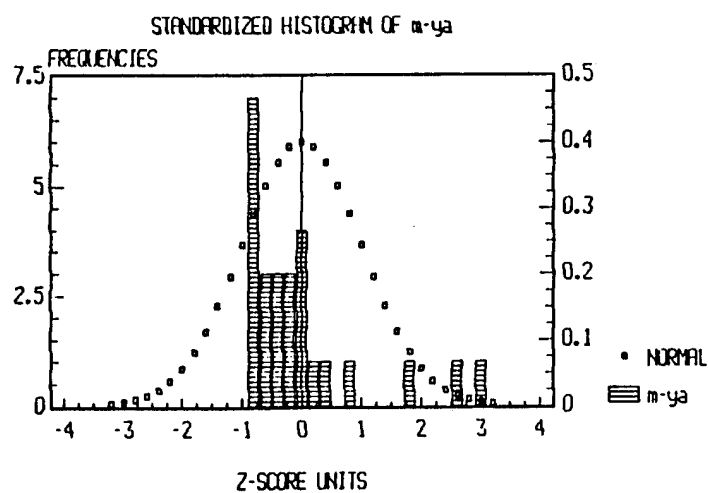
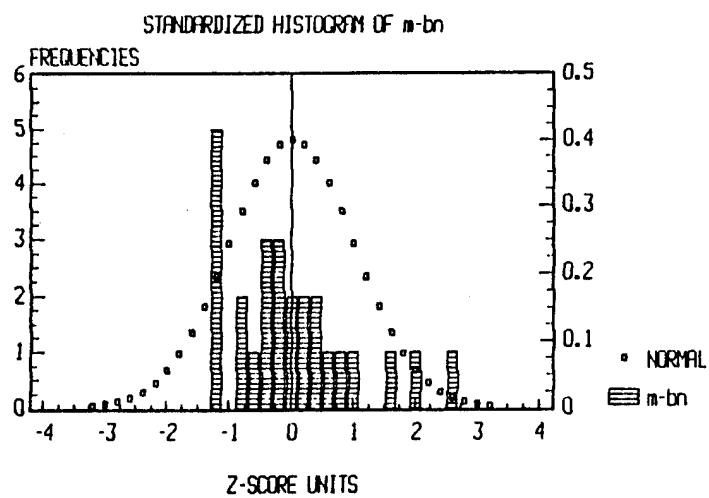


FIGURE A42

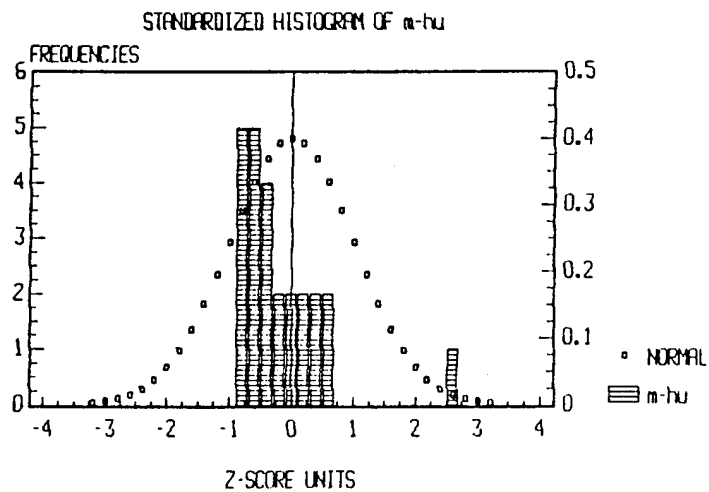
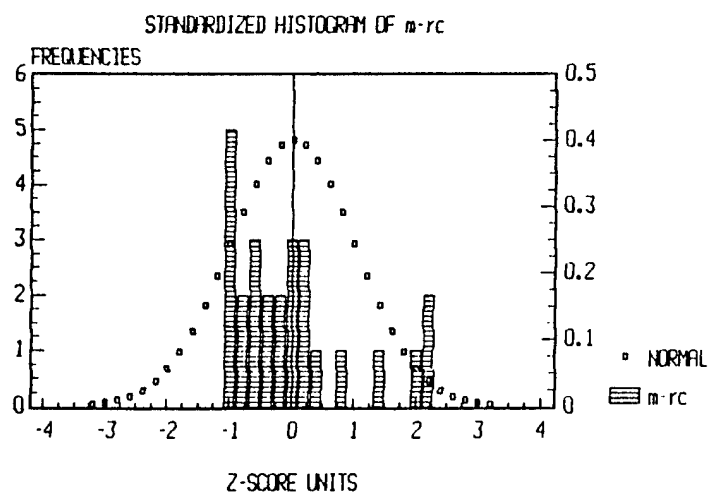
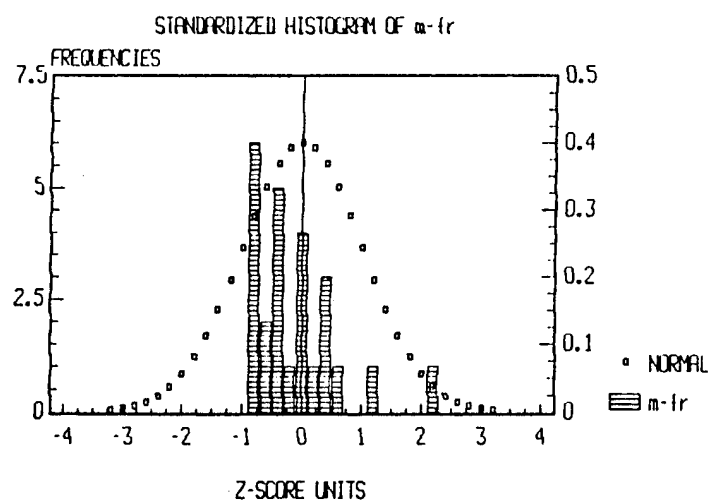


FIGURE A43

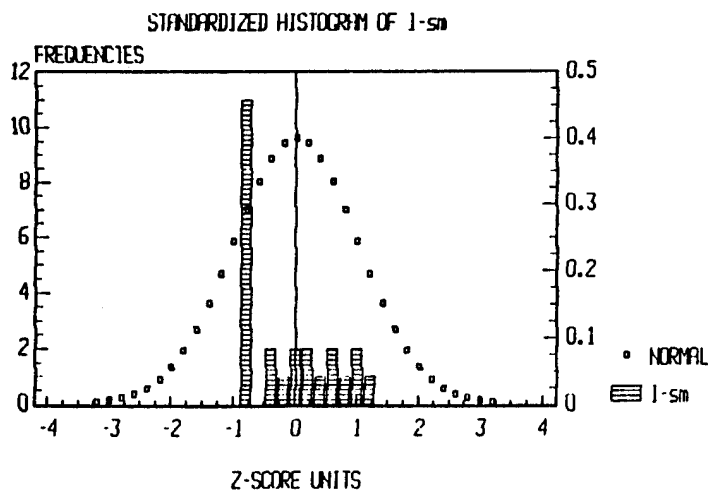
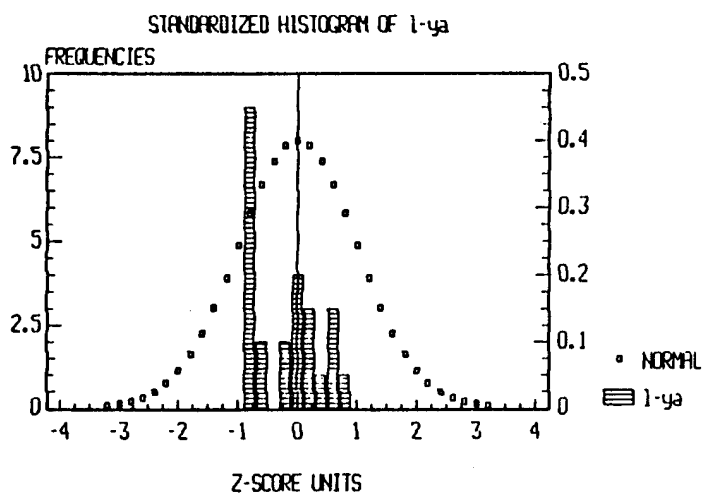
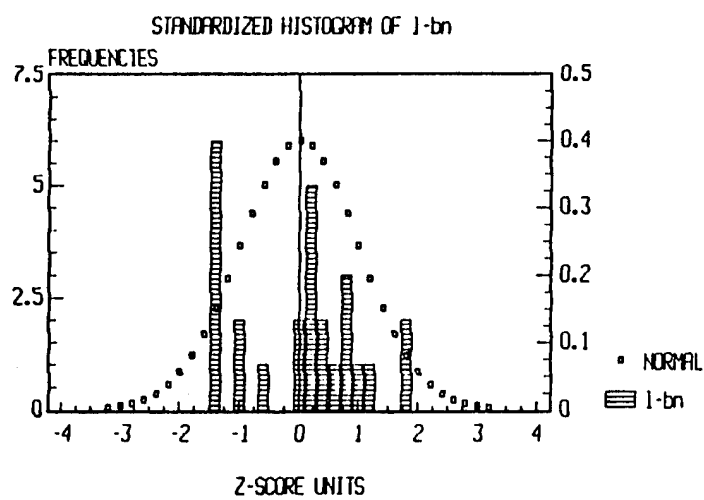


FIGURE A44

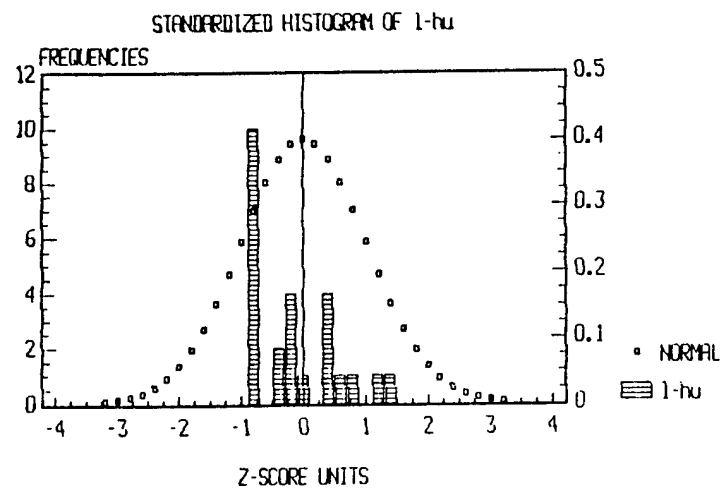
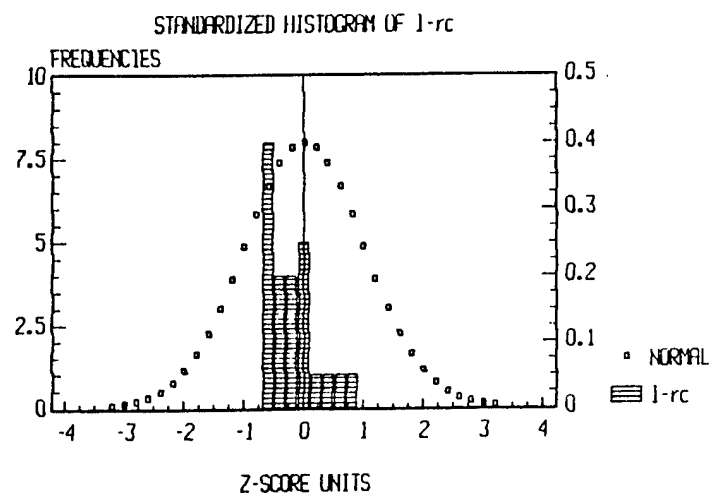
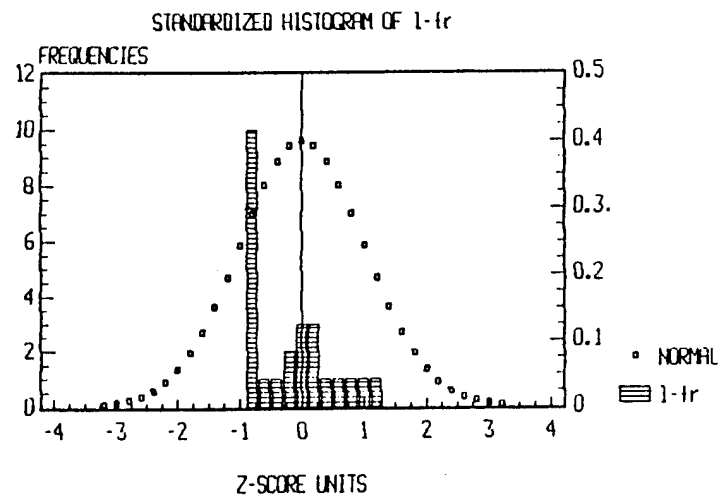


FIGURE A45

VAR NAME	MEAN	STD ERR	LOWER 95%	UPPER 95%	LOWER 99%	UPPER 99%
s-ff	190876.6	14346.57	162370	219383.2	153331.6	228421.6
m-ff	124123	8777.822	106681.4	141564.5	101151.4	147094.5
l-ff	92799.52	13777.38	65244.75	120354.3	56537.45	129061.6

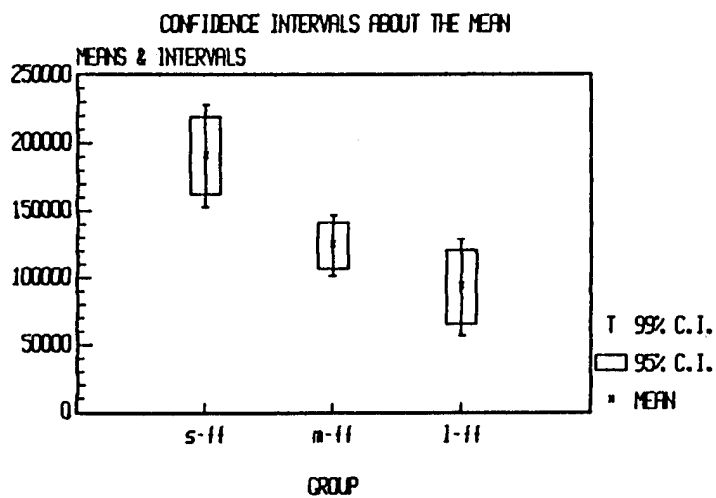
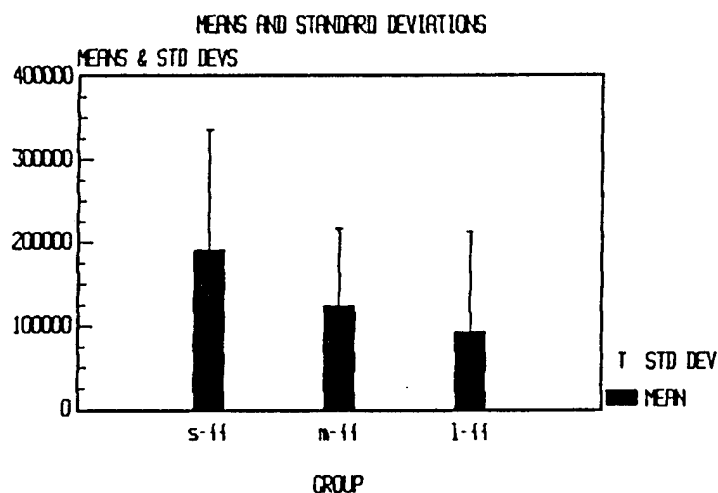


FIGURE A46

VAR NAME	SIZE	MEAN	SAMPLE STD DEV	SAMPLE VARIANCE	COEF. OF VARIATION
----	----	----	-----	-----	-----
s-ff	103	190876.6	145601.8	2.119987E+10	.76281
m-ff	111	124123	92480.09	8.552568E+09	.74507
l-ff	76	92799.52	120108.4	1.442604E+10	1.29428



NAME	SIZE	MEAN	STD ERR	T-TEST MEAN=0	2-TAILED PROB.
----	----	----	-----	-----	-----
s-ff	103	190876.6	14346.57	13.30469	<.001
m-ff	111	124123	8777.822	14.14052	<.001
l-ff	76	92799.52	13777.38	6.73564	<.001

FIGURE A47

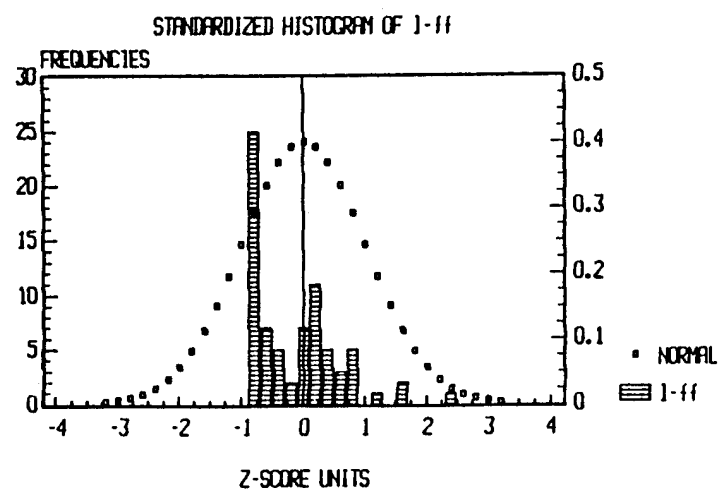
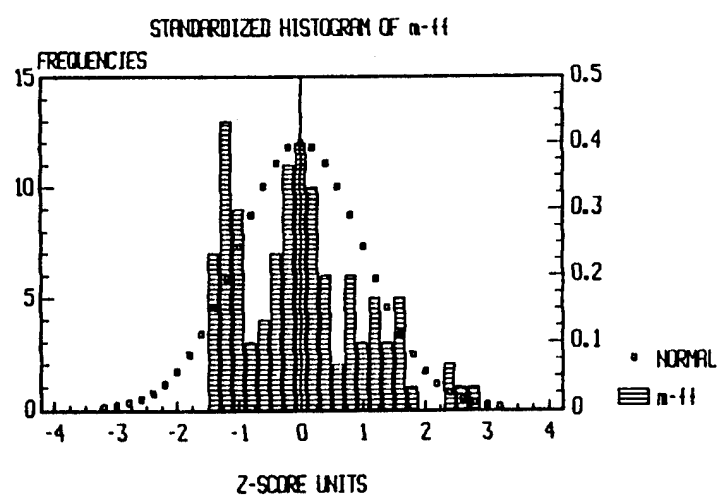
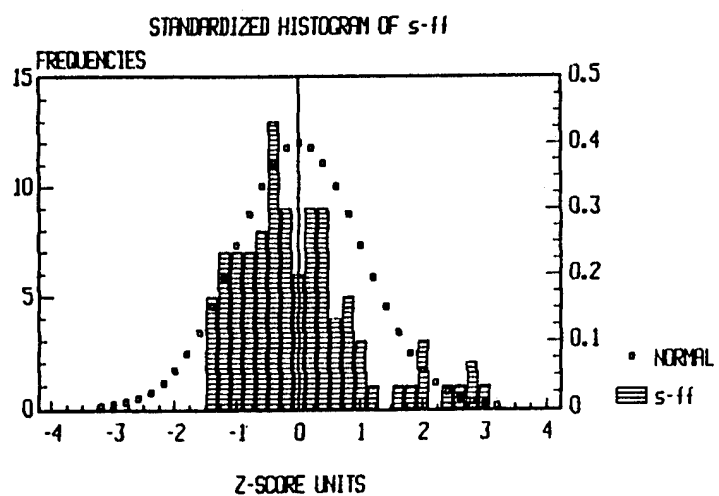


FIGURE A48

DESCRIPTIVE ESTIMATES FOR... s-ff

SAMPLE SIZE	103
NUMBER MISSING	9
MEAN	190876.6
HARMONIC MEAN	8870.681
MEDIAN	160000
VARIANCE	2.119987E+10
STANDARD DEVIATION	145601.8
MEAN ABS. DEVIATION	111889.4
STANDARD ERROR	14346.57
SKEWNESS	1.06471
KURTOSIS	.96184
MINIMUM	260
MAXIMUM	620000
RANGE	619740
SUM	1.966029E+07
SUM OF SQUARES	5.915077E+12

DESCRIPTIVE ESTIMATES FOR... m-ff

SAMPLE SIZE	111
NUMBER MISSING	1
MEAN	124123
HARMONIC MEAN	6804.309
MEDIAN	120000
VARIANCE	8.552568E+09
STANDARD DEVIATION	92480.09
MEAN ABS. DEVIATION	73614.52
STANDARD ERROR	8777.822
SKEWNESS	.61138
KURTOSIS	-.11513
MINIMUM	180
MAXIMUM	390000
RANGE	389820
SUM	1.377765E+07
SUM OF SQUARES	2.650906E+12

DESCRIPTIVE ESTIMATES FOR... l-ff

SAMPLE SIZE	76
NUMBER MISSING	36
MEAN	92799.52
HARMONIC MEAN	1479.672
MEDIAN	63000
VARIANCE	1.442604E+10
STANDARD DEVIATION	120108.4
MEAN ABS. DEVIATION	81342.54
STANDARD ERROR	13777.38
SKEWNESS	2.60039
KURTOSIS	9.11626
MINIMUM	84
MAXIMUM	670000
RANGE	669916
SUM	7052763
SUM OF SQUARES	1.736446E+12

FIGURE A49

VAR NAME	SIZE	MEAN	SAMPLE STD DEV	SAMPLE VARIANCE	COEF. OF VARIATION
s-m	102	68772.73	153012.7	2.34129E+10	2.2249
m-l	76	44553.9	128645.3	1.65496E+10	2.88741
s-l	68	82384.95	137441.3	1.88901E+10	1.66828

ANOVA SUMMARY TABLE

SOURCE	SUM SQRES	DF	MEAN SQRES	F-RATIO	PROB
BETWEEN GRPS	5.377454E+10	2	2.688727E+10	1.3412	.2635
WITHIN GRPS	4.871556E+12	243	2.004756E+10		
TOTAL	4.925331E+12	245			

$f_{CRIT} \approx 3.6$
THEREFORE DO NOT REJECT $\frac{\mu_{S-M}}{\mu_{M-L}} = \frac{\mu_{S-L}}{\mu_{M-L}}$

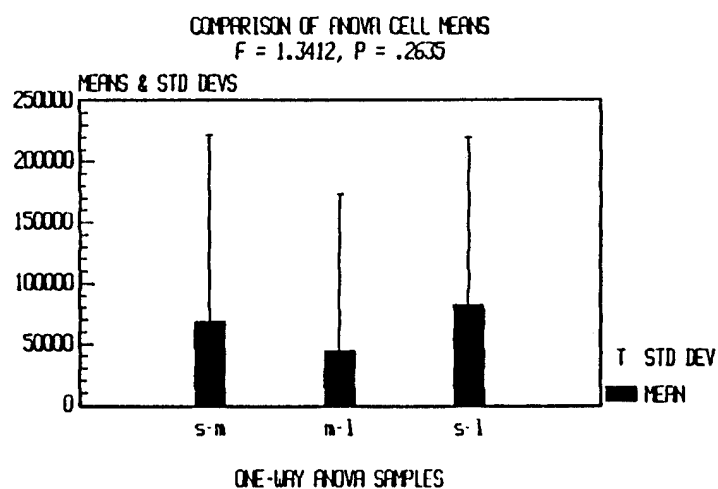


FIGURE A50

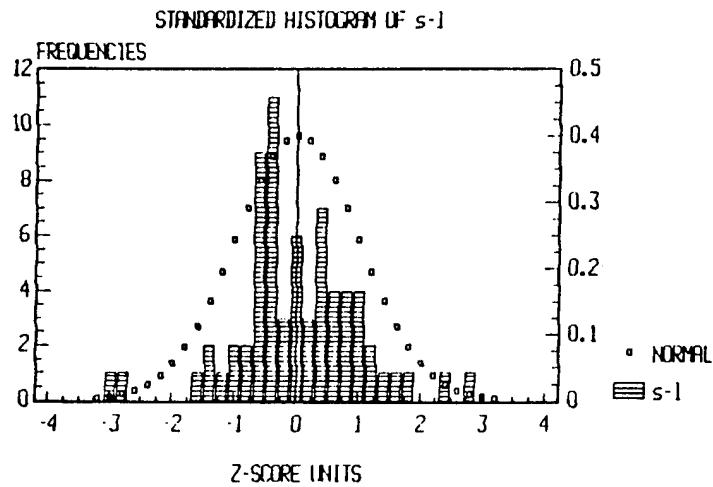
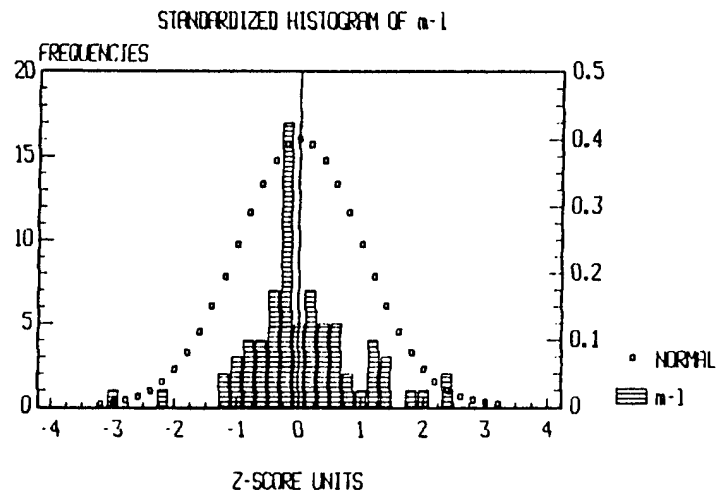
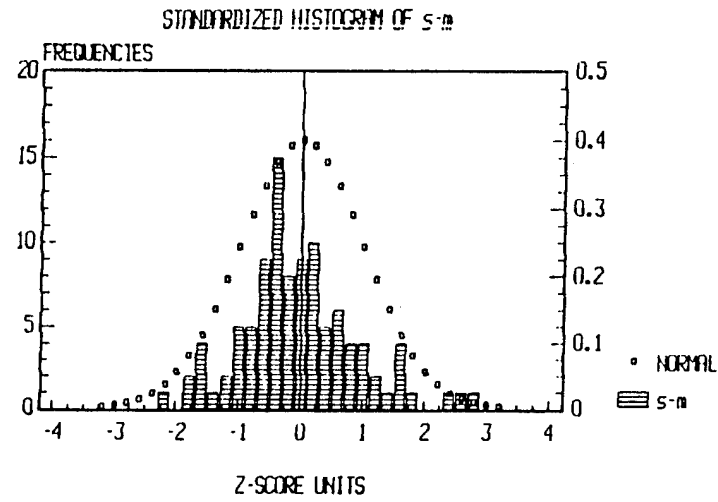


FIGURE A51

VAR NAME	MEAN	STD ERR	LOWER 95%	UPPER 95%	LOWER 99%	UPPER 99%
s-m	68772.73	15150.52	38668.66	98876.81	29123.82	108421.6
m-l	44553.9	14756.62	15040.65	74067.14	5714.465	83393.33
s-l	82384.95	16667.2	49050.56	115719.4	38516.89	126253

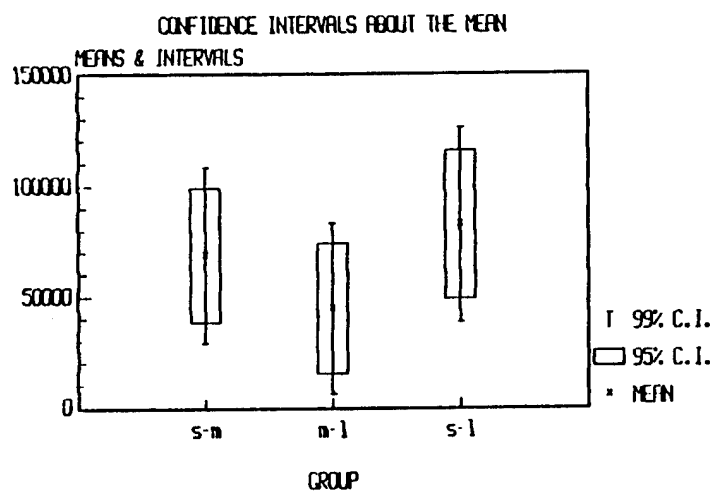


FIGURE A52

DESCRIPTIVE ESTIMATES FOR... m-0

SAMPLE SIZE	102
NUMBER MISSING	10
MEAN	-68772.73
HARMONIC MEAN	-31924.22
MEDIAN	-45000
VARIANCE	2.34129E+10
STANDARD DEVIATION	153012.7
MEAN ABS. DEVIATION	114447.3
STANDARD ERROR	15150.52
SKEWNESS	-.7401
KURTOSIS	1.34588
MINIMUM	-587000
MAXIMUM	269580
RANGE	856580
SUM	-7014819
SUM OF SQUARES	2.847131E+12

DESCRIPTIVE ESTIMATES FOR... m-1

SAMPLE SIZE	76
NUMBER MISSING	36
MEAN	44553.9
HARMONIC MEAN	22433.98
MEDIAN	30000
VARIANCE	1.65496E+10
STANDARD DEVIATION	128645.3
MEAN ABS. DEVIATION	88152.94
STANDARD ERROR	14756.82
SKEWNESS	-.71009
KURTOSIS	3.76726
MINIMUM	-470000
MAXIMUM	384000
RANGE	854000
SUM	3386096
SUM OF SQUARES	1.392084E+12

DESCRIPTIVE ESTIMATES FOR... s-1

SAMPLE SIZE	68
NUMBER MISSING	44
MEAN	82384.95
HARMONIC MEAN	19866.98
MEDIAN	70900
VARIANCE	1.88901E+10
STANDARD DEVIATION	137441.3
MEAN ABS. DEVIATION	103450.8
STANDARD ERROR	16667.2
SKEWNESS	-.01985
KURTOSIS	1.61706
MINIMUM	-320000
MAXIMUM	479810
RANGE	799810
SUM	5602177
SUM OF SQUARES	1.727171E+12

FIGURE A53

VAR NAME ----	SIZE ----	MEAN ----	SAMPLE STD DEV -----	SAMPLE VARIANCE -----	COEF. OF VARIATION -----	
bf-s	65	231219.9	156264.7	2.441865E+10	.67583	
bf-m	38	178767.9	96492.91	9.310881E+09	.53977	
bf-l	9	283333.3	208866	4.3625E+10	.73717	

NAME ----	SIZE ----	MEAN ----	STD ERR -----	T-TEST MEAN=0 -----	2-TAILED PROB. -----	
bf-s	65	231219.9	19382.25	11.92947	<.001	
bf-m	38	178767.9	15653.22	11.42052	<.001	
bf-l	9	283333.3	69621.99	4.0696	.004	

VAR NAME ----	MEAN ----	STD ERR ----	LOWER 95% -----	UPPER 95% -----	LOWER 99% -----	UPPER 99% -----
bf-s	231219.9	19382.25	192455.4	269984.3	180205.8	282233.9
bf-m	178767.9	15653.22	146991.9	210543.9	136128.5	221407.3
bf-l	283333.3	69621.99	122785	443881.7	49751.56	516915.1

FIGURE A54

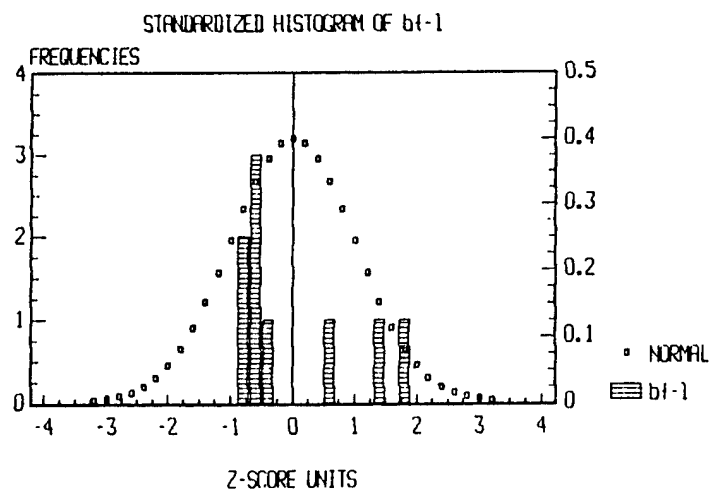
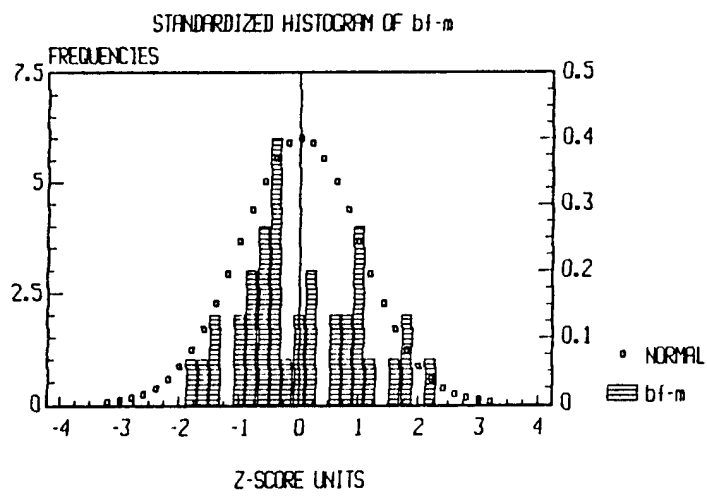
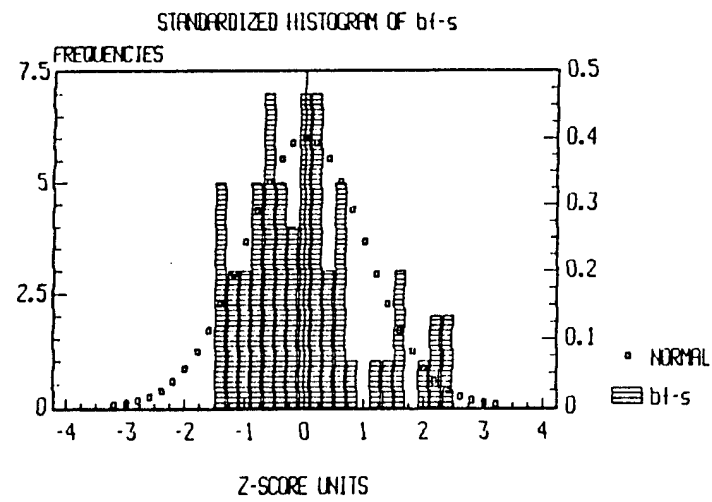


FIGURE A55

DESCRIPTIVE ESTIMATES FOR... bf-a

SAMPLE SIZE	65
NUMBER MISSING	47
MEAN	231219.9
HARMONIC MEAN	27038.82
MEDIAN	220000
VARIANCE	2.441865E+10
STANDARD DEVIATION	156284.7
MEAN ABS. DEVIATION	119294.3
STANDARD ERROR	19382.25
SKEWNESS	.80589
KURTOSIS	.20382
MINIMUM	990
MAXIMUM	620000
RANGE	619010
SUM	1.502929E+07
SUM OF SQUARES	5.037864E+12

DESCRIPTIVE ESTIMATES FOR... bf-b

SAMPLE SIZE	38
NUMBER MISSING	74
MEAN	178787.9
HARMONIC MEAN	6507.432
MEDIAN	145000
VARIANCE	9.310881E+09
STANDARD DEVIATION	96492.91
MEAN ABS. DEVIATION	78997.15
STANDARD ERROR	15653.22
SKEWNESS	.40324
KURTOSIS	-.47471
MINIMUM	180
MAXIMUM	390000
RANGE	389820
SUM	6793181
SUM OF SQUARES	1.558905E+12

DESCRIPTIVE ESTIMATES FOR... bf-1

SAMPLE SIZE	9
NUMBER MISSING	103
MEAN	283333.3
HARMONIC MEAN	193807.3
MEDIAN	170000
VARIANCE	4.3625E+10
STANDARD DEVIATION	208868
MEAN ABS. DEVIATION	173333.3
STANDARD ERROR	69621.99
SKEWNESS	1.19139
KURTOSIS	-.14386
MINIMUM	110000
MAXIMUM	670000
RANGE	560000
SUM	2550000
SUM OF SQUARES	1.0715E+12

FIGURE A56

OCCURRENCE OF LATERAL SKIN DISPLACEMENT RELATIVE TO MASKPOINTS FOR ALTERNATE EXERCISES PRESENTED BY SUBJECT NUMBER FOR SELECTED S, M, L AND MISFIT SAMPLE POPULATIONS

NOTES	LOW FF EXERCISE YAWN				LOW FF EXERCISE SMILE				FROWN				CHIN LT				CHIN RT				LOW FF EXERCISE HEAD UP				POINT	COUNT POINT
	S	M	L	MF	S	M	L	MF	S	M	L	MF	S	M	L	MF	S	M	L	MF	S	M	L	MF		
1		12	02	19										2	2		6				22	23			1	
2				42													4				2				2	20
3				2																9	2				2	19
4 no data for 5 - in hair		1	56	11						2	2						15			19					3	19
		0	02	34						2	2						06			42					4	18
			9	9													03			49					4	18
5		2	56	1						22	23						125			02					5	17
		2	02	4						2	2						021			34					3	
6		15		49						2	2						6			1					6	16
		01		02						2	2						00			3					0	
7	6	126	56	11										6	1225		6			11					7	15
	4	030	02	34										4	0231		4			34					2	
			9	9										5	5		5			0						
8				11										2	3		6								8	14
				34										3			3									
9				1													6								9	13
				3													3								10	12
10* couldn't reset after yawn for 13 -- our of view		2		14						2	3						12								11	
		3		30													03								12	
11 no data for 14 - holes not in contact with skin seal pucker observed at chin for head up during ff test - 92		2	5	14						2	3						125									
		3	0	30													031									
			9	9																						
12* out of view after yawn for 40 - "unright fitting"		2	56	14						2	2						22								12	10
		3		30						2	2						23								13	9
13				1																					14	8
				3																					15	7
14		5	5	1													6								16	6
		3	0	3													4								17	5
15	6	225	6	14						2	3						1225								18	4
	4	231	0	30						3	3						0231								19	3
			9	9													22								20	2
			2	2													02									
16		5		11													25									
		1		34													21									
17		1225	55	1													2256									
		0231	0	4													2310									
		5																								
18		12	55	11						6	2						22								18	4
		02	0	34						3	2						23								19	3
			9	9																					20	2
		2		2																						
		2		9																						
		2		2																						

SUBJECTS NO OBSERVED: 41, 68, 70, 72, 73, 74, 88, 89, 90, 93, 94, 96, 101, 103, 105, 106, 107, 108, 109, 112, 113, 81, 91, 76, 87, 100

FIGURE A57

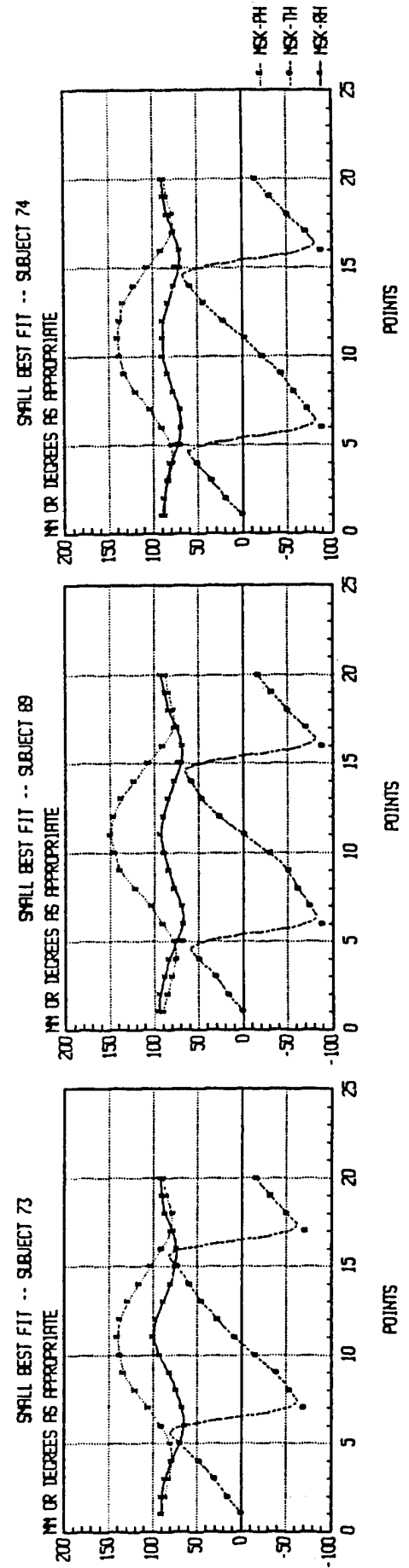
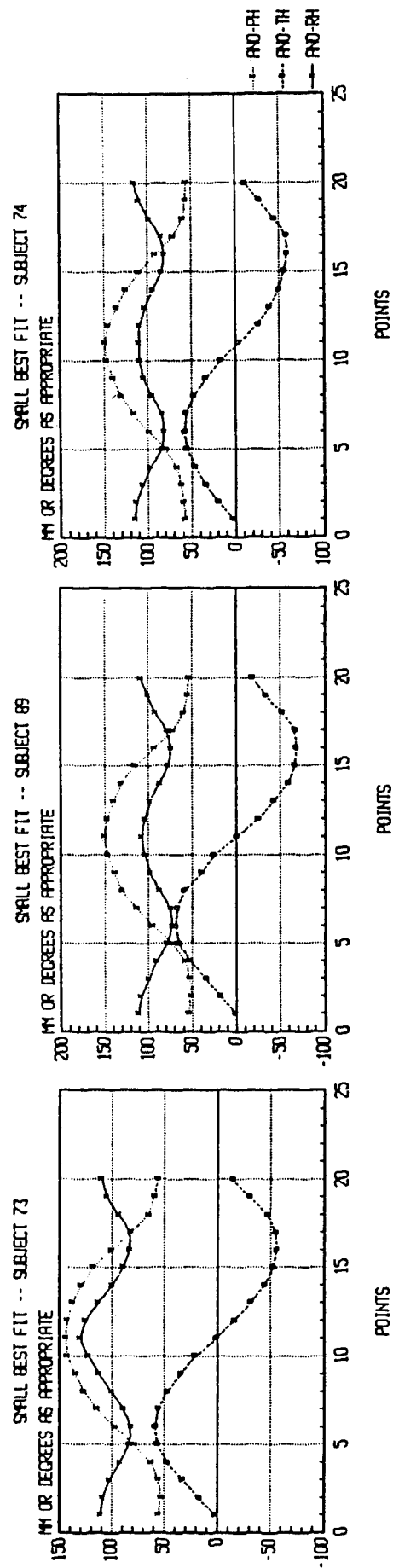


FIGURE A58

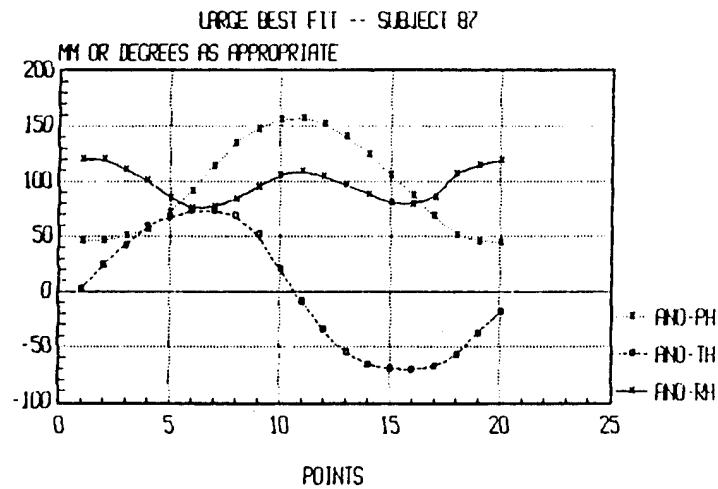
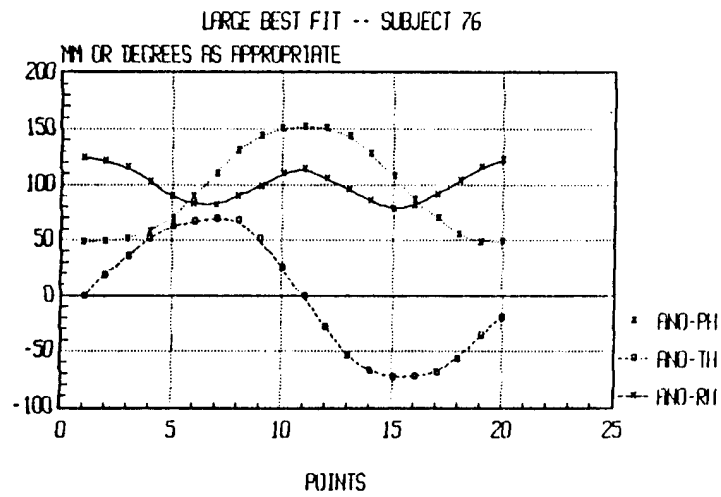
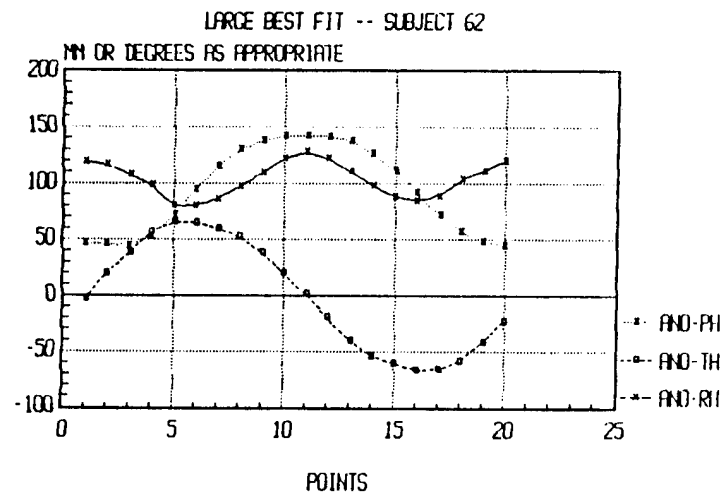


FIGURE A59

RANGE OF RHO, THETA AND PHI IN MASK COORDINATES FOR SELECTED S, M AND L SAMPLE POPULATIONS
FOR COMPARISON TO MASK, MISFITS, ANATOMICAL COORDINATES AND EACH OTHER

	PT1	PT2	PT3	PT4	PT5	PT6	PT7	PT8	PT9	PT10	PT11
MASK ρ (mm)	86-95 89 98-104 102 97-103 100-104 102	87-95 88 97-103 100 100-104 100	84-90 87 94-102 94 98-100 97	78-87 85 86-95 88 87-96 91	69-78 78 75-84 80 78-85 83	63-77 72 71-82 76 72-84 78	64-78 73 69-82 78 75-86 80	72-84 77 78-89 82 82-95 87	81-90 84 89-96 94 91-98 96	87-97 93 95-103 102 98-106 104	89-102 94 97-111 103 103-109 106
S misfit 40 M misfit 13	93 95	92 96	88 96	81 90	— 80	68 78	68 78	76 82	83 90	87 99	89 98
MASK θ (deg)	0	14-18 15	29-34 32	47-52 51	68-72 71	90	69-76 72	53-65 57	36-51 43	15-32 25	89-97 0
NOTE: absolute value shown for PT7-PT10	0	11-17 15	26-33 31	46-50 47	68-72 71	90	69-77 74	54-62 58	38-49 42	16-32 25	810-87 -3
M misfit 40 M misfit 13	0	17-19 16	31-33 32	49-51 50	68-71 70	90	70-73 70	51-58 52	37-46 36	16-30 19	-10-84 0
MASK ϕ (deg)	90	83-89 89	79-84 82	74-81 76	75-82 80	90	102-112 104	114-126 117	126-139 130	131-145 139	133-149 142
S misfit 40 M misfit 13	90	84-90 88	81-86 83	78-82 76	79-83 83	90	104-108 103	117-124 117	125-137 129	135-146 139	137-147 141
ANATOMICAL ρ (mm)	90	86-88 87	78-84 82	74-80 78	76-83 81	90	99-105 101	110-117 114	118-129 123	127-141 132	132-147 135
S misfit 40 M misfit 13	90	89 86	82 81	78 78	— 80	90	103 102	118 118	132 131	140 140	141 140
ANATOMICAL θ (mm)	106-122	104-121	98-113	87-102							
(n=9) M	114-126	113-124	106-117	94-106							
(n=5) L	119-124	116-121	107-117	98-105							

FIGURE A60

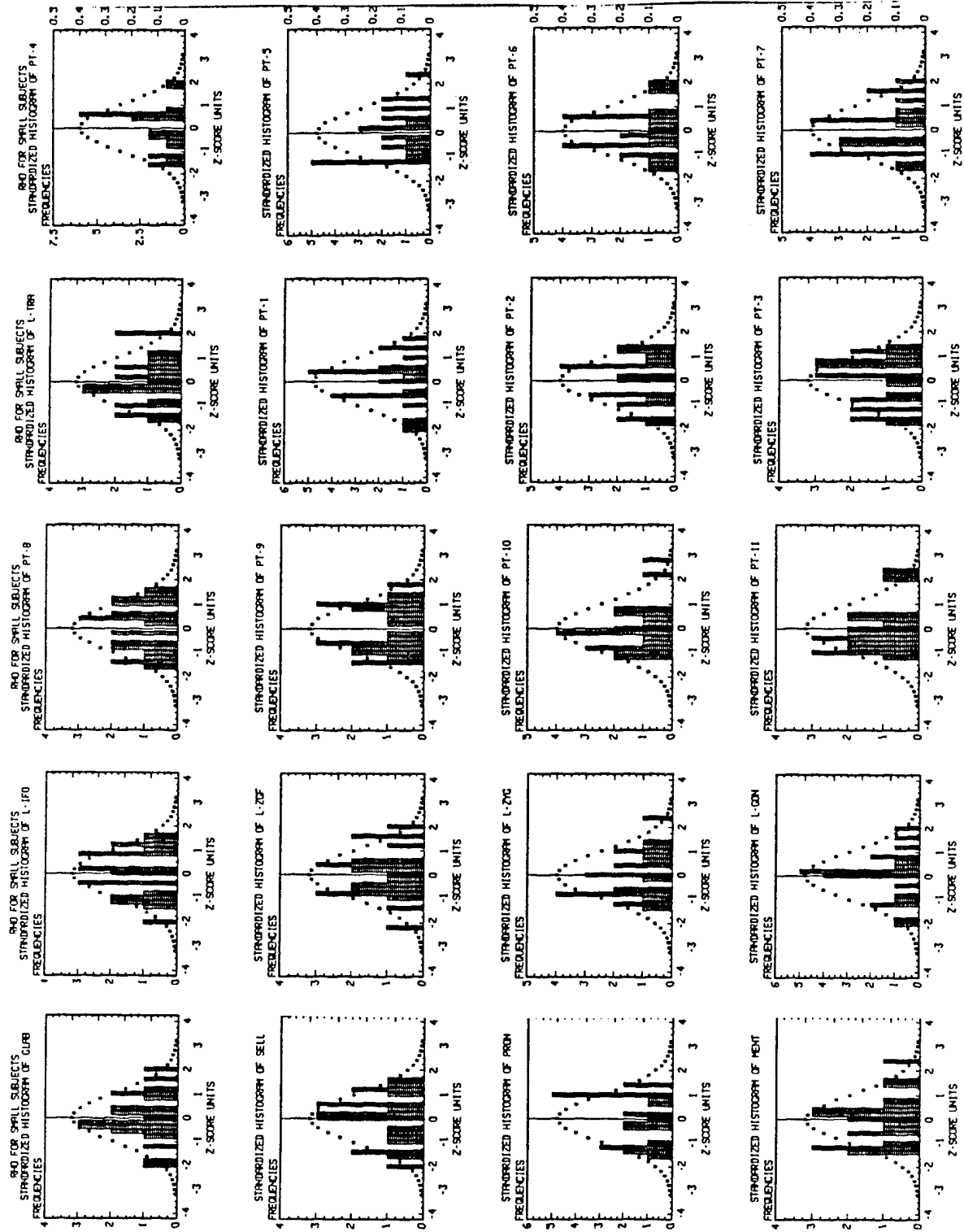


FIGURE A61

MASKRHO FOR SMALL SUBJECTS

VAR NAME	MEAN	STD ERR	LOWER 95%	UPPER 95%	LOWER 99%	UPPER 99%
GLAB	74.86	.882	73.03	76.69	72.373	77.347
SELL	62.851	.832	61.126	64.576	60.507	65.195
PRON	81.342	.875	79.526	83.157	78.874	83.809
MENT	97.103	.59	95.88	98.327	95.441	98.766
L-IFO	54.187	.813	52.5	55.874	51.894	56.48
L-ZGF	70.673	.821	68.97	72.376	68.358	72.988
L-ZYG	72.806	.911	70.918	74.694	70.239	75.373
L-GON	84.737	.886	82.899	86.574	82.239	87.234
L-TRA	82.154	1.197	79.672	84.636	78.781	85.527

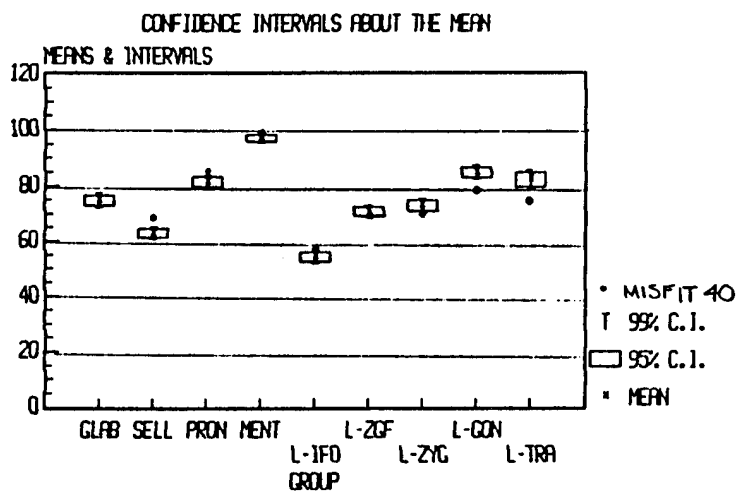


FIGURE A62

MASKRHO FOR SMALL SUBJECTS

VAR NAME	MEAN	STD ERR	LOWER 95%	UPPER 95%	LOWER 99%	UPPER 99%
PT-1	90.637	.487	89.628	91.646	89.265	92.009
PT-2	91.016	.503	89.974	92.058	89.599	92.433
PT-3	87.23	.422	86.355	88.104	86.041	88.419
PT-4	81.87	.496	80.841	82.899	80.471	83.269
PT-5	72.982	.699	71.532	74.432	71.011	74.953
PT-6	69.151	.796	67.5	70.802	66.907	71.395
PT-7	70.282	.779	68.666	71.898	68.085	72.478
PT-8	77.948	.754	76.384	79.511	75.823	80.073
PT-9	85.123	.58	83.92	86.326	83.488	86.758
PT-10	90.29	.521	89.21	91.371	88.822	91.759
PT-11	93.134	.74	91.6	94.668	91.048	95.219

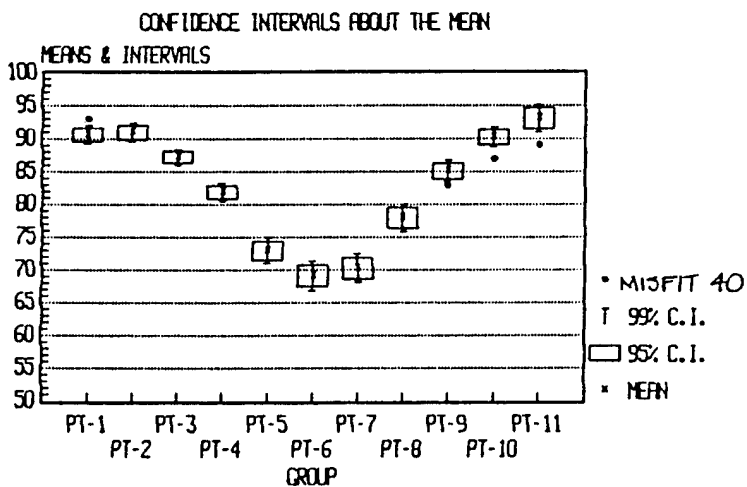


FIGURE A63

MASKRHO FOR MEDIUM SUBJECTS						
VAR NAME	MEAN	STD ERR	LOWER 95%	UPPER 95%	LOWER 99%	UPPER 99%
GLAB	83.019	1.45	79.674	86.363	78.153	87.885
SELL	74.01	1.585	70.354	77.666	68.691	79.329
PRON	94.409	1.322	91.36	97.458	89.973	98.845
MENT	110.821	1.242	107.958	113.685	106.655	114.987
L-IFO	65.23	1.644	61.439	69.021	59.715	70.745
L-ZGF	75.367	1.502	71.903	78.831	70.327	80.406
L-ZYG	74.961	1.51	71.478	78.444	69.894	80.028
L-GON	89.318	1.13	86.711	91.925	85.525	93.11
L-TRA	79.886	1.639	76.106	83.665	74.387	85.385

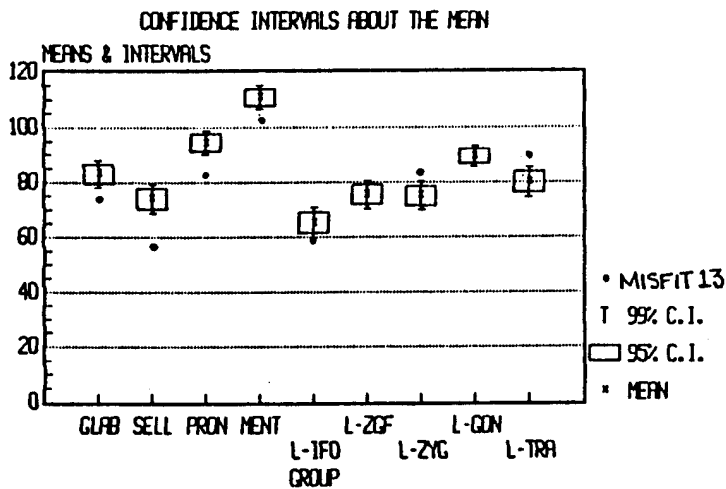


FIGURE A64

VAR NAME	MEAN	STD ERR	MASKRHO FOR MEDIUM SUBJECTS			
			LOWER 95%	UPPER 95%	LOWER 99%	UPPER 99%
PT-1	101.344	.673	99.792	102.897	99.085	103.604
PT-2	100.969	.55	99.701	102.237	99.124	102.813
PT-3	97.218	.911	95.117	99.318	94.162	100.274
PT-4	89.443	1.056	87.009	91.878	85.902	92.985
PT-5	79.257	.908	77.162	81.351	76.200	82.304
PT-6	74.356	1.177	71.642	77.069	70.407	78.304
PT-7	74.989	1.172	72.286	77.692	71.056	78.922
PT-8	84.449	1.031	82.071	86.826	80.99	87.908
PT-9	93.138	.692	91.542	94.733	90.817	95.459
PT-10	100.053	.845	98.105	102.001	97.219	102.888
PT-11	104.231	1.3	101.232	107.23	99.868	108.594

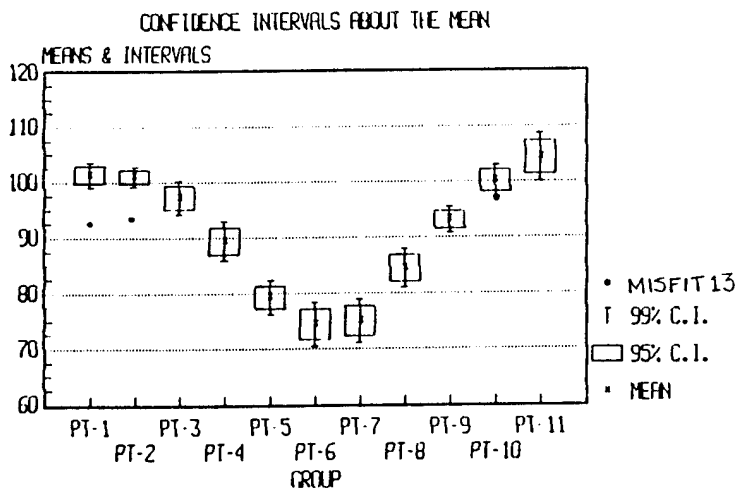


FIGURE A65

RHO FOR EACH SMALL SUBJECT

NOTE: A • IN THE FIRST 5 VARIABLES INDICATES THE VALUE IS OUTSIDE THE 97% CONFIDENCE INTERVAL ABOUT THE MEAN

	GLAB	SELL	PRON	MENT	L-IFO
1	72.89	63.76	• 84.27	• 93.36	• 51.09
4	• 78.83	• 67.38	• 85.59	97.63	• 57.61
7	• 83.34	• 68.02	• 84.95	97.88	• 57.25
10	74.38	63.79	82.33	95.9	• 49.56
13	76.88	62.72	• 85.18	• 101.47	54.94
16	75.96	• 57.01	79.6	97.51	• 49.82
19	75.36	63.05	81.99	• 99	• 48.94
22	72.67	• 58.92	• 75.73	• 95.34	52.76
25	• 77.83	• 68.36	• 87.13	98.48	• 60.69
28	76.48	64.86	• 85.9	• 101.08	• 59.03
31	• 81.57	64.98	80.88	• 94.42	55.33
34	• 66.04	• 54.83	• 76.69	• 93.1	• 46.72
37	• 71.48	• 60.02	• 75.46	98.25	• 50.19
40	73.2	62.96	• 85.62	98.2	• 59.46
43	74.91	• 57.43	• 74.9	• 93.75	54.35
46	• 80.04	• 69.28	• 76.61	97.34	• 50.03
49	73.23	64.75	• 85.31	• 104.13	• 57.39
52	• 72	• 60.44	• 76.36	• 93.91	52.95
55	• 67.01	• 56.68	79.56	• 93.72	55.04
58	• 79.27	• 65.25	• 76.77	95.68	• 57.79
61	74.25	• 66.52	• 87.63	• 99.5	• 58.83
64	70	61.28	81.55	97.09	53.92
67	74.16	63.28	80.85	96.64	52.61
	L-ZGF	L-ZYG	L-GON	L-TRA	PT-1
1	65.45	68.98	82.9	74.31	91.54
4	72.5	74.61	87.1	81.09	91.87
7	70.67	70.41	75.97	79.66	89.14
10	68.87	69.3	85.29	82.51	90.83
13	67.37	67.99	77.46	73.75	90.65
16	72.11	75.87	89.91	89.6	86.33
19	69.31	67.51	85.17	82.95	89.28
22	68.26	74.53	85.42	85.77	86.96
25	72.75	69.1	80.02	79.44	91.51
28	70.18	66.97	81.19	73.23	94.01
31	78.38	79.17	85.82	84.76	88.48
34	62.03	69.6	85.41	80.3	89.11
37	68.06	71.51	79.37	83.6	91.34
40	71.51	73.07	86.74	81.45	91.66
43	77.24	83.52	93.35	93.25	92.22
46	75.16	77.52	80.37	93.88	86.07
49	67.8	68.15	84.7	76.23	94.89
52	71.6	75.54	84.99	86.32	93.89
55	71.9	77.26	88.19	87.96	91.6
58	76.94	78.13	85.05	85.18	89.74
61	72.8	72.68	88.39	76.38	92.93
64	67.55	72.6	91.27	80.73	89.46
67	67.04	70.52	84.86	77.19	91.14

FIGURE A65 CONT.

	PT-2	PT-3	PT-4	PT-5	PT-6
1	92.31	87.64	83.12	71.28	65.29
4	92.38	89.25	80.93	73.93	72.19
7	92.45	89.85	83.06	72.5	67.33
10	93.4	88.29	81.13	71.74	64.96
13	88.61	84.67	81.26	69.91	66.65
16	86.79	83.87	78.19	69.12	64.93
19	89.53	86.04	78.43	69.12	63.68
22	87.34	84.16	80.68	71.25	68.27
25	94.34	89.94	83.04	75.1	71.77
28	93.87	87.77	83.19	73.92	66.86
31	89.36	88.52	86.5	80.78	74.95
34	89.37	84.9	79.74	68.78	66.79
37	91.44	86.88	82.99	73.95	68.93
40	93.98	88.61	83.3	74.24	71.78
43	91.41	89.84	83.46	78.01	76.25
46	87.03	85.5	79.08	70.06	63.24
49	94.61	87.29	78.07	69.26	69.88
52	92.6	88.71	81.62	72.03	68.73
55	91.21	87.77	86.35	76.35	76.73
58	90.85	88.77	82.8	76.24	71.69
61	92.72	88.8	83.43	77.43	71.46
64	88.97	85.45	83.75	74.96	70.97
67	88.8	83.76	78.89	68.63	67.14
	PT-7	PT-8	PT-9	PT-10	PT-11
1	68.63	75.8	83.29	87.49	89.86
4	74.61	82.52	89.28	95.86	101.59
7	66.74	71.89	81.15	87.66	90.17
10	66.43	74.07	82.34	87.87	89.47
13	65.37	74.73	83.1	90.38	94.59
16	68.79	78.58	87.62	90.44	95.38
19	66.71	73.02	81.08	92.07	99.92
22	68.9	77.27	83.36	88.54	88.56
25	71.66	79.08	85.63	87.48	90.49
28	67.99	77.3	83.02	88.66	92.54
31	76.3	82.06	85.96	89.17	91.93
34	68.37	75.77	81.89	89.7	91.2
37	68.31	73.77	82.3	88.47	91.34
40	71.64	80.21	87.12	91.81	92.78
43	76.2	81.78	87.67	92.24	92.13
46	64.19	72.6	83.78	91.87	95.06
49	70.88	79.45	90.19	97.34	100.64
52	71.95	81.25	88.39	89.92	91.84
55	77.86	83.75	88.08	89.92	89.26
58	72.58	79.67	84.52	88.25	91.68
61	73.6	82.67	87.98	89.75	93.22
64	72.03	80.37	86.86	91.24	94.6
67	66.74	75.19	83.22	90.55	93.83

FIGURE A66

RHO FOR EACH MEDIUM SUBJECT

	GLAB	SELL	PRON	MENT	L-1PO
1	76.44	66.55	86.53	105.69	59.89
2	78.78	71.62	92.38	106.92	65
3	77.85	67.84	93.14	110.96	62.2
4	83.99	76.39	96.75	115.21	69.26
5	83.23	75.98	95.83	113.17	55.92
6	84.85	76.05	94.7	109.24	70.42
7	87.98	82.17	101.01	116.85	68.16
8	88.13	74.48	92.83	108.41	67.16
9	85.92	75.01	96.51	110.94	69.06
	L-ZGF	L-ZYG	L-GON	L-TRA	PT-1
1	70.56	75.49	87.92	80.09	100.06
2	68.13	66.21	85.85	71.51	97.67
3	76.16	78.75	94.66	86.23	99.75
4	77.96	74.21	83.04	77.59	103.89
5	73.33	77.13	90.31	83.81	101.42
6	76.46	73.58	90.56	75.45	103.01
7	77.69	73.27	89.61	78.4	103.58
8	83.61	82.72	89.93	86.24	101.95
9	74.4	73.29	91.98	79.65	100.77
	PT-2	PT-3	PT-4	PT-5	PT-6
1	100.27	95.86	86.83	75.04	70.78
2	97.47	95.31	87.64	79.72	71.06
3	101	98.35	89.75	79.24	77.29
4	102.35	98.21	91.13	80.84	73.32
5	100.07	95.69	89.67	76.64	72.19
6	101.13	94.22	86.34	79.32	74.42
7	102.22	101.62	92.78	80.88	74.98
8	103.14	101.05	95.14	84.32	82.08
9	101.07	94.65	85.71	77.31	73.08
	PT-7	PT-8	PT-9	PT-10	PT-11
1	74.2	83.91	92.99	97.93	99.71
2	68.93	78.27	89.06	95.36	104.08
3	77.36	87.34	96.14	103.08	105.9
4	73.73	86.25	94.62	97.73	97.46
5	72.91	81.49	91.23	102.77	110.57
6	76.73	85.25	93.72	100.93	102.86
7	75.21	84.14	92.34	100.8	106.75
8	81.78	88.55	93.72	101.02	106.28
9	74.05	84.84	94.42	100.86	104.47
SUBJEC					
1	10				
2	22				
3	23				
4	51				
5	53				
6	56				
7	60				
8	81				
9	91				

FIGURE A67

RHO FOR EACH LARGE SUBJECT

	GLAB	SELL	PRON	MENT	L-IFO
1	80.85	66.51	92.18	110.09	64.14
4	76.66	64.26	84.65	108.68	58.52
7	76.07	63.27	91.53	113.73	67.21
10	83.23	74.61	88.78	114.32	64.72
13	79.88	68.6	86.19	114.94	62.21
	L-ZGF	L-ZYG	L-GON	L-TRA	PT-1
1	82.93	87.31	95.74	95.66	96.66
4	72.75	76.24	89.3	84.88	100.54
7	79.18	78.28	96.04	82.17	100.2
10	78.9	76.9	88.78	81.26	102.42
13	72.8	71.79	76.6	77.29	102.74
	PT-2	PT-3	PT-4	PT-5	PT-6
1	100.1	98.83	95.82	85.43	84.42
4	100.2	99.96	93.05	78.39	73.52
7	101.4	99.31	94.95	79.74	77.35
10	100.39	97.77	89.24	79.61	75.65
13	104.4	97.56	91.38	78.27	71.7
	PT-7	PT-8	PT-9	PT-10	PT-11
1	86.42	94.87	97.83	106.28	108.88
4	74.59	83.88	93.19	97.69	103.74
7	79.61	87.93	94.89	103.99	106.8
10	78.26	87.49	94.3	102.73	106.66
13	74.51	81.79	90.77	100.05	103.49
	CODE	SUBJEC			
1	1	5			
4	1	50			
7	1	62			
10	1	76			
13	1	87			

FIGURE A68

SEQUENTIAL DELTA ρ RANGE BETWEEN MASKPOINTS FOR SELECTED S, M & L SAMPLE POPULATIONS AND COMPARISONS TO MISFITS

$\Delta \rho$ range (mm)	1-2	2-3	3-4	4-5	5-6	6-7	7-8	8-9	9-10	10-11
(n=23) s	-3 2	1 7	1 9	5 12	-1 7	-4 1	-10 -5	-11 -4	-11 -2	-8 1
(n=9) m	-1 2	1 7	6 9	7 13	2 9	-3 2	-13 -7	-11 -5	-12 -3	-9 0
(n=5) l	-3 2	0 7	3 9	10 15	1 7	-3 -1	-9 -7	-9 -3	-9 -5	-6 -3
m misfit 13	-1	0	6	10	2	1	-5	-8	-10	2
s misfit 40	1	4	7	—	—	0	-8	-7	-4	-2
misfit 92	-2	-3	-5	-7	-3	-1	-7	-7	0	-2

KEY:

 = OUT OF RANGE

FIGURE A69

POLYGONAL PERIMETER (mm) FOR SELECTED SMALL POPULATION & COMPARISON TO FF SCORES AND UNDEFORMED MASK

ENDPOINTS →	1-2	1-3	1-4	1-5	1-6	1-7	1-8	1-9	1-10	1-11	FF FOR SHORT PERIMETER	FF FOR LONG PERIMETER
SUBJECT	41 63 64 68 70	52 53 49 56 49	80 81 78 83 77	109 111 107 108 107	137 138 138 137 134	165 167 164 166 161	191 193 190 192 189	217 223 216 222 214	242 245 240 245 237	264 273 264 267 263		140000
	72 73 74 88 89	47 47 53 55 51	75 74 77 82 79	103 103 104 111 107	131 130 132 140 137	159 158 157 148 142	186 184 185 194 191	211 210 210 222 219	232 237 234 241 240	257 264 255 265 267	210000 260000 180000	
	90 93 94 96 101	52 49 53 55 51	82 77 78 84 81	110 107 107 111 110	140 133 137 140 137	168 162 164 165 164	196 190 190 194 194	223 216 217 219 222	247 237 242 242 242	272 263 264 268 270	340000	400000 230000
	103 105 106 107 108	48 51 52 54 52	74 78 79 81 82	103 107 110 109 110	131 133 140 140 137	158 166 169 165 164	187 192 198 192 191	211 220 223 220 218	233 244 242 242 241	258 269 265 265 264	230000	590000 110000
	109 112 113	53 54 50	81 81 77	110 108 102	139 136 131	145 163 157	193 190 183	220 215 211	241 241 234	262 267 261	310000	
SMALL MASK	24	51	80	109	137	166	191	217	242	268		
MED MASK	27	56	86	121	150	179	208	238	266	292		
LARGE MASK	28	58	88	119	150	181	212	240	269	295		



KEY:  INDICATES TOP OF RANGE
 INDICATES BOTTOM OF RANGE

FIGURE A70

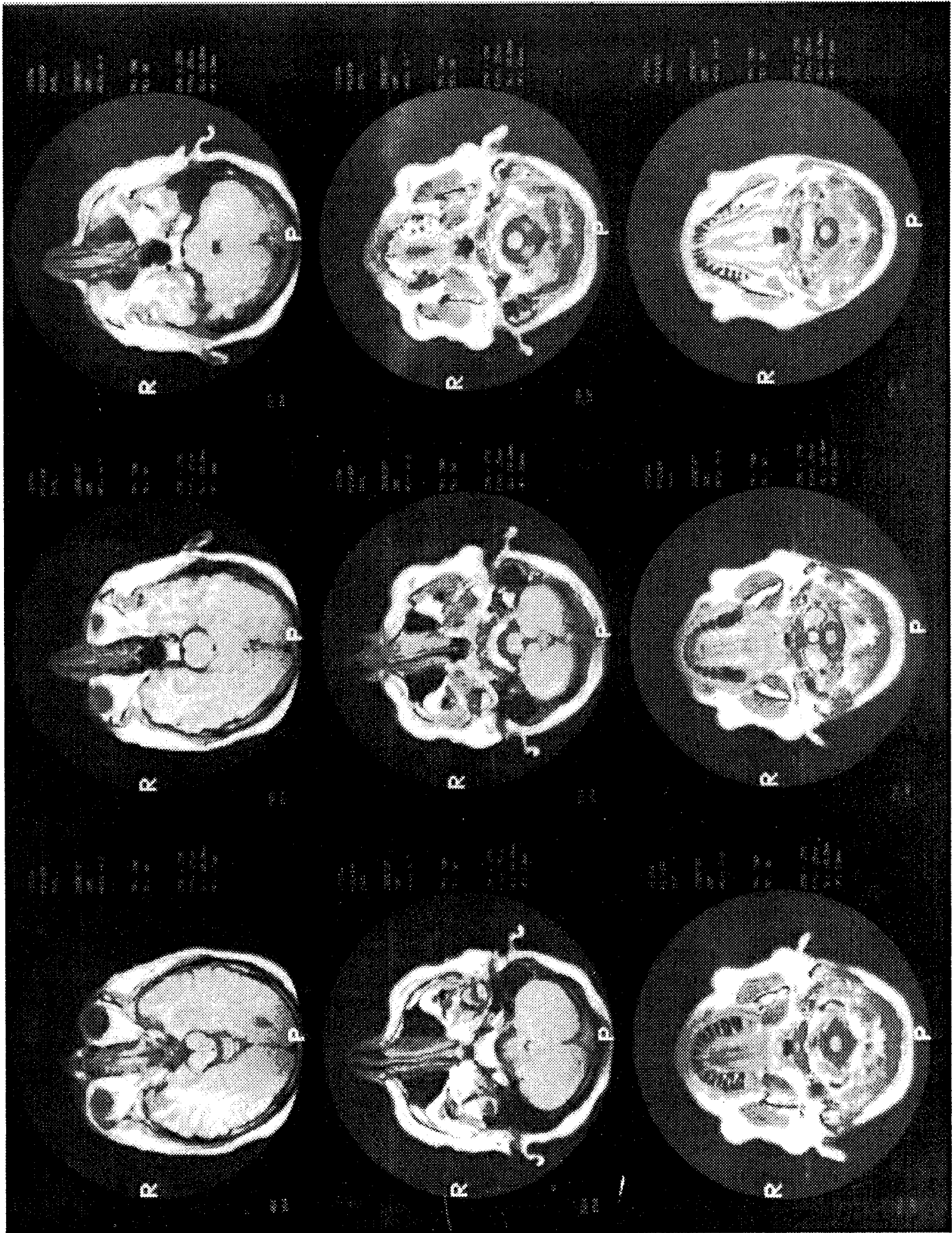


FIGURE A71

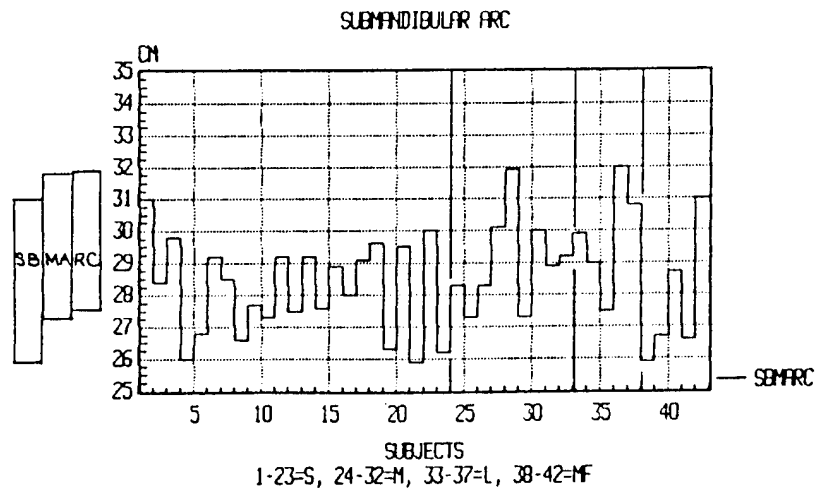
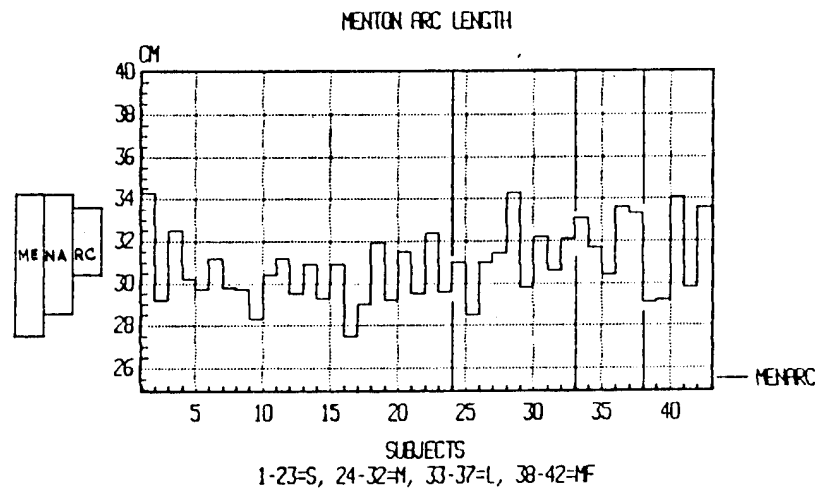
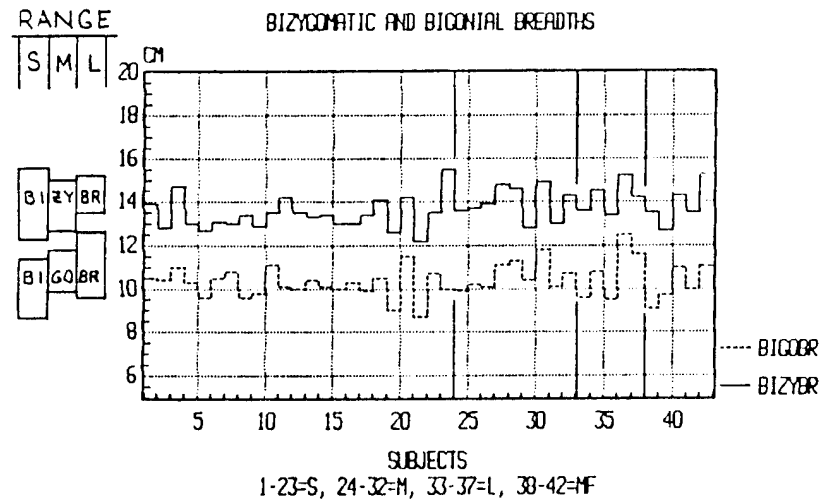


FIGURE A72

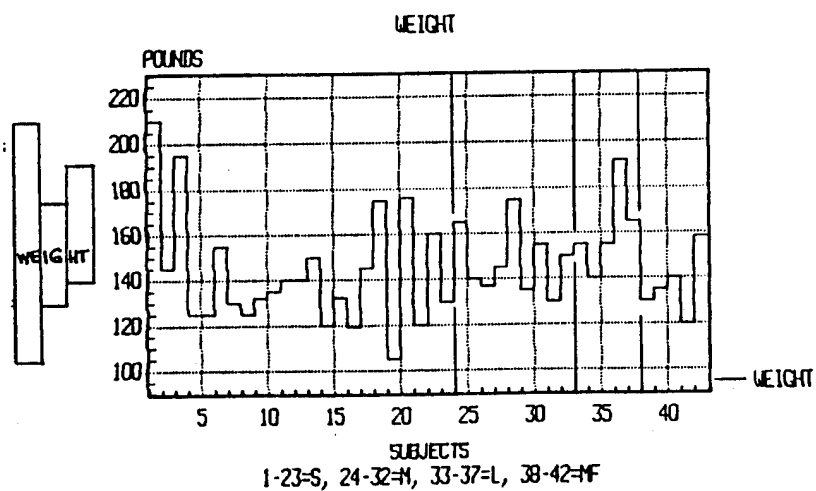
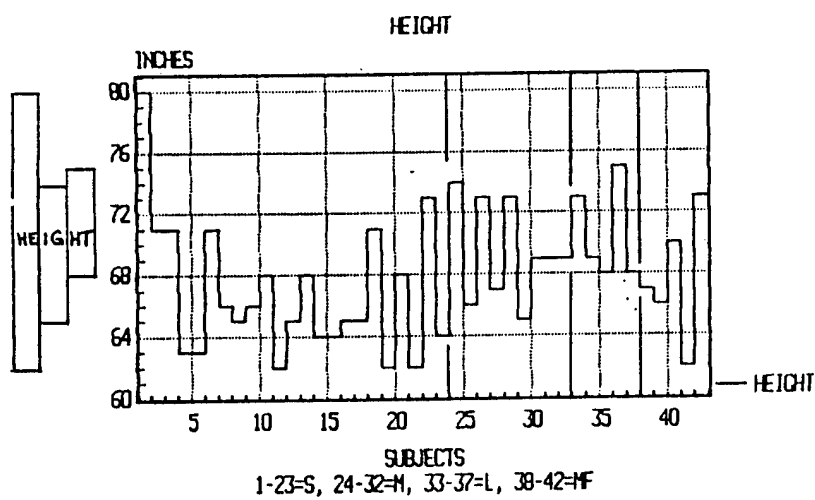
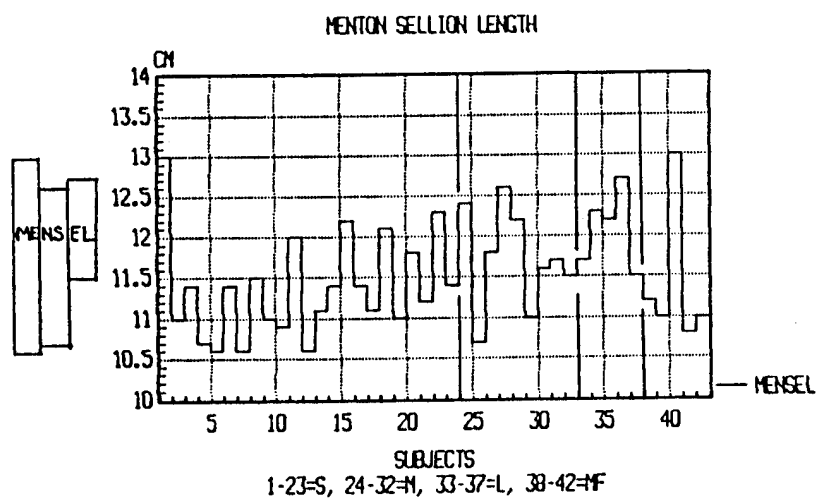


FIGURE A73

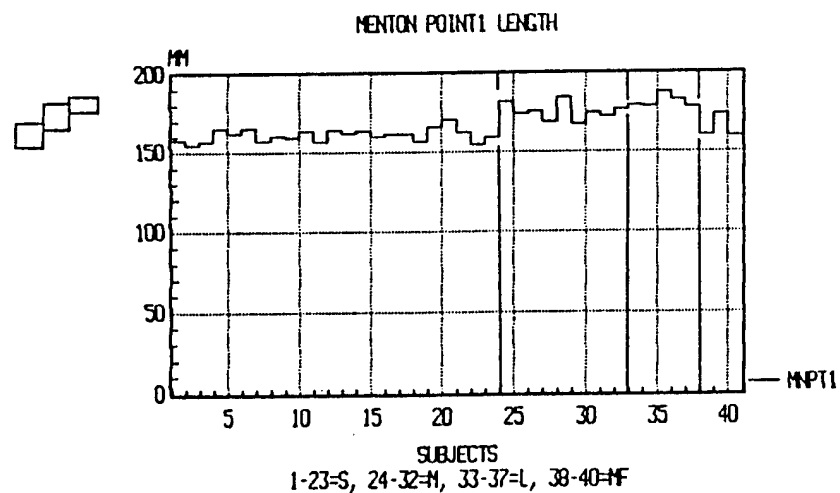
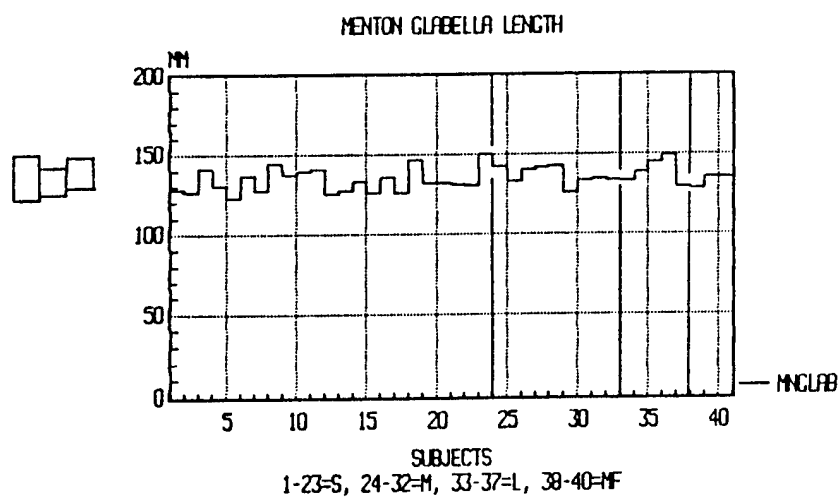
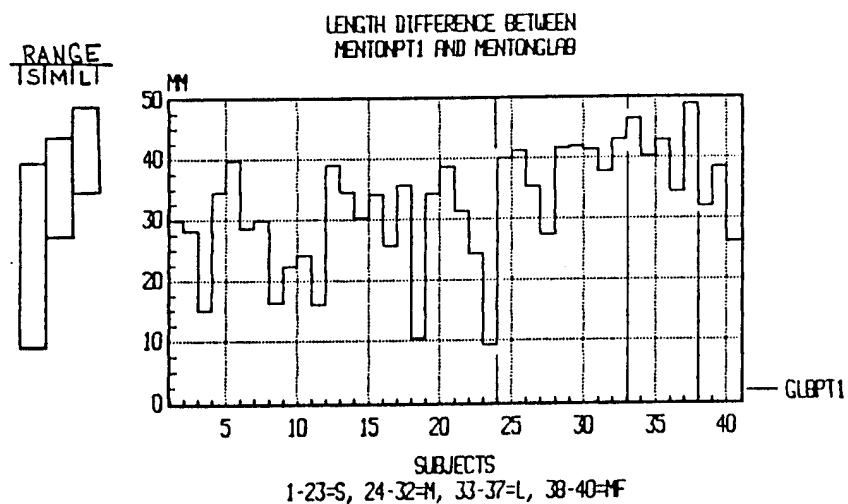


FIGURE A74

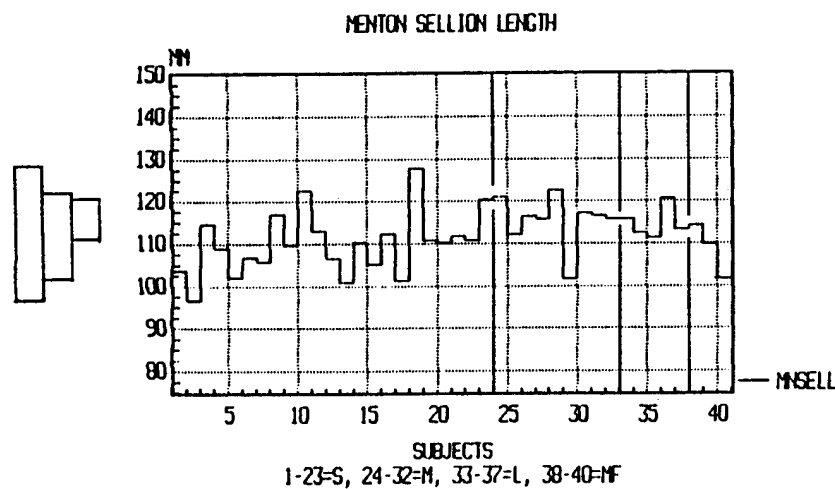
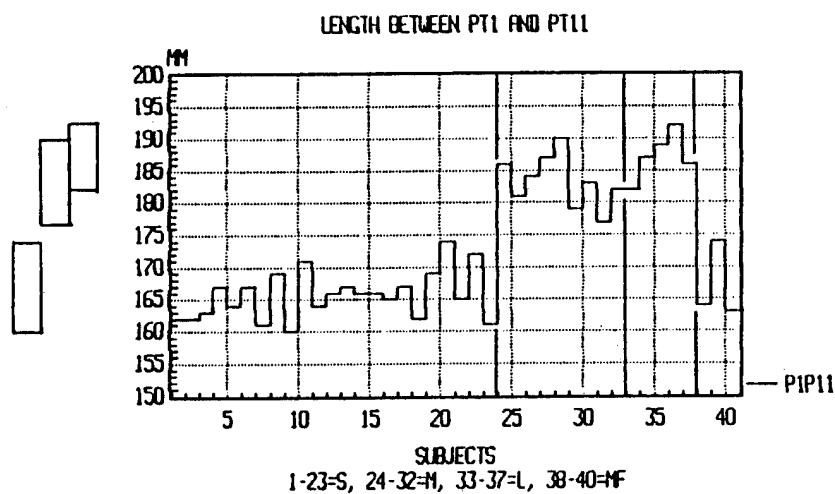
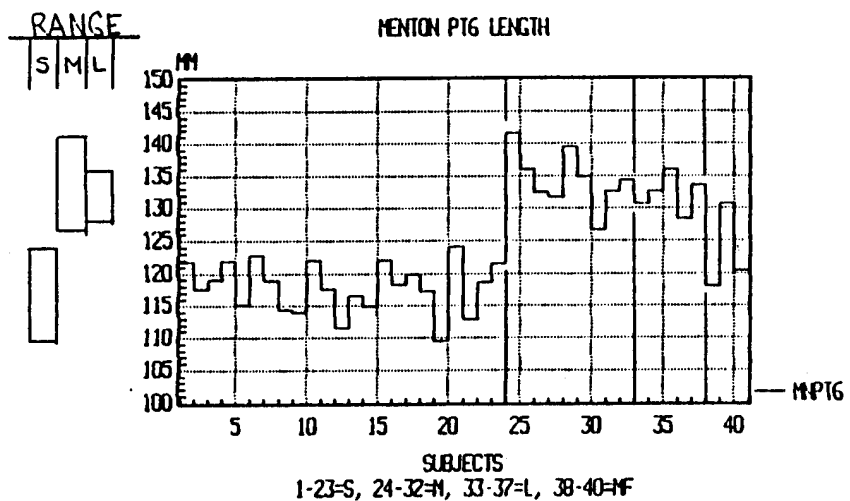


FIGURE A75

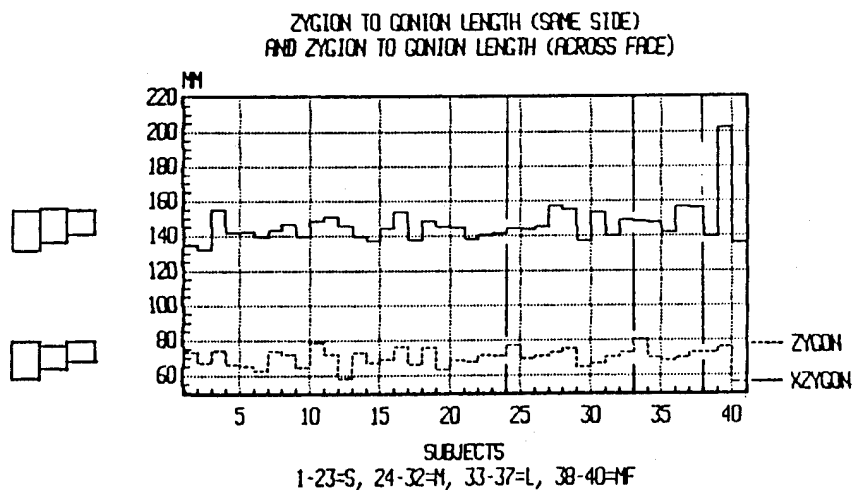
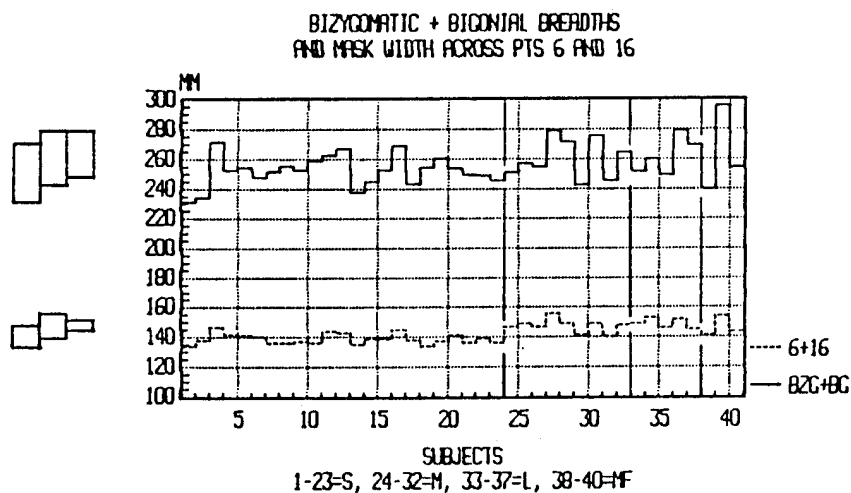
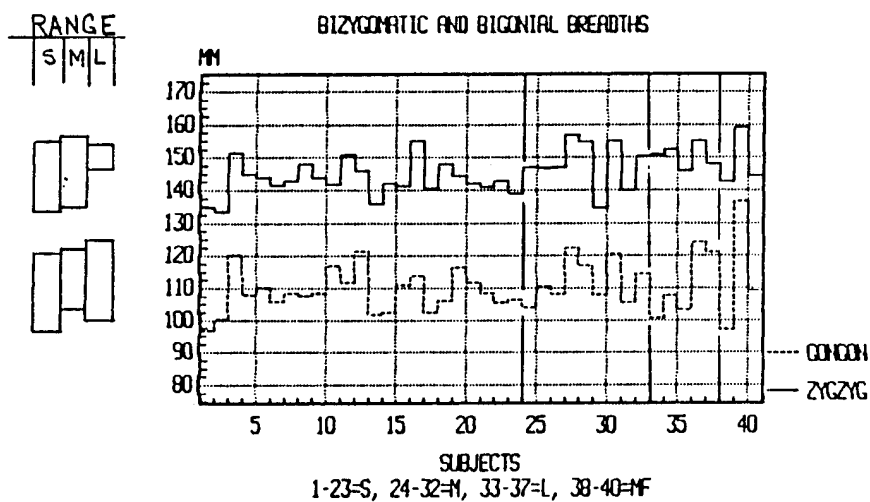


FIGURE A76

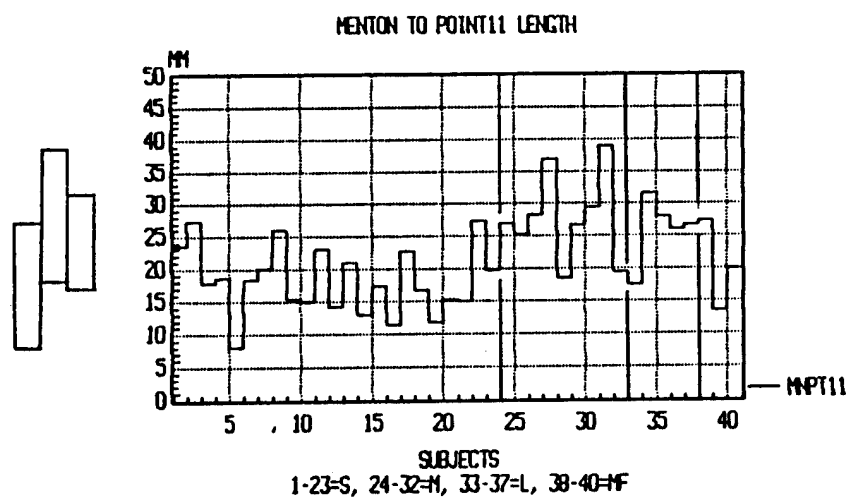
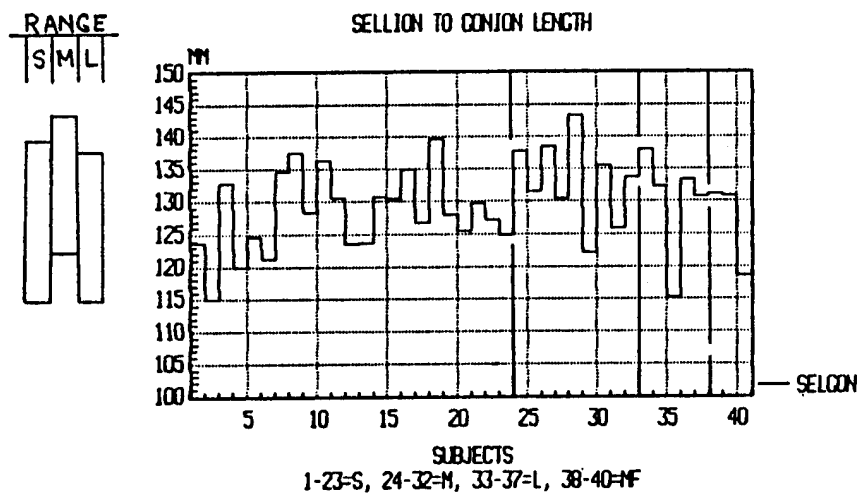


FIGURE A77

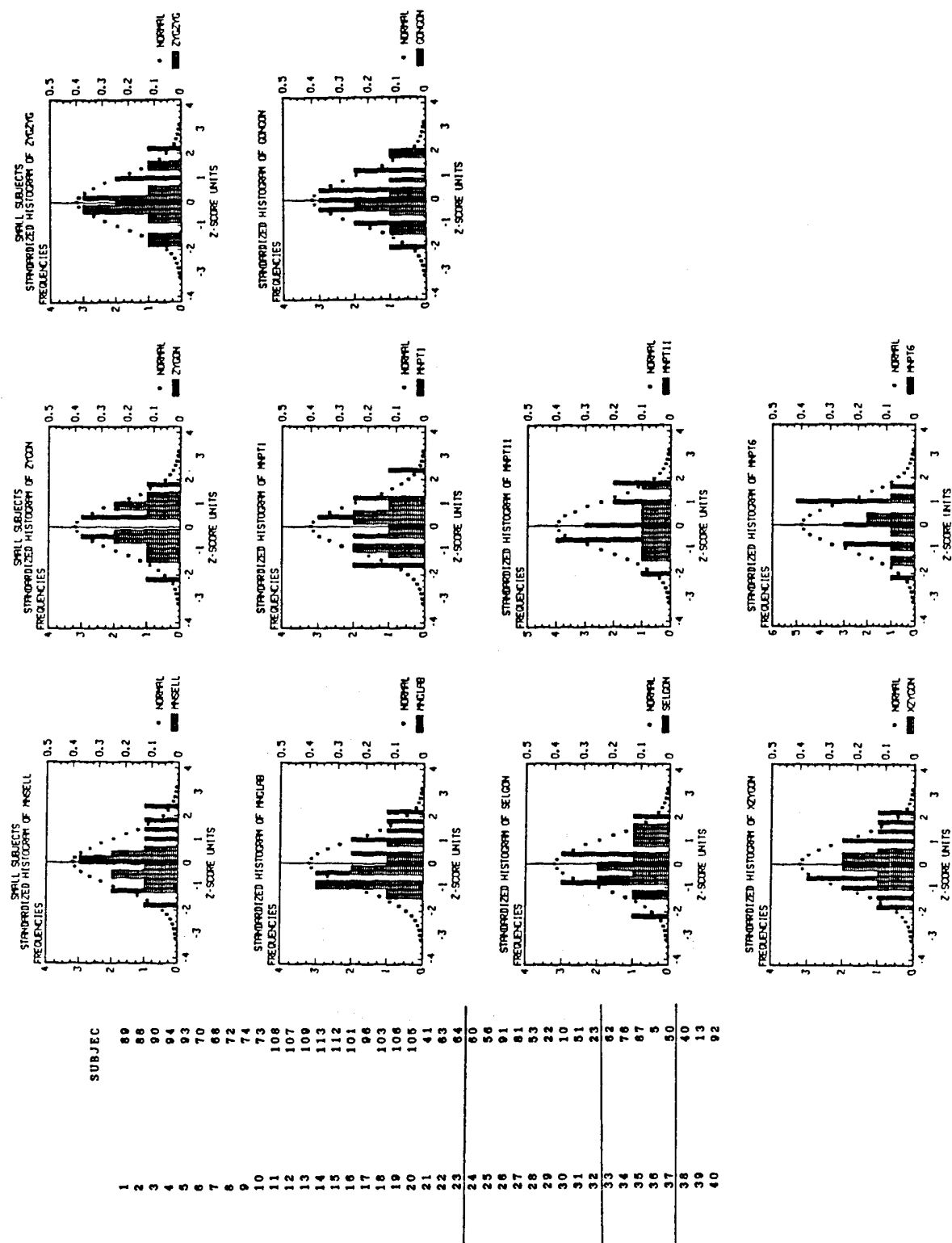


FIGURE A78

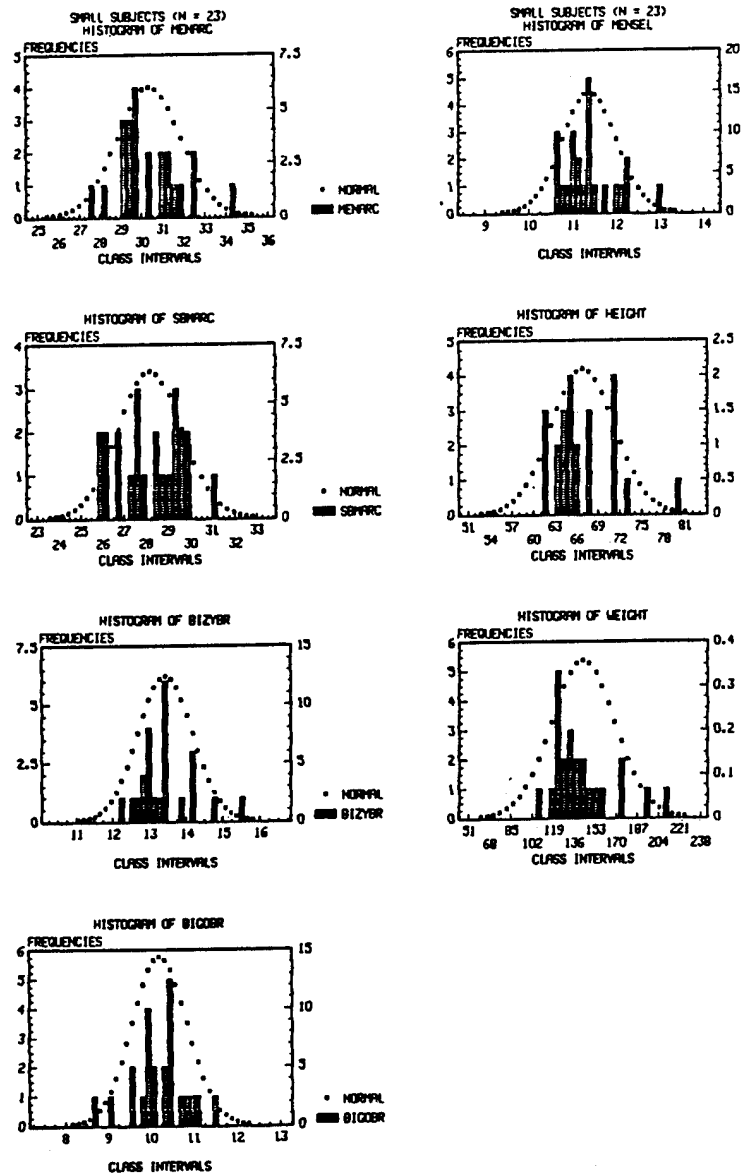


FIGURE A79

VAR NAME	MEAN	STD ERR	LOWER 95%	UPPER 95%	LOWER 99%	UPPER 99%
MNSELL	109.928	1.534	106.747	113.108	105.605	114.251
MNGLAB	133.52	1.549	130.308	136.732	129.154	137.886
SELGON	128.227	1.248	125.638	130.816	124.708	131.746
XZYGON	142.859	1.209	140.352	145.367	139.451	146.267
ZYGON	69.228	1.045	67.06	71.396	66.281	72.175
MNPT1	161.026	.828	159.309	162.742	158.692	163.359
MNPT11	18.229	1.077	15.996	20.461	15.194	21.263
MNPT6	117.932	.807	116.258	119.606	115.656	120.207
ZYGZYG	143.268	1.069	141.051	145.486	140.255	146.282
GONGON	108.854	1.29	106.179	111.53	105.217	112.491

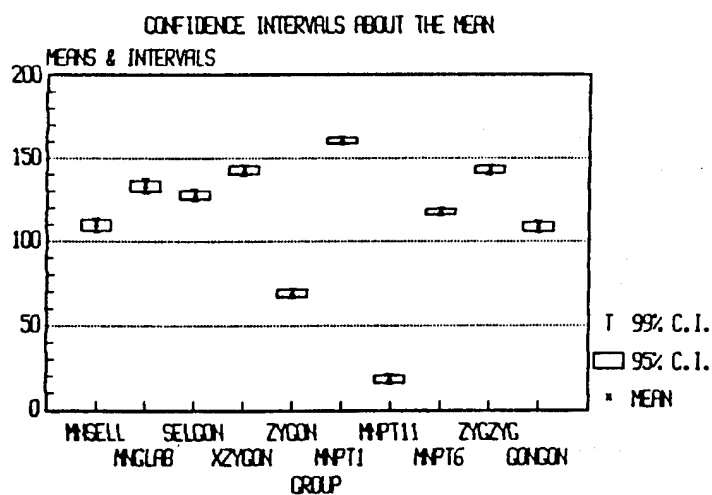


FIGURE A80

VAR NAME	SIZE	MEAN	SAMPLE STD DEV	SAMPLE VARIANCE	COEF. OF VARIATION
MNSELL	23	109.9278	7.35463	54.09054	.0669
MNGLAB	23	133.52	7.42764	55.16988	.05563
SELGON	23	128.2269	5.9864	35.83699	.04669
XZYGON	23	142.8591	5.79833	33.62067	.04059
ZYGON	23	69.22783	5.01353	25.13543	.07242
MNPT1	23	161.0256	3.96984	15.75966	.02465
MNPT11	23	18.2287	5.16283	26.65477	.28323
MNPT6	23	117.9317	3.8708	14.98309	.03282
ZYGZYG	23	143.2683	5.12712	26.28737	.03579
GONGON	23	108.8544	6.18733	38.28311	.05684
BZG+BG	23	252.1226	10.29879	106.065	.04085
6+16	23	138.8261	3.56309	12.69564	.02567
PIP11	23	165.6522	3.67558	13.5099	.02219
GLBPT1	23	27.50565	8.99165	80.84975	.3269

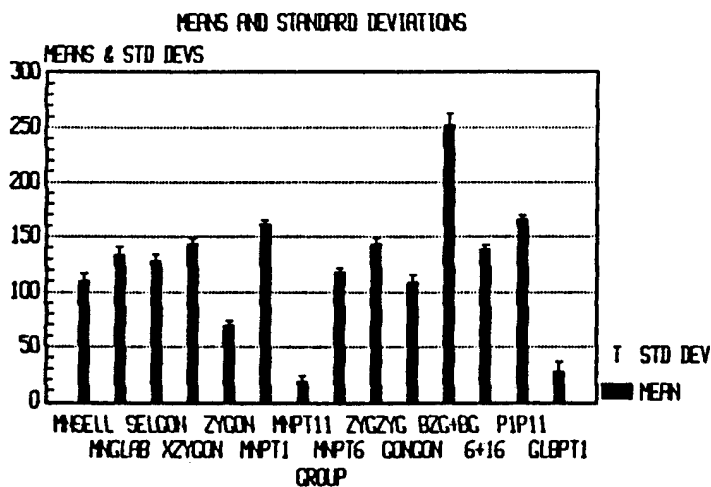


FIGURE A81

VAR NAME	MEAN	STD ERR	LOWER 95%	UPPER 95%	LOWER 99%	UPPER 99%
MENARC	30.335	.318	29.675	30.995	29.437	31.232
SBMARC	28.187	.301	27.562	28.812	27.338	29.036
BIZYBR	13.43	.154	13.11	13.75	12.995	13.865
BIGOBR	10.209	.133	9.933	10.484	9.834	10.583
MENSEL	11.378	.129	11.111	11.645	11.016	11.741
HEIGHT	66.826	.915	64.929	68.723	64.248	69.404
WEIGHT	143	5.355	131.895	154.105	127.905	158.095

VAR NAME	SIZE	MEAN	SAMPLE STD DEV	SAMPLE VARIANCE	COEF. OF VARIATION
MENARC	23	30.33478	1.52662	2.33055	.05033
SBMARC	23	28.18696	1.44484	2.08755	.05126
BIZYBR	23	13.43044	.74005	.54767	.0551
BIGOBR	23	10.2087	.63669	.40538	.06237
MENSEL	23	11.37826	.61715	.38087	.05424
HEIGHT	23	66.8261	4.38647	19.24111	.06564
WEIGHT	23	143	25.67985	659.4546	.17958

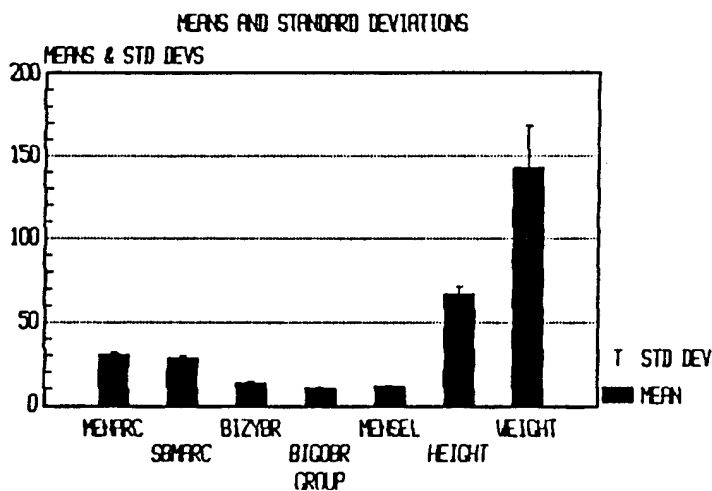


FIGURE A82

VAR NAME	MEAN	STD ERR	LOWER 95%	UPPER 95%	LOWER 99%	UPPER 99%
MNSELL	114.062	2.256	108.96	119.164	106.731	121.393
MNGLAB	136.316	1.741	132.378	140.254	130.658	141.974
SELGON	131.727	2.43	126.231	137.223	123.83	139.624
XZYGON	145.946	2.325	140.687	151.206	138.389	153.503
ZYGON	69.435	1.864	65.219	73.651	63.377	75.493
MNPT1	173.928	2.208	168.934	178.922	166.753	181.103
MNPT11	27.035	2.175	22.115	31.955	19.966	34.104
MNPT6	133.002	1.922	128.655	137.349	126.756	139.248
ZYGZYG	147.697	2.196	142.729	152.665	140.558	154.836
GONGON	112.052	2.003	107.521	116.583	105.542	118.562

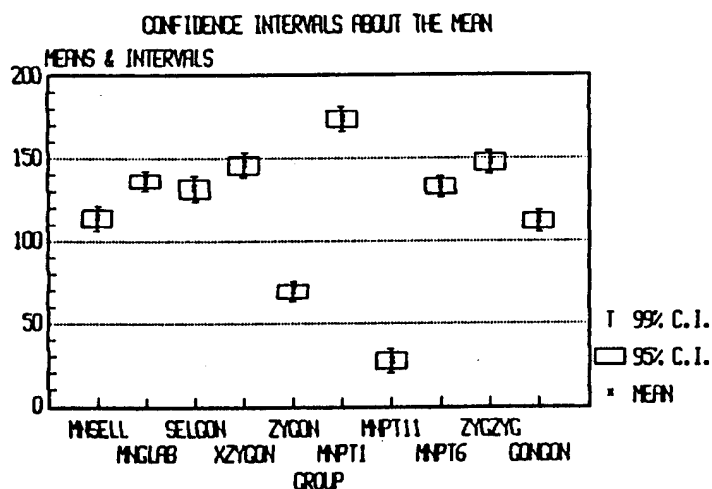


FIGURE A83

VAR NAME -----	SIZE -----	MEAN -----	SAMPLE STD DEV -----	SAMPLE VARIANCE -----	COEF. OF VARIATION -----
MNSELL	9	115.44	5.98953	35.87451	.05188
MNGLAB	9	136.5267	5.79588	33.59222	.04245
SELGON	9	133.1767	6.5405	42.77819	.04911
XZYGON	9	147.0478	6.86767	47.16484	.0467
ZYGON	9	70.90444	3.84605	14.79213	.05424
MNPT1	9	175.4044	5.50477	30.30254	.03138
MNPT11	9	27.80778	6.81987	46.51063	.24525
MNPT6	9	134.4067	4.39876	19.34909	.03273
ZYGZYG	9	147.9878	7.30242	53.32538	.04934
GONGON	9	112.3022	6.66569	44.43145	.05935
BZG+BG	9	260.29	13.28175	176.4048	.05103
6+16	9	147.3333	4.71699	22.25001	.03202
P1P11	9	183.2222	4.05518	16.44445	.02213
GLBPT1	9	38.87778	4.93633	24.36733	.12697

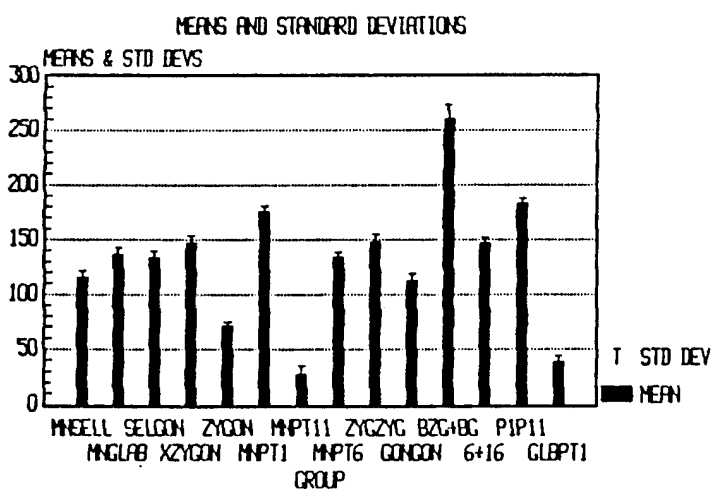
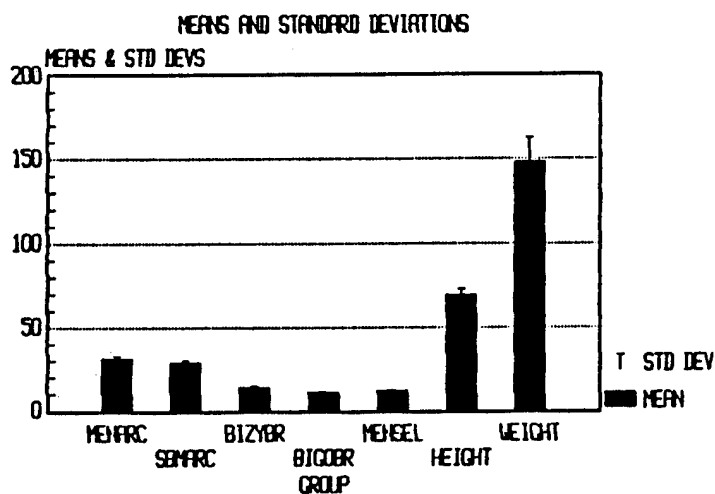


FIGURE A84

MEDIUM STATS

VAR NAME	SIZE	MEAN	SAMPLE STD DEV	SAMPLE VARIANCE	COEF. OF VARIATION
----	----	----	-----	-----	-----
MENARC	9	31.21111	1.82592	2.64361	.05209
SBMARC	9	29.03334	1.47564	2.1775	.05083
BIZYBR	9	13.95556	.75682	.57278	.05423
BIGOBR	9	10.62222	.64957	.42194	.06115
MENSEL	9	11.72222	.62205	.38694	.05307
HEIGHT	9	69.44445	3.24465	10.52778	.04672
WEIGHT	9	148	14.82397	219.75	.10016



VAR NAME	MEAN	STD ERR	LOWER 95%	UPPER 95%	LOWER 99%	UPPER 99%
----	----	----	----	----	----	----
MENARC	31.211	.542	29.961	32.461	29.393	33.029
SBMARC	29.033	.492	27.899	30.168	27.383	30.684
BIZYBR	13.956	.252	13.374	14.537	13.109	14.802
BIGOBR	10.622	.217	10.123	11.122	9.896	11.349
MENSEL	11.722	.207	11.244	12.2	11.027	12.418
HEIGHT	69.444	1.082	66.95	71.939	65.816	73.073
WEIGHT	148	4.941	136.605	159.395	131.422	164.578

FIGURE A85

LARGE STATS

VAR NAME	MEAN	STD ERR	LOWER 95%	UPPER 95%	LOWER 99%	UPPER 99%
MNSELL	114.666	1.651	110.081	119.251	107.063	122.269
MNGLAB	139.076	3.615	129.04	149.112	122.431	155.721
SELGON	129.916	3.835	119.269	140.563	112.258	147.574
XZYGON	149.866	2.801	142.091	157.641	136.97	162.762
ZYGON	72.11	2.105	66.267	77.953	62.419	81.801
MNPT1	181.704	1.732	176.895	186.513	173.728	189.68
MNPT11	25.936	2.306	19.533	32.339	15.317	36.555
MNPT6	132.228	1.27	128.702	135.754	126.379	138.077
ZYGZYG	150.424	1.609	145.957	154.891	143.015	157.833
GONGON	111.388	4.759	98.176	124.6	89.475	133.301

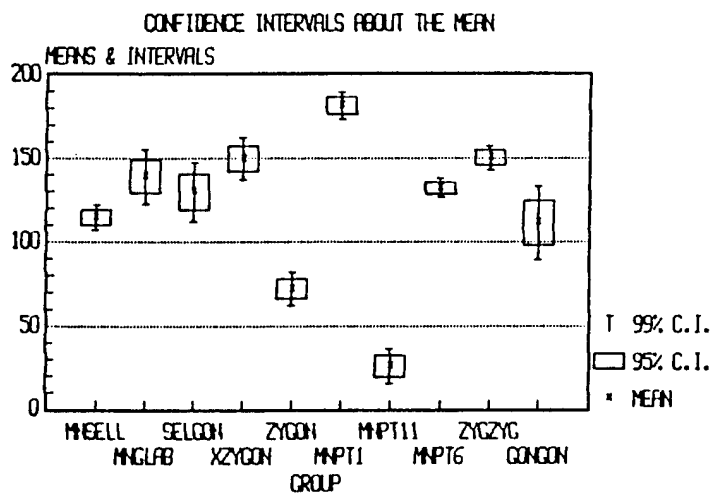


FIGURE A86

LARGE STATS

VAR NAME	SIZE	MEAN	SAMPLE STD DEV	SAMPLE VARIANCE	COEF. OF VARIATION
MNSELL	5	114.666	3.69283	13.63697	.03221
MNGLAB	5	139.076	8.0841	65.35275	.05813
SELGON	5	129.916	8.57623	73.55169	.06601
XZYGON	5	149.866	6.26309	39.22627	.04179
ZYGON	5	72.11	4.70676	22.1536	.06527
MNPT1	5	181.704	3.87374	15.00583	.02132
MNPT11	5	25.936	5.15729	26.59763	.19885
MNPT6	5	132.228	2.84059	8.06898	.02148
ZYGZYG	5	150.424	3.59847	12.94895	.02392
GONGON	5	111.388	10.64253	113.2635	.09554
BZG+BG	5	261.812	12.52268	156.8174	.04783
6+16	5	149	3.53553	12.5	.02373
PIP11	5	187.2	3.70135	13.7	.01977
GLBPT1	5	42.628	5.69889	32.47729	.13369

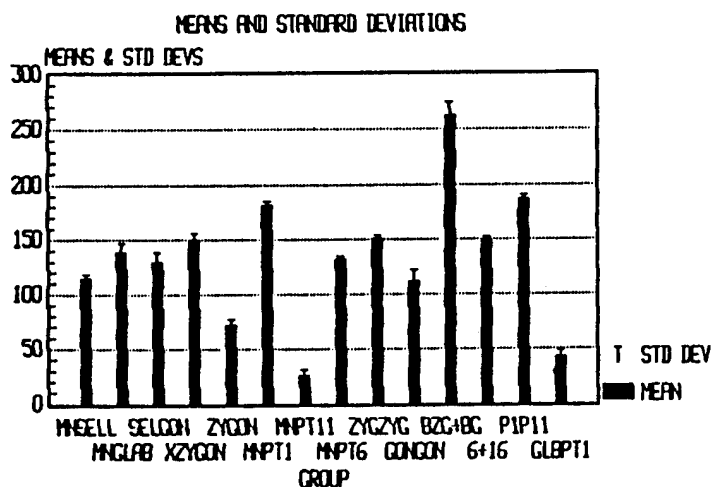
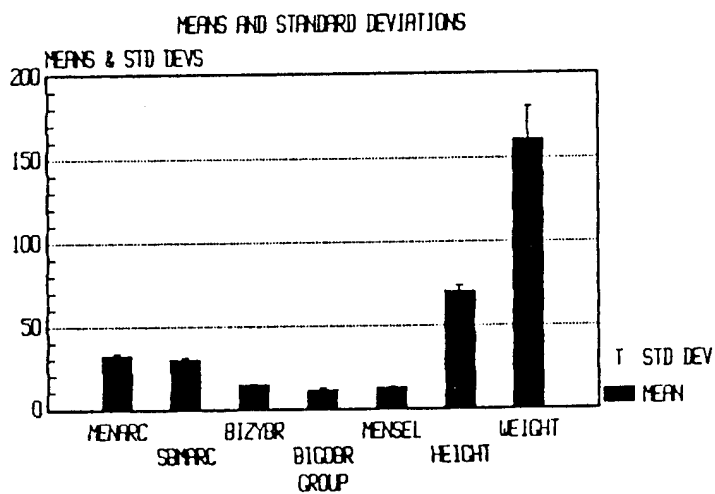


FIGURE A87

LARGE STATS

VAR NAME	SIZE	MEAN	SAMPLE STD DEV	SAMPLE VARIANCE	COEF. OF VARIATION
MENARC	5	32.42	1.34425	1.807	.04146
SBMARC	5	29.84	1.71552	2.943	.05749
BIZYBR	5	14.18	.7225	.522	.05095
BIGOBR	5	10.8	1.29035	1.665	.11948
MENSEL	5	12.08	.48166	.232	.03987
HEIGHT	5	70.6	3.20936	10.3	.04546
WEIGHT	5	161.4	19.29508	372.3001	.11955



VAR NAME	MEAN	STD ERR	LOWER 95%	UPPER 95%	LOWER 99%	UPPER 99%
MENARC	32.42	.601	30.751	34.089	29.652	35.188
SBMARC	29.84	.767	27.71	31.97	26.308	33.372
BIZYBR	14.18	.323	13.283	15.077	12.692	15.668
BIGOBR	10.8	.577	9.198	12.402	8.143	13.457
MENSEL	12.08	.215	11.482	12.678	11.088	13.072
HEIGHT	70.6	1.435	66.616	74.584	63.992	77.208
WEIGHT	161.4	8.629	137.446	185.354	121.672	201.128

FIGURE A88

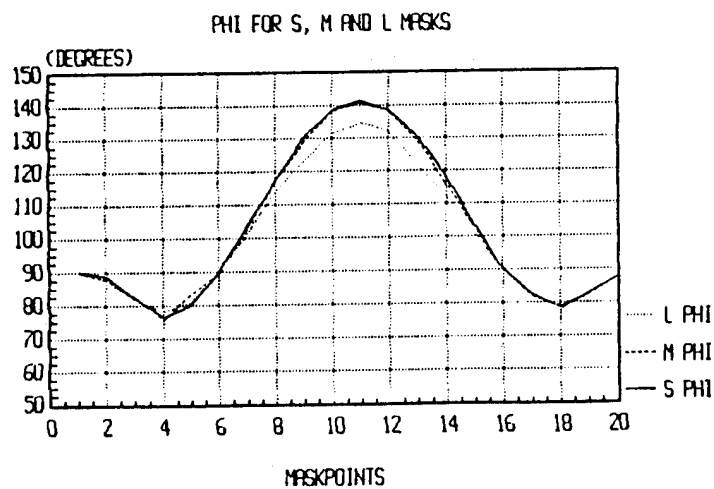
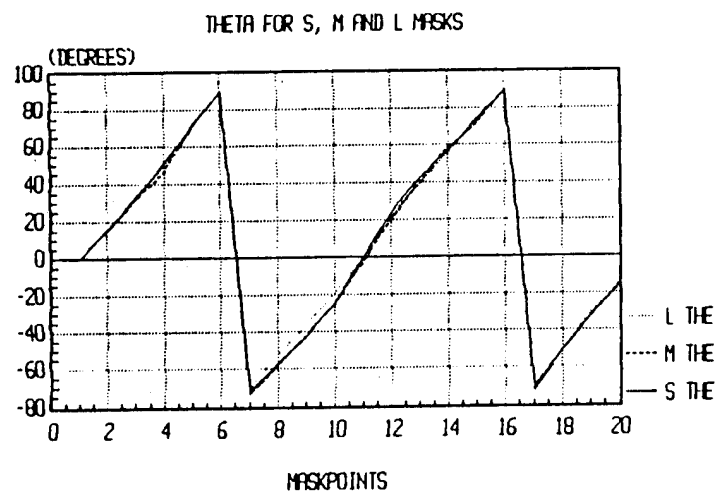
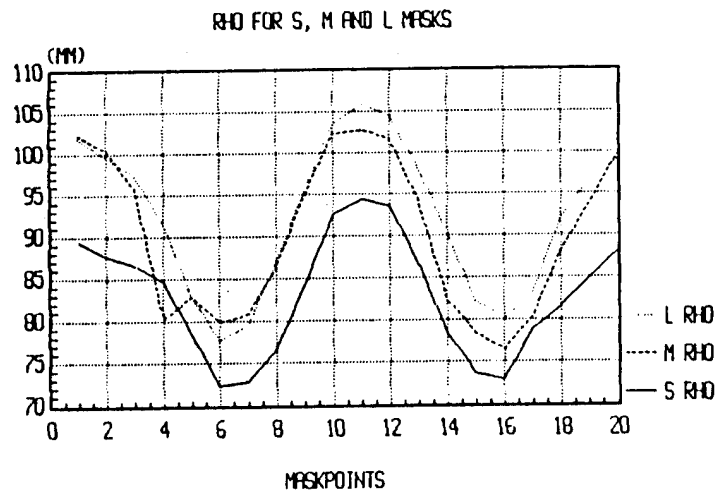


FIGURE A89

RHO, THETA AND PHI FOR SMALL MASK

	S RHO	S THE	S PHI
1	89.43	0	90
2	87.88	15.46	88.81
3	86.82	32	82.41
4	84.54	51	78.35
5	78.44	71.01	79.85
6	72.22	90	90
7	72.72	-72.24	104.08
8	78.67	-57.23	117.3
9	84.21	-43	130.23
10	92.6	-24.6	138.95
11	94.42	-0.01	141.64
12	93.49	23.78	138.85
13	86.69	41.89	130.74
14	78.36	57.01	118.18
15	73.58	73.55	103.59
16	72.81	90	90
17	78.91	-71.48	82.36
18	81.57	-50.74	78.43
19	84.92	-32.69	82.64
20	88.08	-15.1	87.67

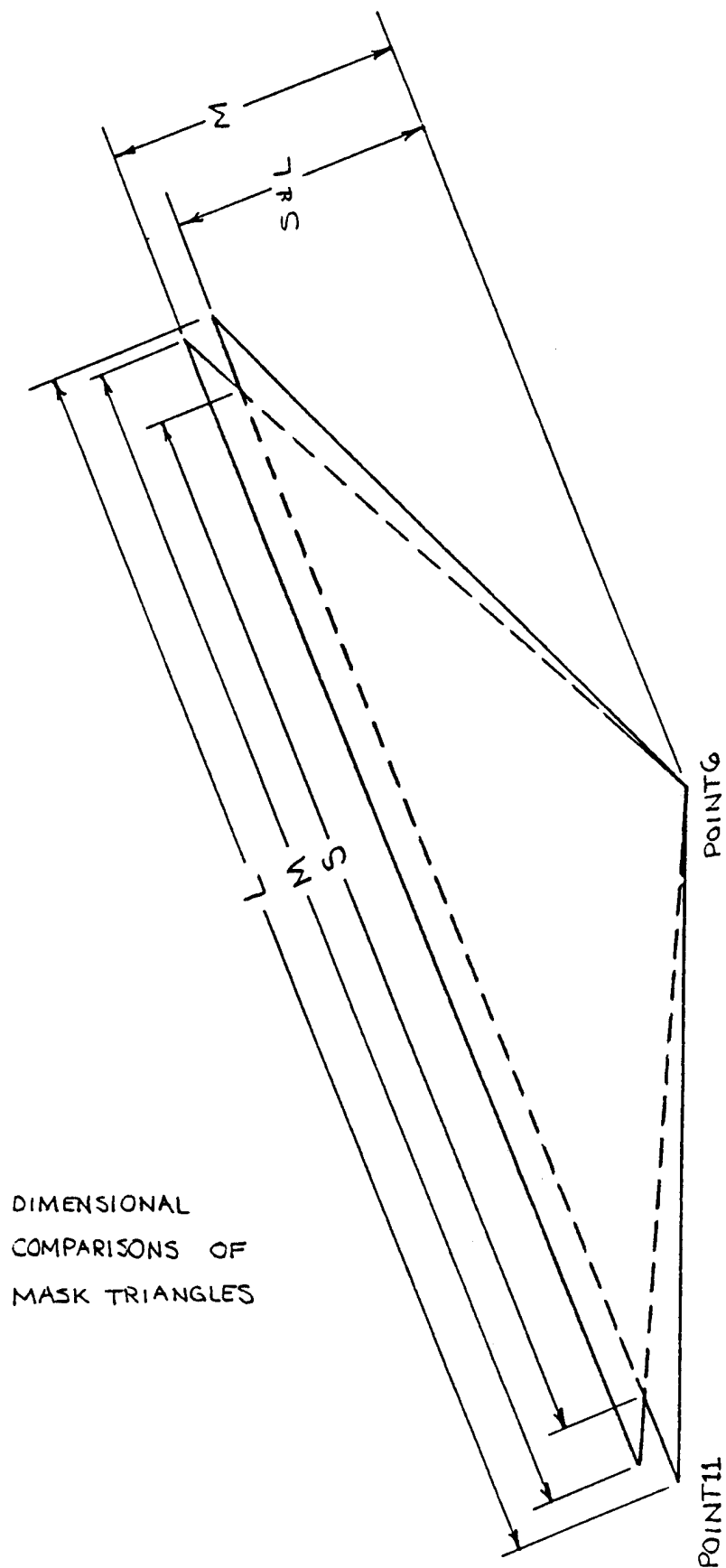
RHO, THETA AND PHI FOR MEDIUM MASK

	M RHO	M THE	M PHI
1	102.37	0	90
2	100.41	14.83	87.64
3	95.84	31.02	82.87
4	80.32	48.56	75.78
5	82.84	70.58	83.25
6	79.87	90	90
7	80.85	-73.54	102.75
8	86.26	-58.34	116.97
9	94.87	-41.99	128.65
10	102.4	-25.1	138.55
11	102.82	-2.79	141.17
12	101.76	19.77	138.19
13	94.24	39.27	129.46
14	82.41	58.57	116.06
15	78.36	70.78	102.78
16	76.33	90	90
17	80.42	-69.94	81.96
18	88.07	-51.24	78.71
19	93.67	-32.29	82.36
20	99.78	-14.32	87.72

RHO, THETA AND PHI FOR LARGE MASK

	L RHO	L THE	L PHI
1	101.93	0	90
2	99.57	15.95	87.47
3	97.49	32.38	81.84
4	91.46	50.03	78.29
5	82.95	69.95	80.97
6	77.71	90	90
7	79.61	-70.43	101.37
8	86.97	-52.3	113.94
9	95.61	-36.4	122.94
10	103.81	-19.4	131.57
11	105.96	.02	134.82
12	104.47	21.49	132.15
13	98.24	38.85	122.09
14	90.29	55.34	112.32
15	82.23	72.75	100.87
16	80.04	90	90
17	83.23	-72.91	82.63
18	91.98	-50.83	77.81
19	98.64	-30.29	82.68
20	99.08	-16.7	87.48

FIGURE A90



DIMENSIONAL
COMPARISONS OF
MASK TRIANGLES

FIGURE A91

FACE AND MASK TRIANGLES

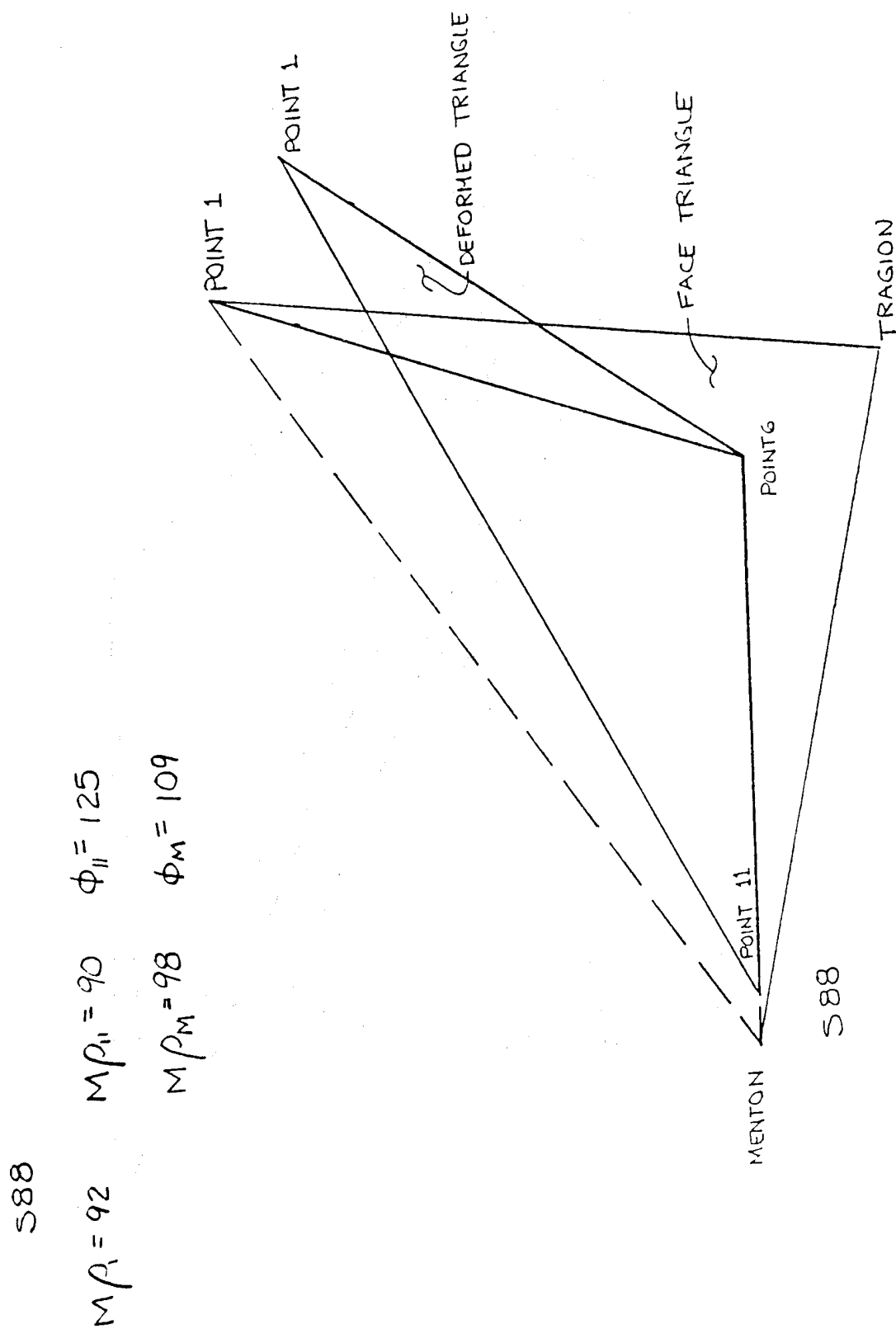


FIGURE A92

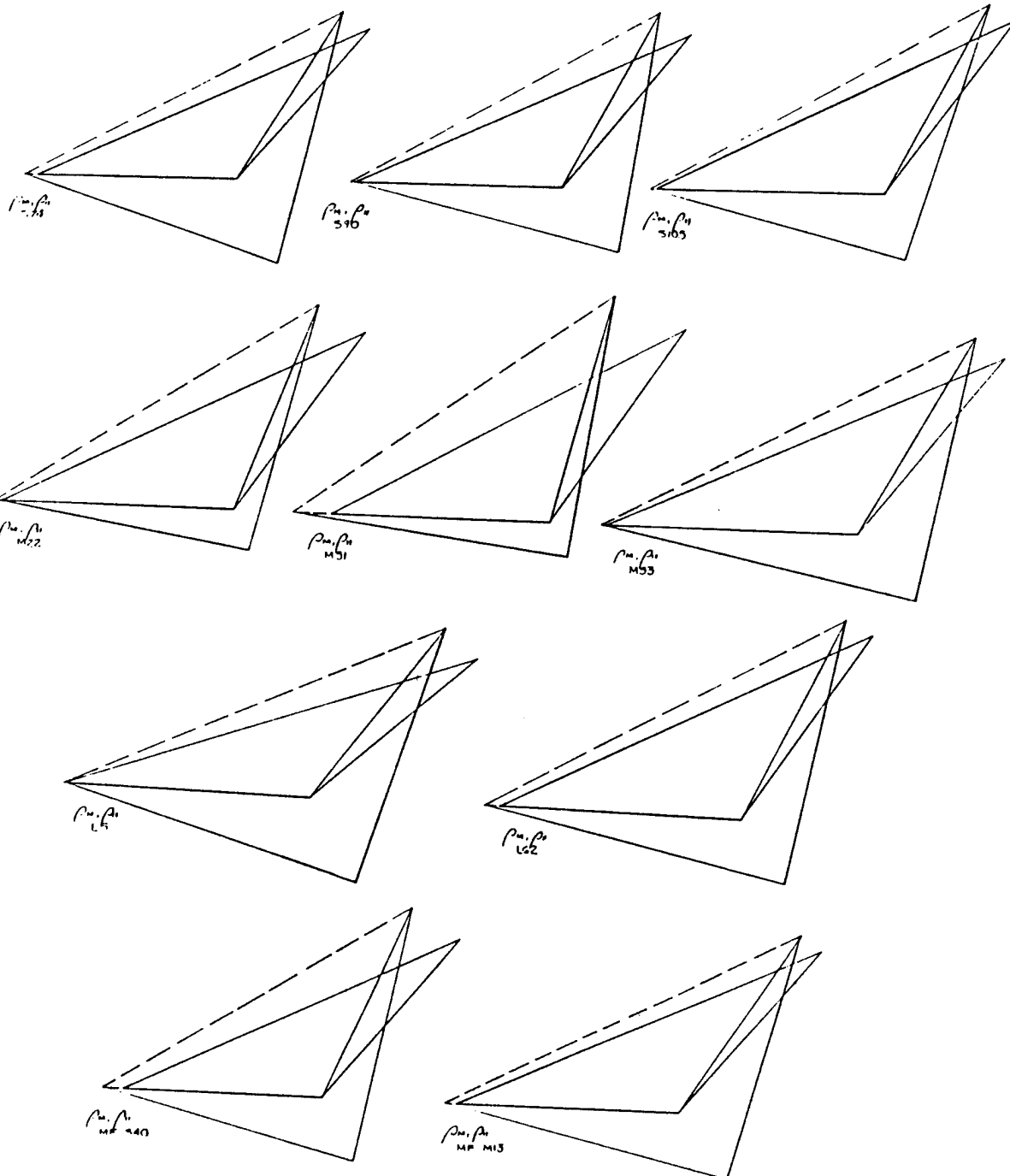
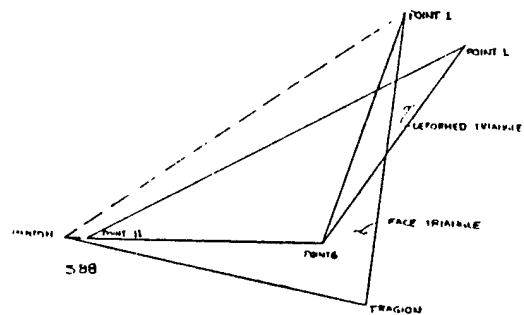


FIGURE A93

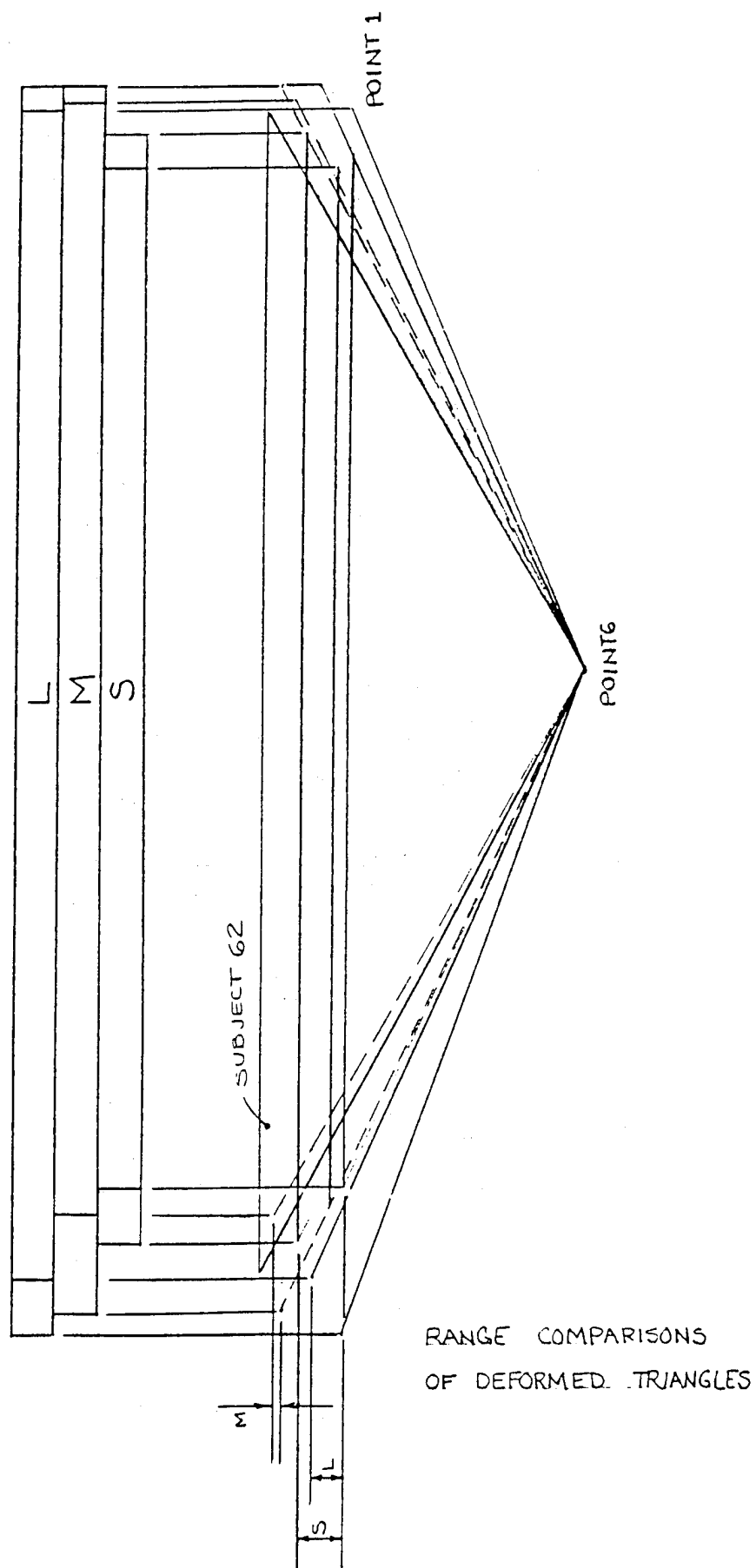
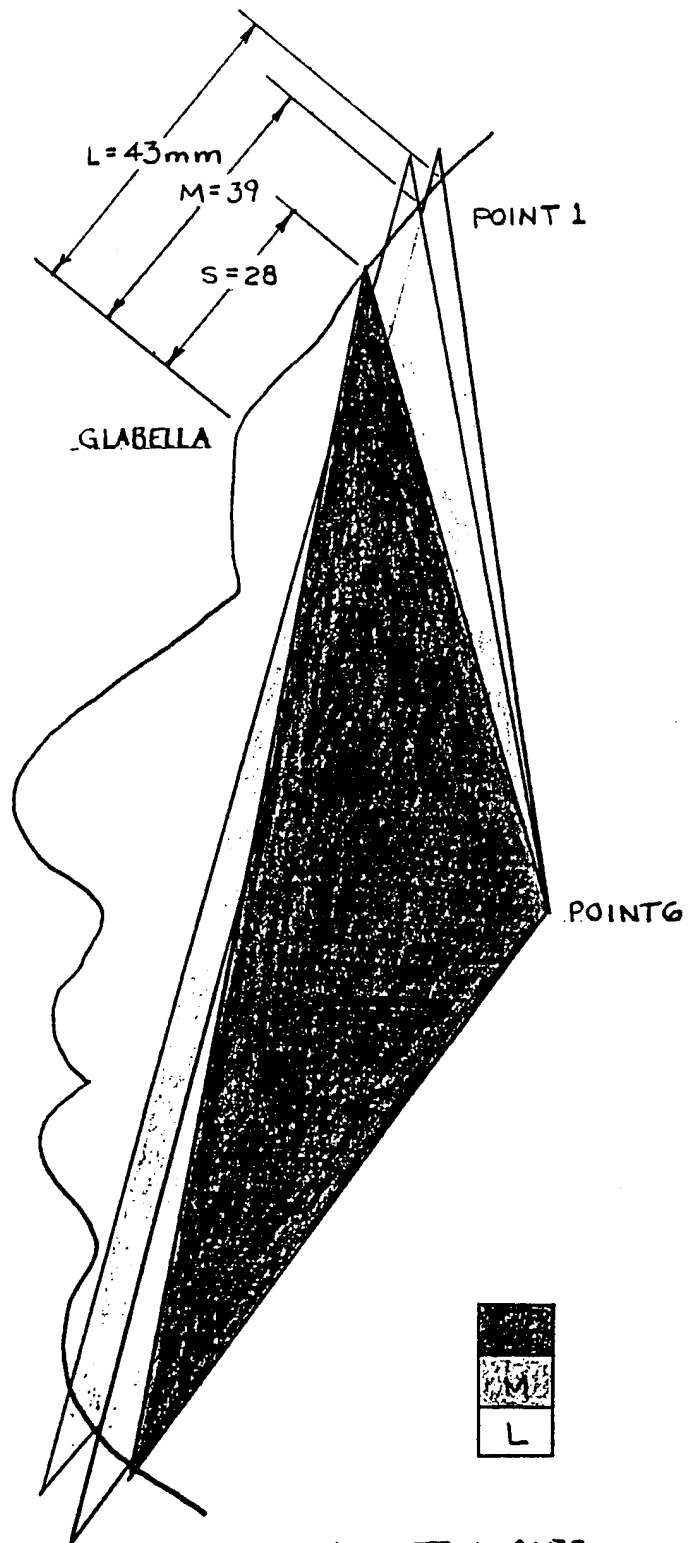


FIGURE A94



MASK TRIANGLES ON A PROFILE

FIGURE A95

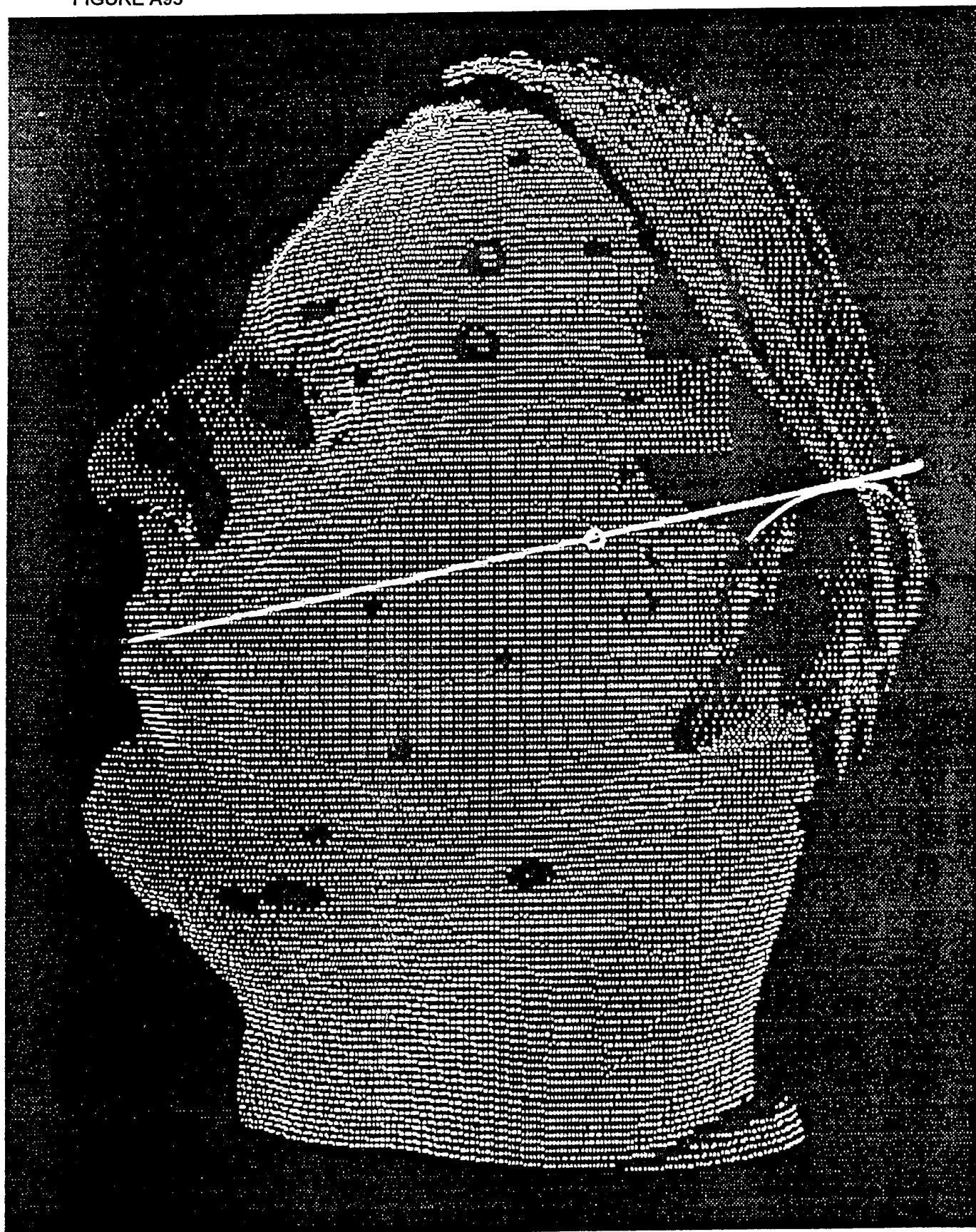
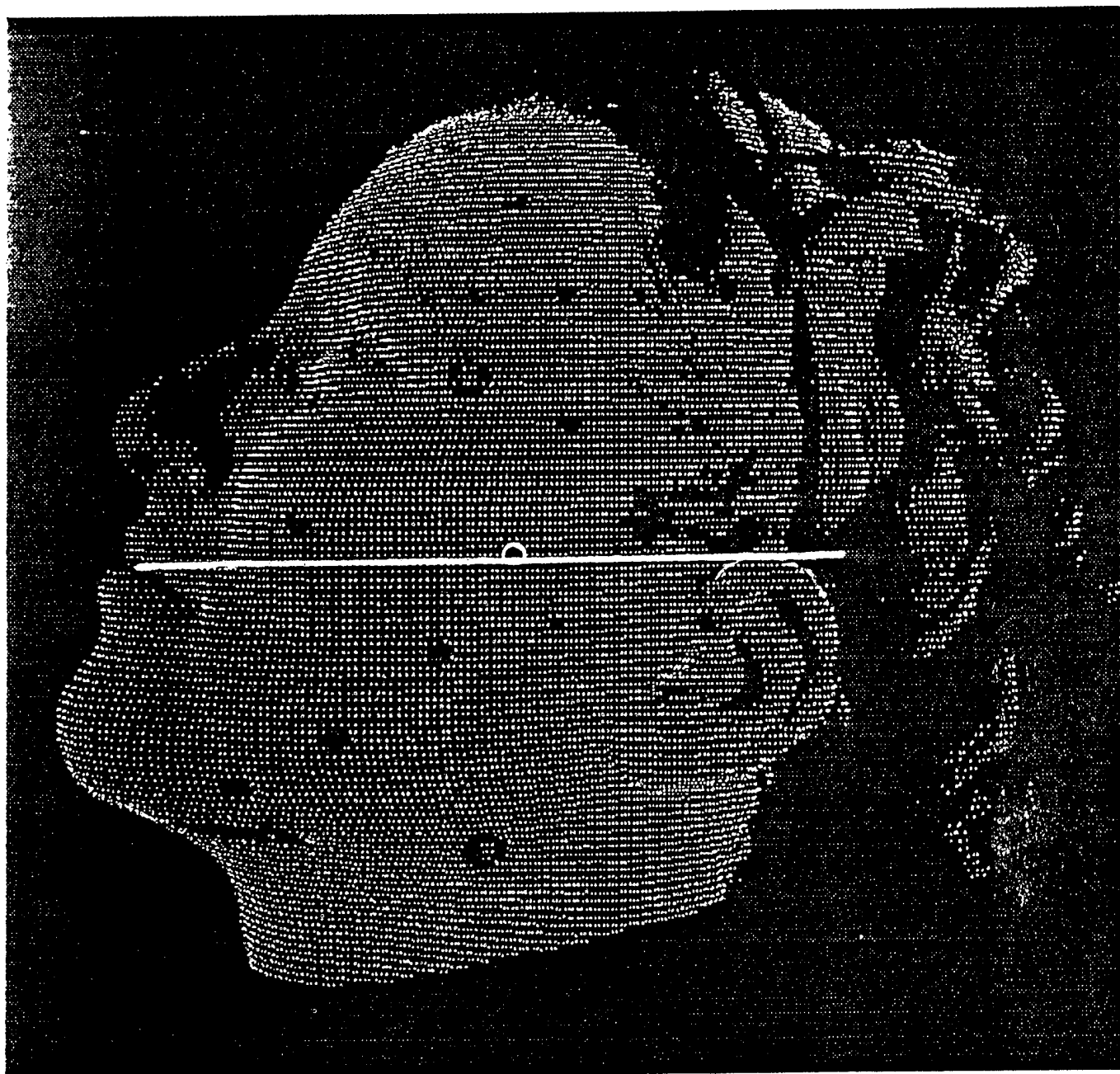
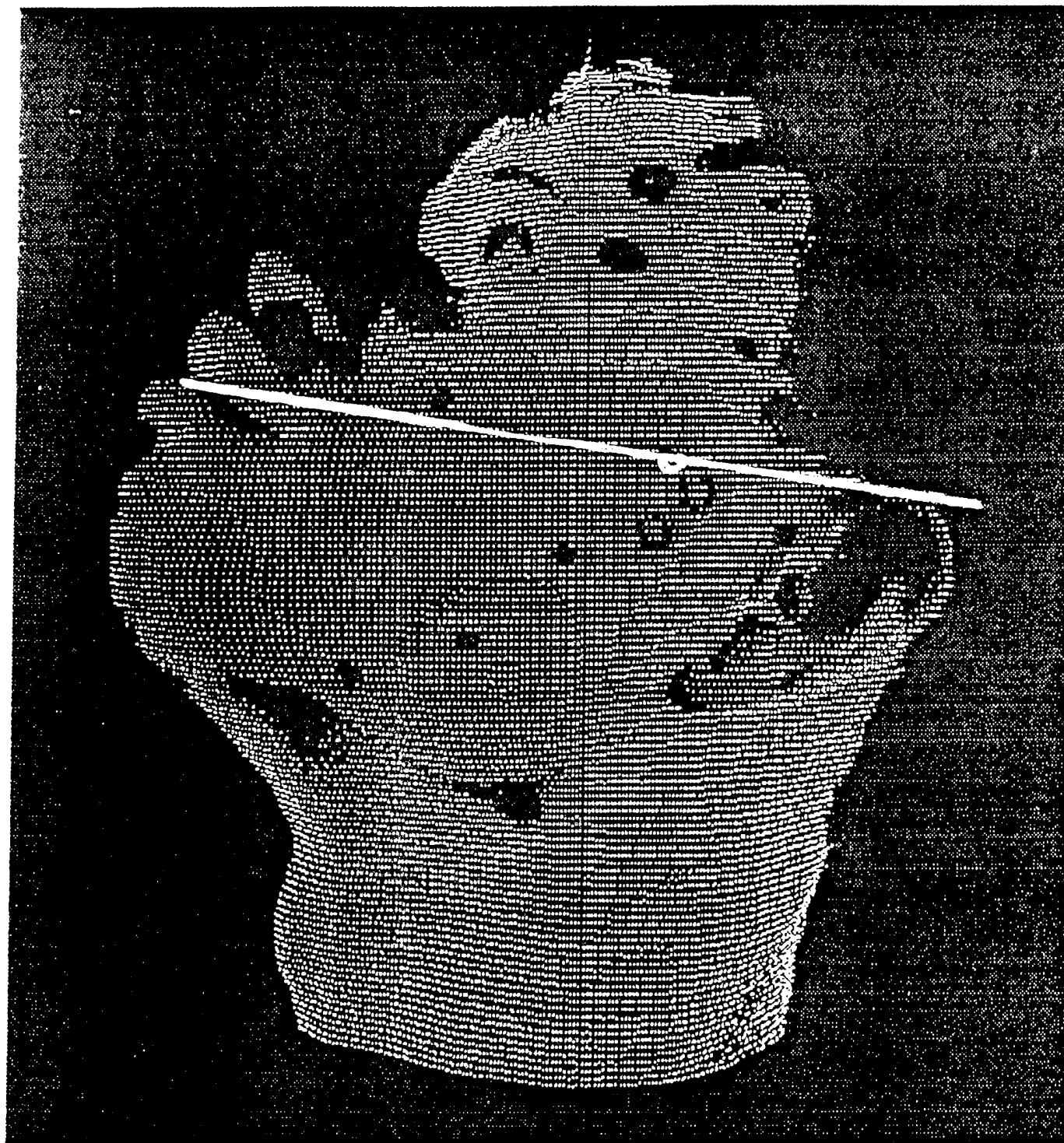


FIGURE A96



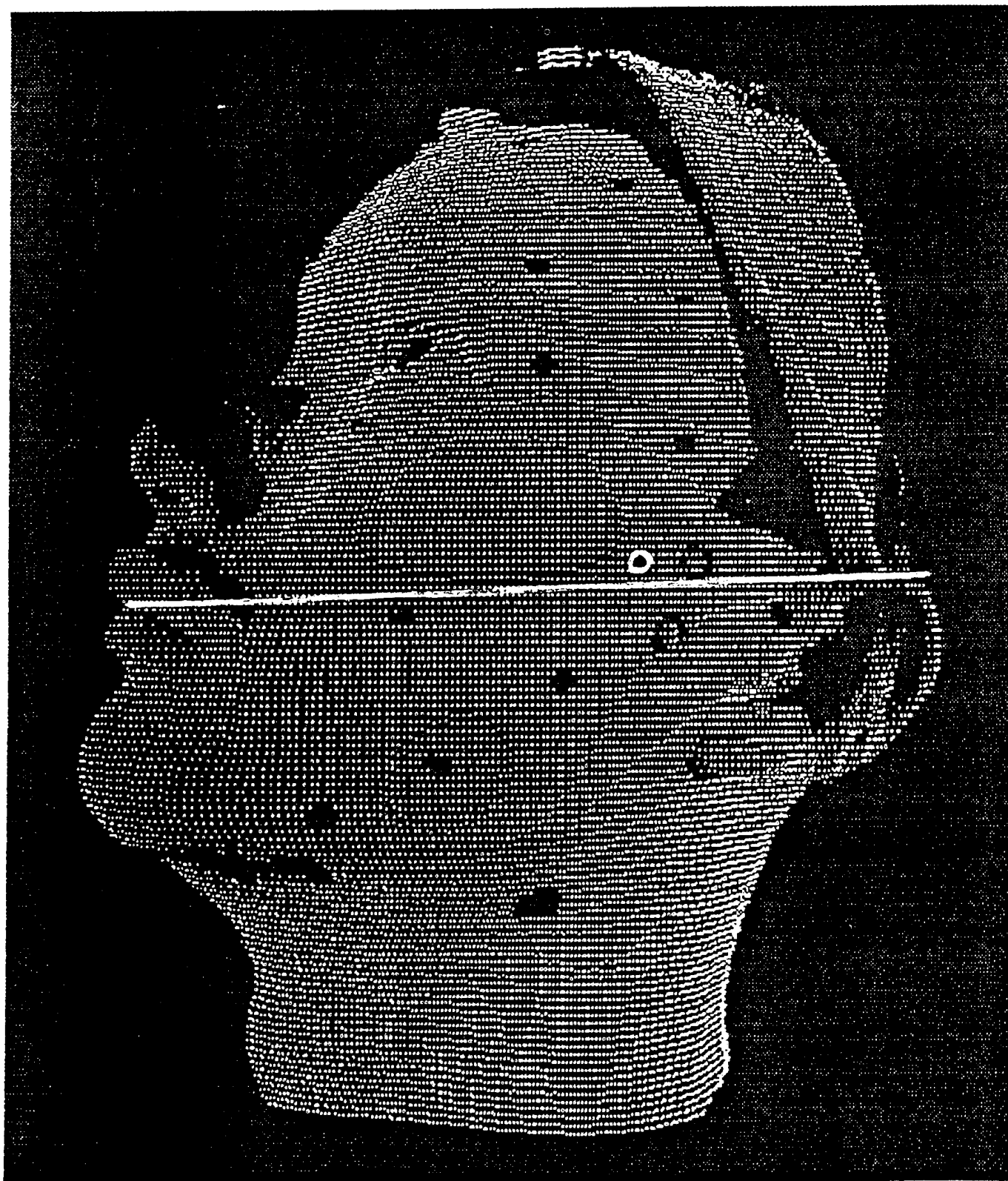
Subject # 74

FIGURE A97



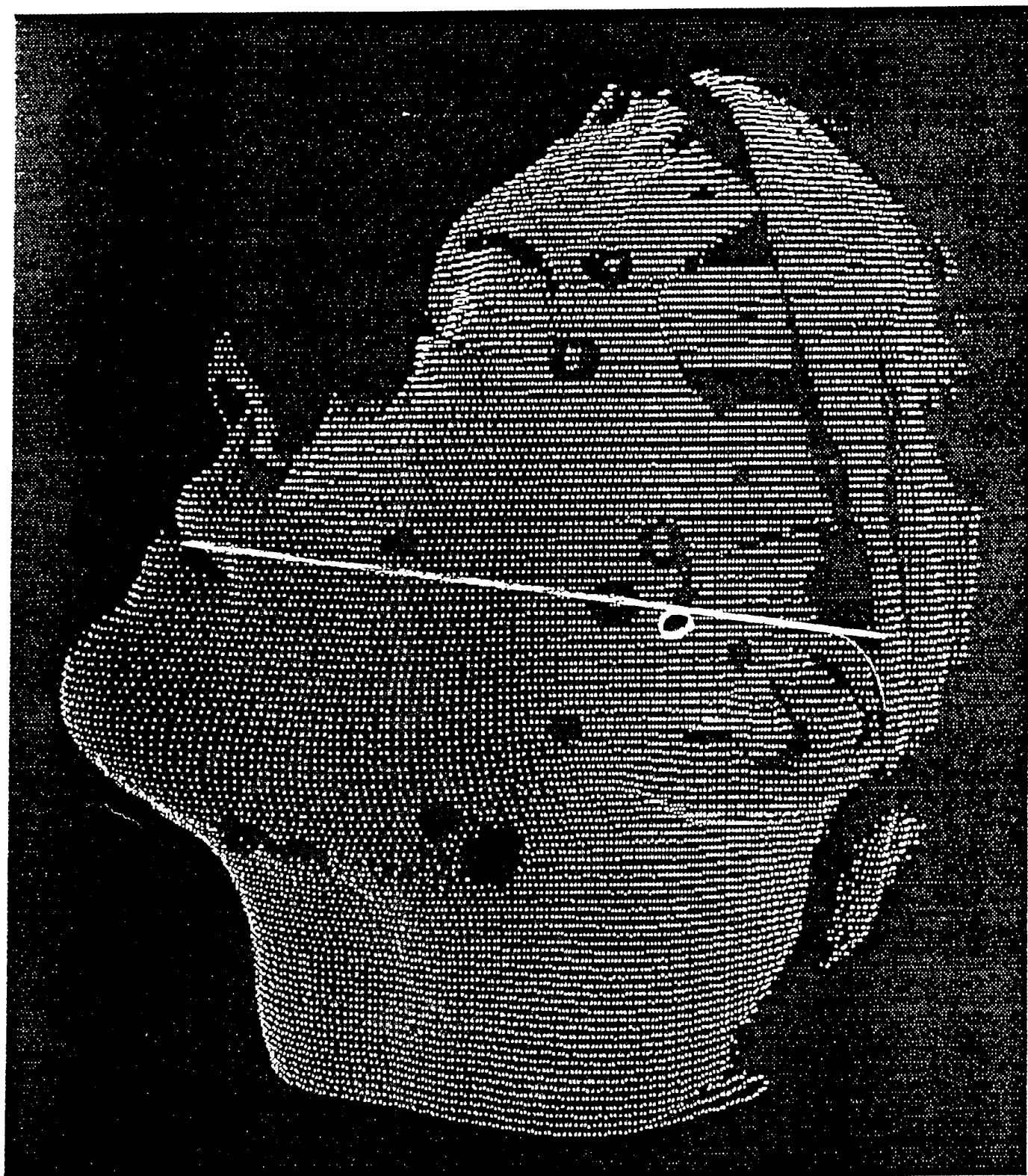
Subject #62

FIGURE A98



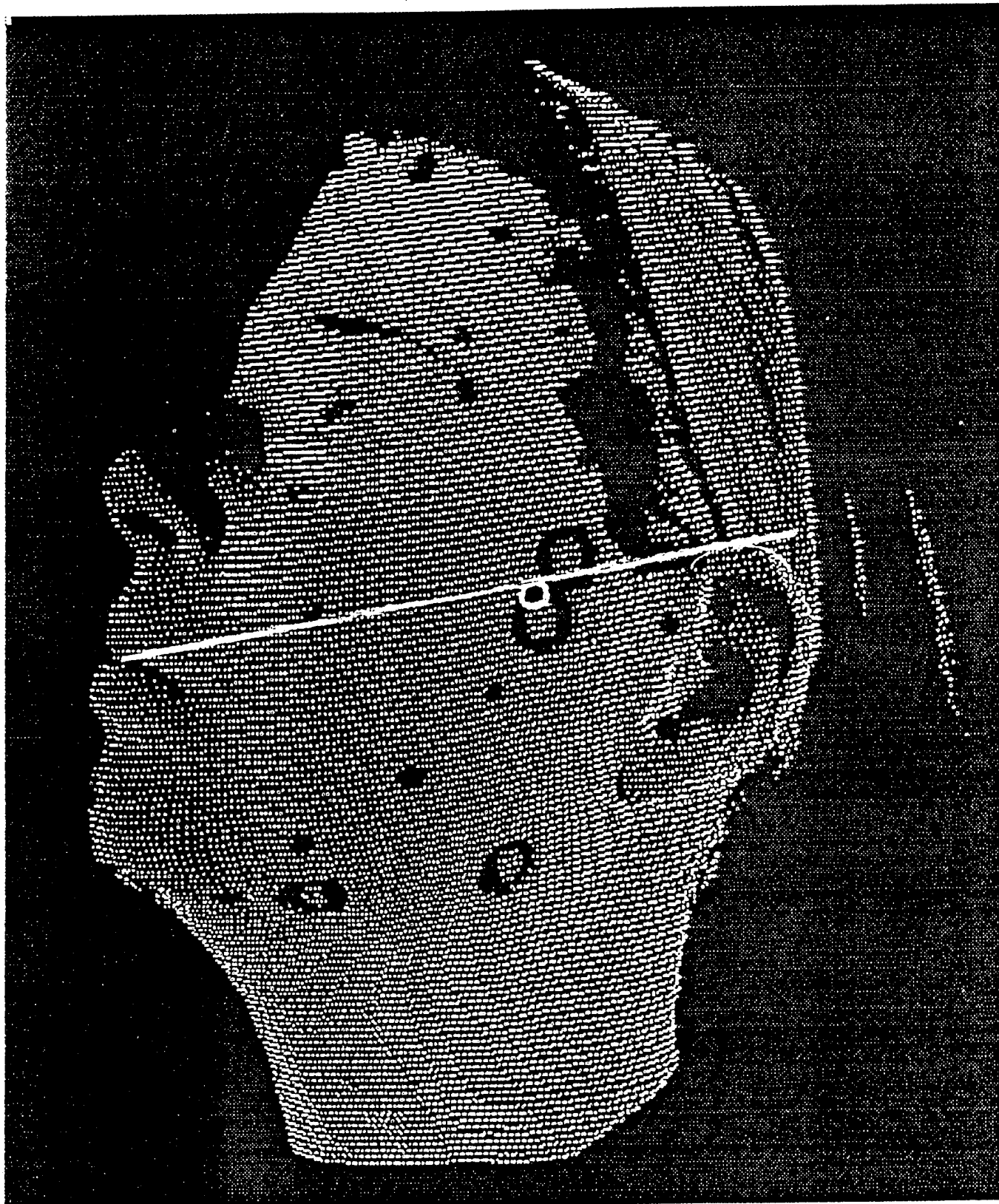
Subject #13

FIGURE A99



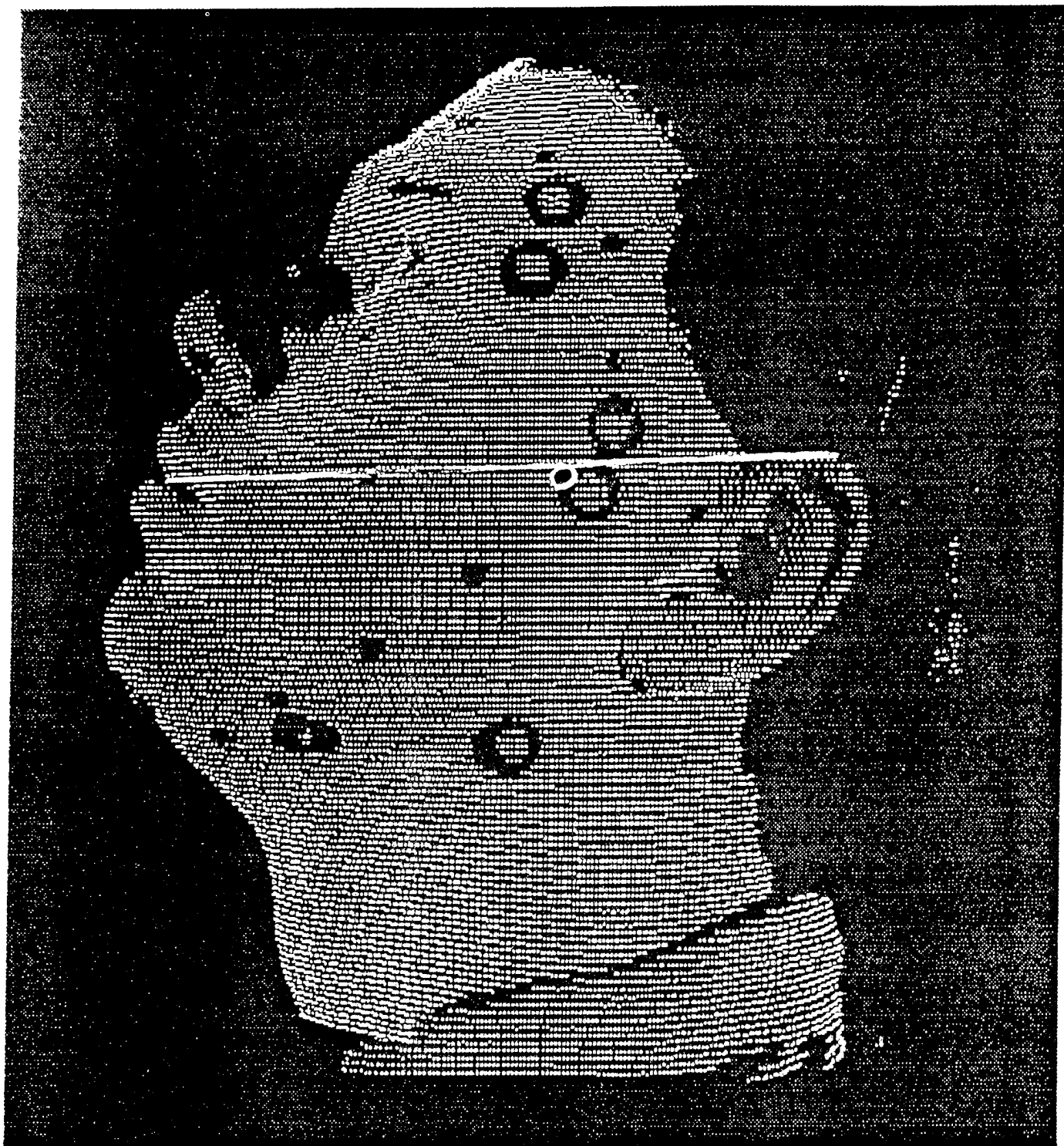
Subject #57

FIGURE A100



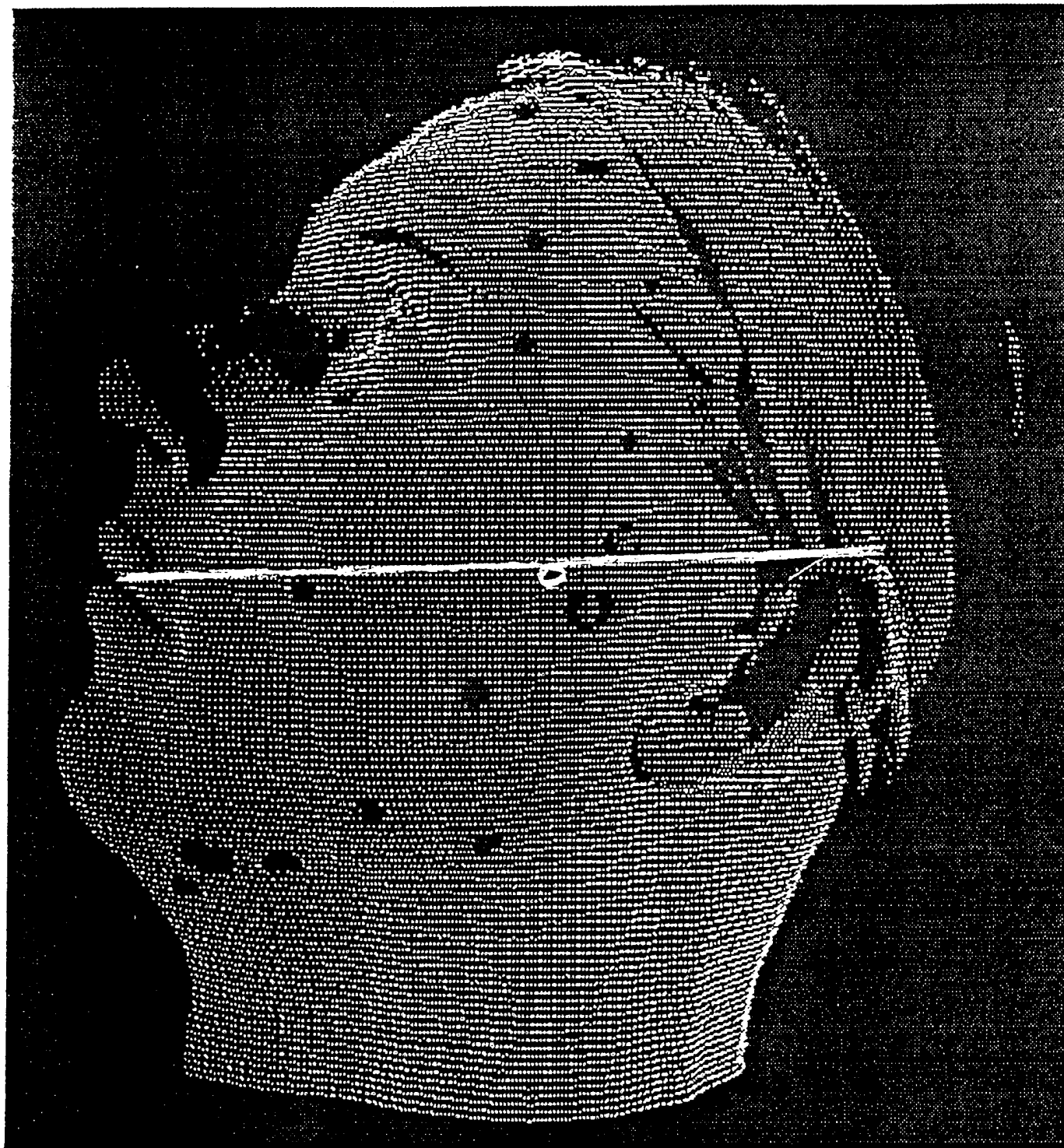
Subject #105

FIGURE A101



Subject #90

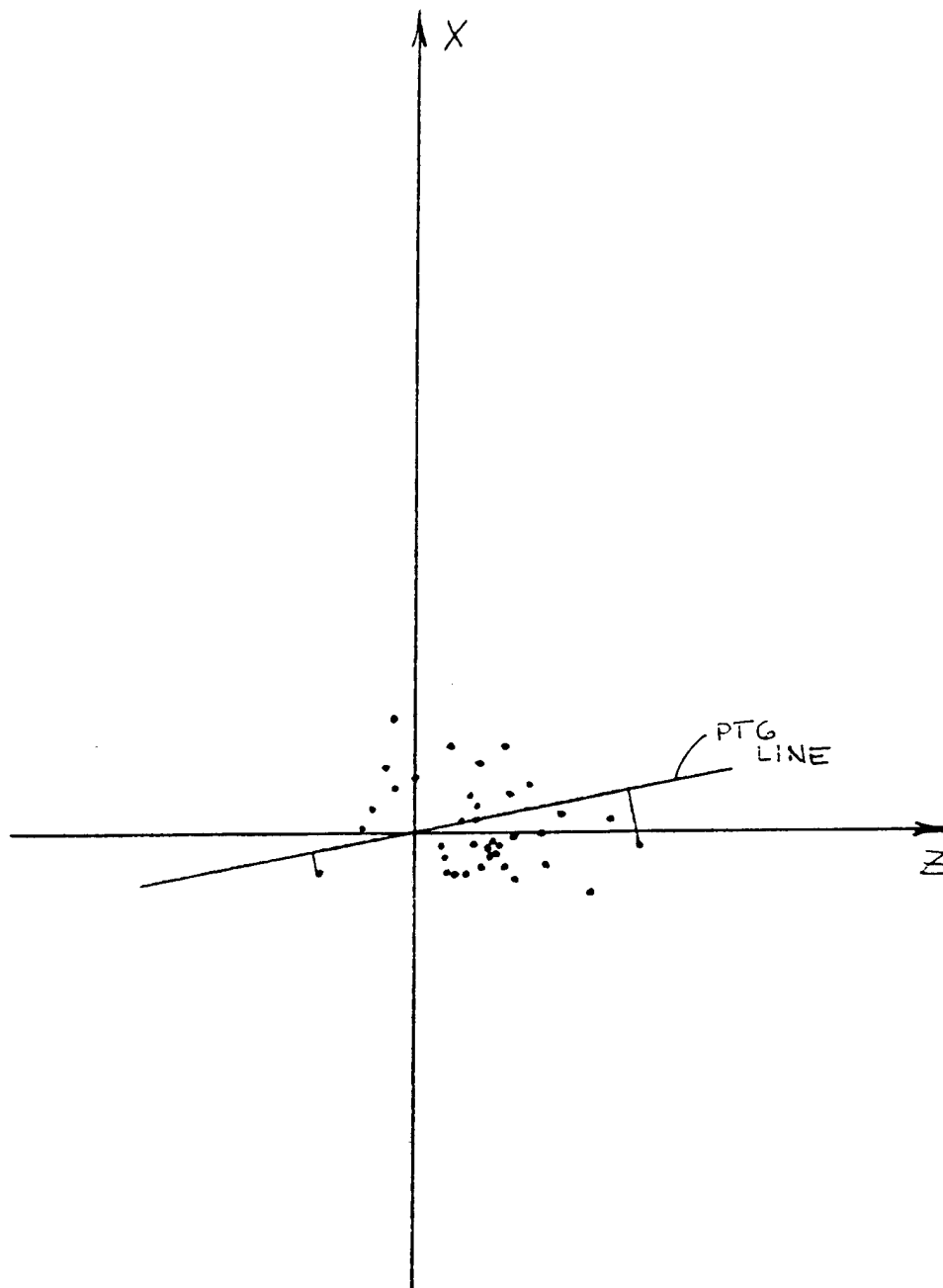
FIGURE A102



SUBJECT #5

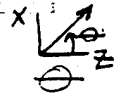
FIGURE A103

PLOT OF L. ZYGION ABOUT PTG ORIGIN



L. ZYGION COORDINATES

FIGURE A104

SUB.	mask system			r $\sqrt{x^2+z^2}$ (mm)	
	x (mm)	y (mm)	z (mm)		
41	-1.15	68.22	10.09	10.2	-7.
63	-2.41	73.93	9.75	10.0	-14.
64	9.27	69.22	8.94	12.9	46.
68	-0.97	68.45	10.82	10.9	-5.
70	-4.41	67.32	8.41	9.5	-28.
72	-8.05	71.50	24.06	25.4	-18.
73	4.27	66.12	12.93	13.6	18.
74	-4.02	72.32	17.54	18.0	-13.
88	9.47	68.34	-3.84	10.2	112.
89	1.21	66.59	7.02	7.1	10.
90	11.76	77.29	12.49	17.2	43.
93	-5.99	67.88	14.17	15.4	-23.
94	-0.93	71.10	7.52	7.6	-7.
96	-5.08	72.69	5.43	7.4	-43.
101	2.81	81.09	19.80	20.0	8.
103	-1.21	71.93	28.76	28.8	-2.
105	6.38	67.80	-2.49	6.8	111.
106	1.29	70.80	26.31	26.3	3.
107	4.28	76.71	8.12	9.2	28.
108	0.21	76.18	17.32	17.3	1.
109	5.13	72.10	7.53	9.1	34.
112	-5.46	72.25	4.58	7.1	-50.
113	-4.32	62.24	12.68	13.4	-19.
92	-2.51	74.33	10.96	11.2	-13.
40	2.09	69.05	7.59	7.9	15.
10	-2.28	74.82	9.80	10.1	-13.
22	-4.66	64.66	-13.48	14.3	-16.
23	-1.93	78.62	3.95	4.4	-26.
51	15.61	72.49	-2.76	15.9	100.
53	-5.54	75.72	13.60	14.7	-22.
56	0.78	73.25	-6.89	6.9	174.
60	3.69	72.93	-5.98	7.0	148.
81	11.81	81.69	-5.44	13.0	65.
91	-2.51	74.33	10.96	11.2	-13.
13	-0.26	80.68	12.88	12.9	-1.
5	6.91	85.54	16.09	17.5	23.
50	-1.09	75.40	11.27	11.3	-6.
62	-5.45	77.73	7.46	9.2	-36.
76	-3.00	76.73	4.18	5.1	-36.
87	7.88	71.36	-0.04	7.9	90.

CURRENT REGRESSION SUMMARY TABLE

DEPENDENT VARIABLE: Z

MULTIPLE R = .7317
 STD ERR EST = 5.9043
 F = 7.2997

IND VAR	B COEF	STD ERR(B)	T-VALUE	PROB
ZYGZYG	.884552	.363302	2.434754	.0249
GONGON	-.231348	.271119	-.853309	.4041
ANARHM	.441155	.209801	2.10273	.049
CONSTANT	-143.3126			

	ACTUAL 'Y'	PREDICTED 'Y'	RESIDUAL
1	10.09	4.822655	5.267346
2	9.75	10.05681	-.306808
3	8.94	10.15089	-1.210887
4	10.82	12.89386	-2.07386
5	8.41	9.716462	-1.306461
6	24.06	18.63769	5.422312
7	12.93	14.26863	-1.338627
8	17.54	11.79966	5.740345
9	-3.84	3.153057	-6.993057
10	7.02	6.55109	.46891
11	12.49	17.16556	-4.675562
12	14.17	8.953178	5.216822
13	7.52	13.70055	-6.18055
14	5.43	9.74331	-4.313309
15	19.8	24.34025	-4.540249
16	28.76	23.98551	4.774489
17	-2.49	7.855	-10.345
18	26.31	12.07334	14.23666
19	8.12	8.10072	.01928
20	17.32	19.60572	-2.285725
21	7.53	2.215424	5.314577
22	4.58	8.258637	-3.678636
23	12.68	9.892232	2.787769

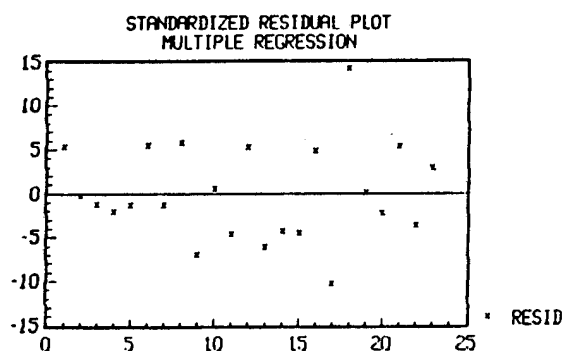


FIGURE A106

CURRENT REGRESSION SUMMARY TABLE

DEPENDENT VARIABLE: Z

MULTIPLE R = .8526
 STD ERR EST = 6.1613
 F = 4.4365

IND VAR	B COEF	STD ERR(B)	T-VALUE
ZYGZYG	.618843	.586475	1.055191
GONGON	.104997	.567514	.185013
ANARHM	.481281	.331057	1.453771

CONSTANT
 -161.9147

	ACTUAL 'Y'	PREDICTED 'Y'	RESIDUAL
24	9.8	6.92899	2.871011
25	-13.48	-11.33472	-2.145279
26	3.95	5.31118	-1.36118
27	-2.76	-4.750133	1.990134
28	13.6	14.82179	-1.221785
29	-6.89	-4.618789	-2.27121
30	-5.98	.407665	-6.387665
31	5.44	7.785759	-2.345759
32	10.96	.08828	10.87172

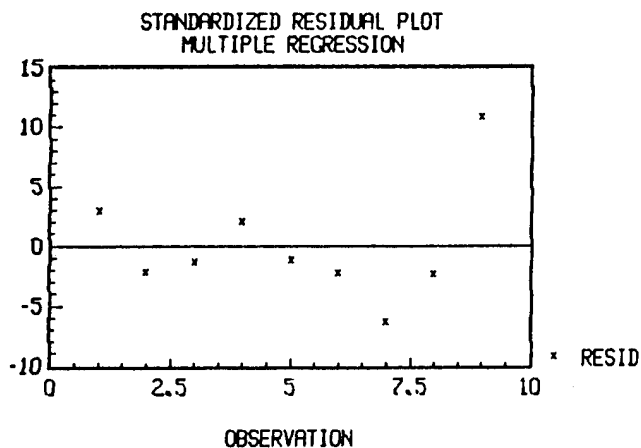


FIGURE A107

PREDICTION OF ZYGION'S Z COMPONENT- LARGE GROUP
CURRENT REGRESSION SUMMARY TABLE

DEPENDENT VARIABLE: Z

MULTIPLE R = .9997
STD ERR EST = .2904
F = 614.1914

IND VAR	B COEF	STD ERR(B)	T-VALUE	PROB
-----	-----	-----	-----	-----
ZYGZYG	.034846	.055398	.629008	.6426
GONGON	.356056	.015037	23.67937	.0269
ANARHM	.630843	.033802	18.66277	.0341

CONSTANT
-120.2754

	ACTUAL 'Y'	PREDICTED 'Y'	RESIDUAL
	-----	-----	-----
33	16.09	16.23269	-.142689
34	11.27	11.13043	.139568
35	7.46	7.426026	.033975
36	4.18	4.049057	.130943
37	-.04	.121803	-.161803

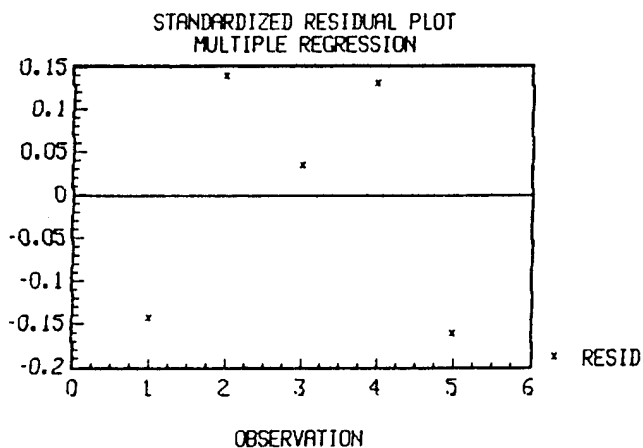


FIGURE A108

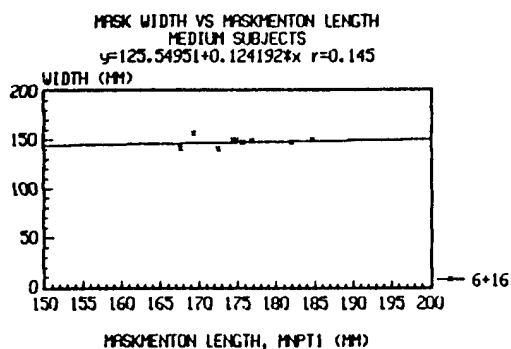
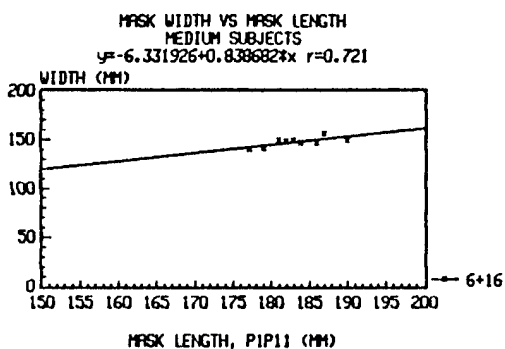
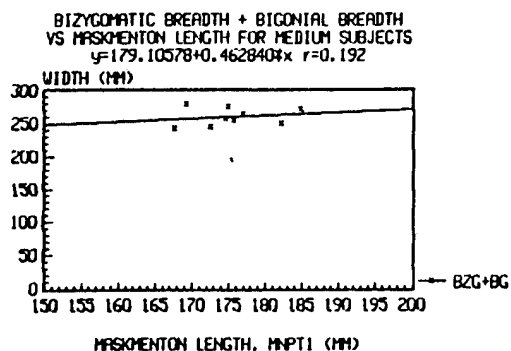
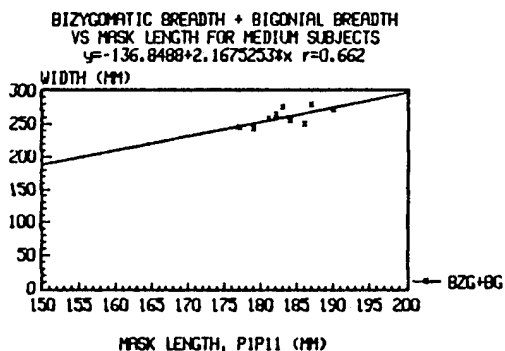
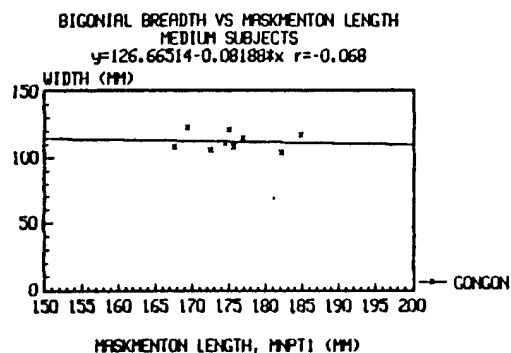
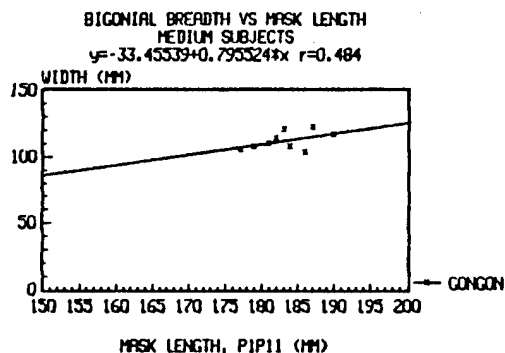
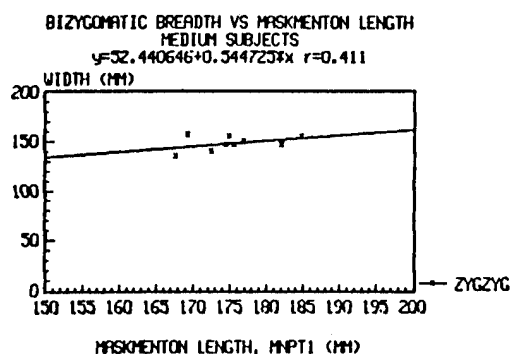
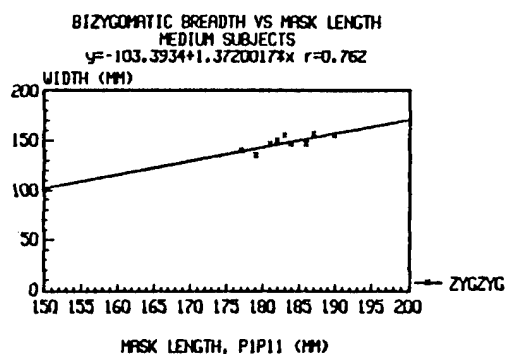


FIGURE A109

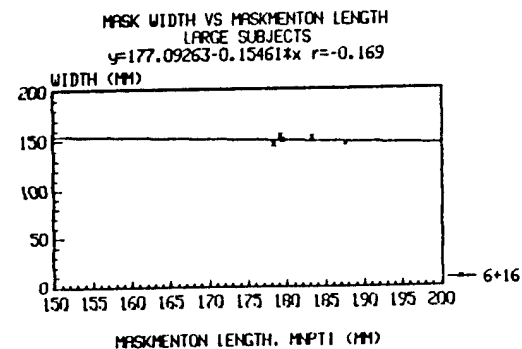
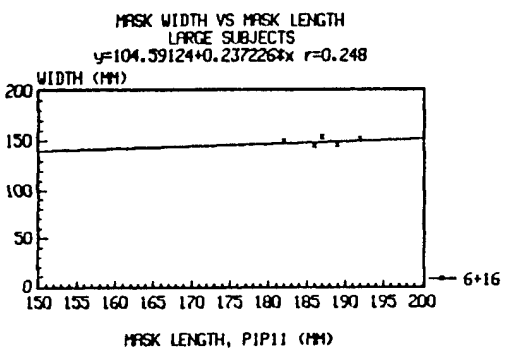
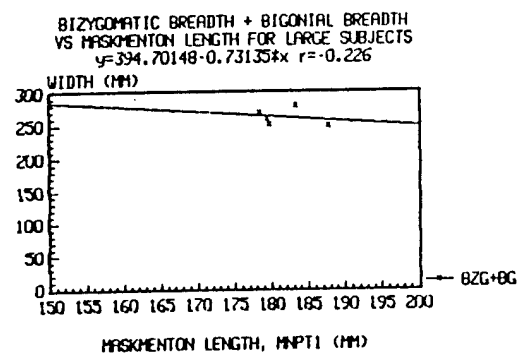
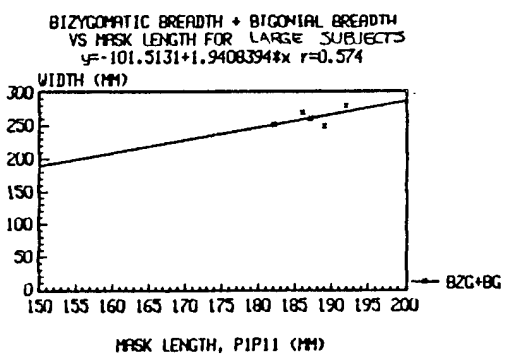
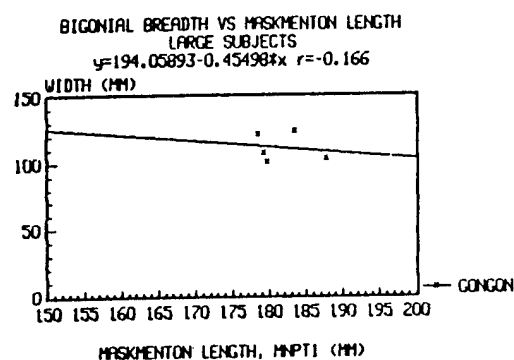
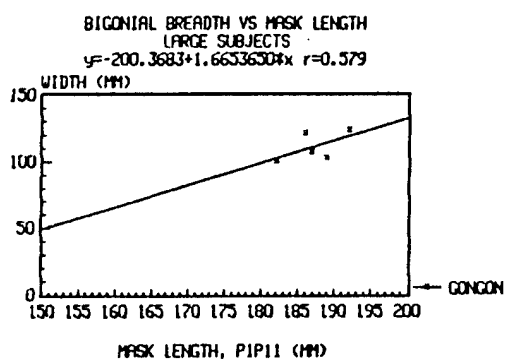
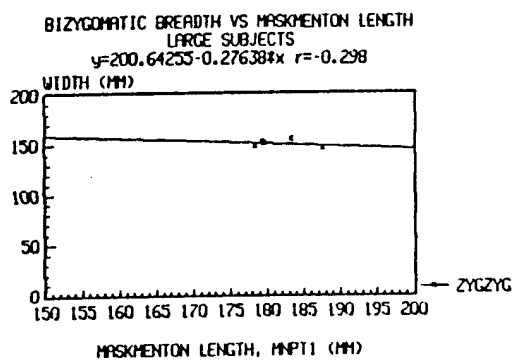
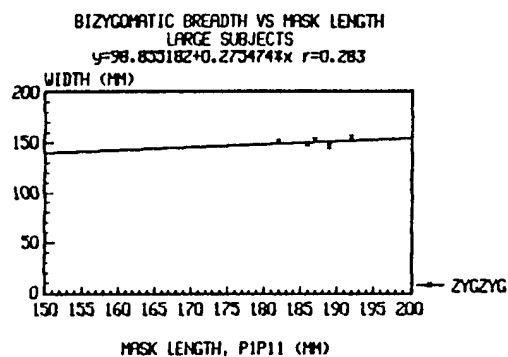


FIGURE A110

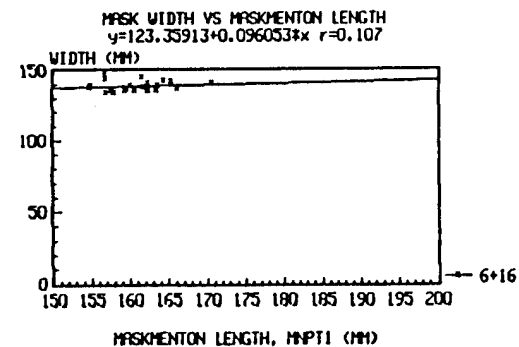
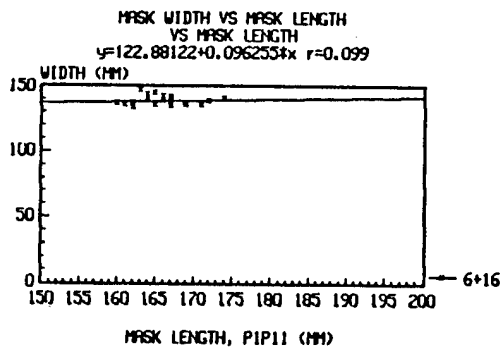
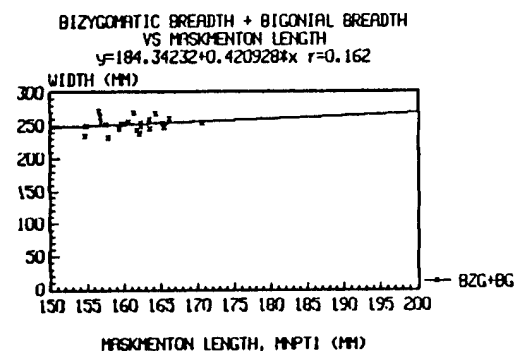
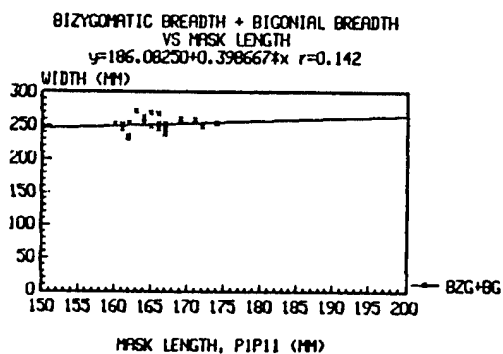
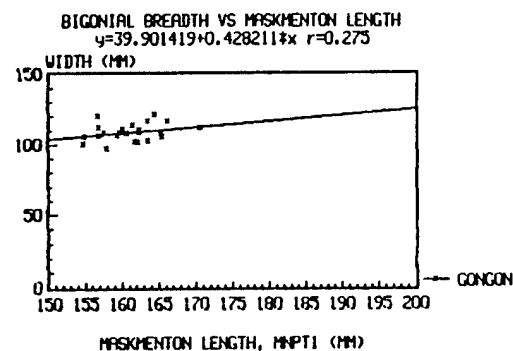
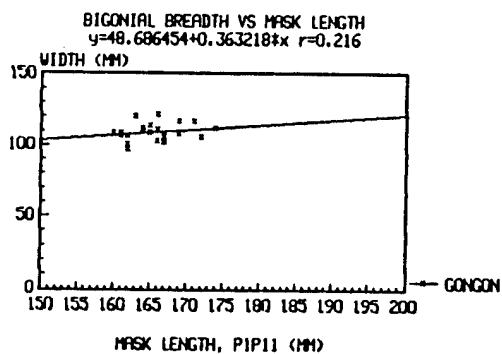
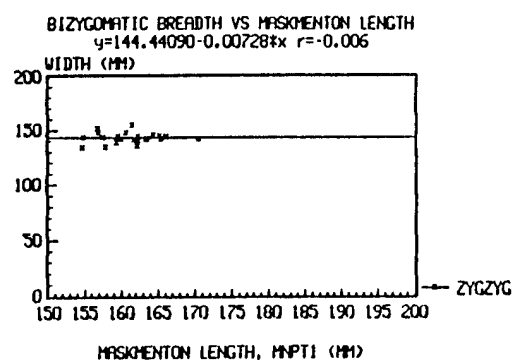
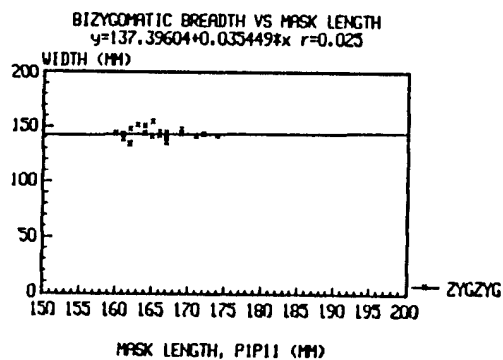


FIGURE A111

COMPARISON OF SIZING METHODS FOR SELECTED SAMPLE POPULATION					MASK SIZE PRESCRIBED BY VARIOUS METHODS				FF SCORE $\times 10^3$ FOR METHOD PRESCRIBED SIZE			
SUBJECT 4 SUBJECTIVES					THEORETICAL							
PREFERENCE	DISCOMFORT				PHASE 1 SIZE	CALIPER SIZE	MSL SIZE	SLATE SIZE	SCORE PHASE 1 SIZE	SCORE CALIPER SIZE	SCORE MSL SIZE	SCORE SLATE SIZE
	S	M	L									
1	S		✓e	41	S	S	M	M	320	320	11	11
2	S	b		63	S	S	M	M	140	140	140	69
3	M	b	✓s	64	M	M	M	M	140	30	30	30
4	M	✓b	b	68	S	S	M	M	310	310	310	220
5	M	✓b	—	70	S	S	M	M	620	620	110	110
6	L	t		72	M	M	M	M	210	100	100	100
7	L			73	M	M	M	M	260	160	160	160
8	M	✓b	—	74	S	M	L	L	180	180	110	59
9	M	✓b,t	—	88	S	S	S	S	600	600	600	600
10	M	✓b,t	✓e	89	S	S	S	S	480	480	480	480
11	M	s	✓e	90	S	M	M	M	340	170	170	170
12	M	✓b,t	✓e	93	S	S	M	M	430	430	430	220
13	M	✓b,t	✓e	94	S	S	M	M	350	350	350	150
14	S	✓c	✓e	96	S	S	S	S	460	460	460	460
15	M	t	✓c	101	S	M	L	L	230	230	110	570
16	L	✓b,t	✓c	103	L	L	L	L	230	95	95	95
17	S	s	✓c	105	S	S	S	S	240	240	240	240
18	S	✓b	✓c	106	S	M	M	M	590	590	270	270
19	S	✓b	o	107	S	S	M	M	110	110	110	16
20	S	✓b	n	108	S/M	M	M	M	550	240*	240	240
21	S	c	✓t	109	S	S	S	S	470	470	470	470
22	S	✓b,t	n	112	S	S	M	M	270	270	270	110
23	M	✓b,t	✓	113	S	M	M	M	310	310	120	120
24	M	—	—	10	M	M	M	L	260	260	260	190
25	M	—	—	22	S	S	S	S	170	13	13	13
26	M	—	—	23	S	M	M	L	130	260	130	1
27	S	—	n	51	M	M	M	M	390	390	390	390
28	S	—	✓n	53	M	M	M	L	140	140	140	110
29	S	b	✓e	56	S	S	M	M	290	290	290	290
30	L	t	✓c	60	M	M	M	M	190	190	190	190
31	L	n	✓c	81	M	L	L	L	230	230	20	20
32	M	s		91	S/M	M	M	M	140	70**	140	140
33	L	—	—	5	L	M	L	L	110	25	110	110
34	L	✓b,t		50	M	M	M	M	120	14	14	14
35	L	✓b,t		62	S	M	M	M	570	250	230	230
36	L	✓b,c	✓c	76	M	M	L	L	170	110	110	170
37	L	b	✓	87	M	M	M	M	670	200	200	200

✓ MEANS DISCOMFORT WAS REPORTED. b MEANS BREATHING RESTRICTED. c MEANS NOSECUP PBM. t MEANS TIGHT. c MEANS CHIN PBM. s MEANS SPEECH PBM. e MEANS EYE OR VISION PBM.

* ASSUMED M
** ASSUMED S

FIGURE A112

SIZE	BESTFIT	CALIPER	MSL	SLATE	
S	23	17	11	5	
M	9	5	6	4	
L	5	0	1	2	
TOTAL	37	22	18	11	88

H_0 : differences between sizing methods due to chance variation

H_a : differences between sizing methods not due to chance variation

$$\chi^2 = 16.45$$

$$df = 3$$

$$\alpha = 0.05$$

$$\chi^2_{crit} = 7.81$$

$\chi^2 > \chi^2_{crit} \therefore$ reject H_0 , differences between sizing methods are significant

SIZE	CALIPER	MSL	SLATE	
S	17	11	5	
M	5	6	4	
L	0	1	2	
TOTAL	22	18	11	51

$$\chi^2 = 3.65$$

$$df = 2$$

$$\alpha = 0.05$$

$$\chi^2_{crit} = 5.99$$

$\chi^2 < \chi^2_{crit} \therefore$ fail to reject H_0 , differences between sizing methods are due to chance variation.

FIGURE A115

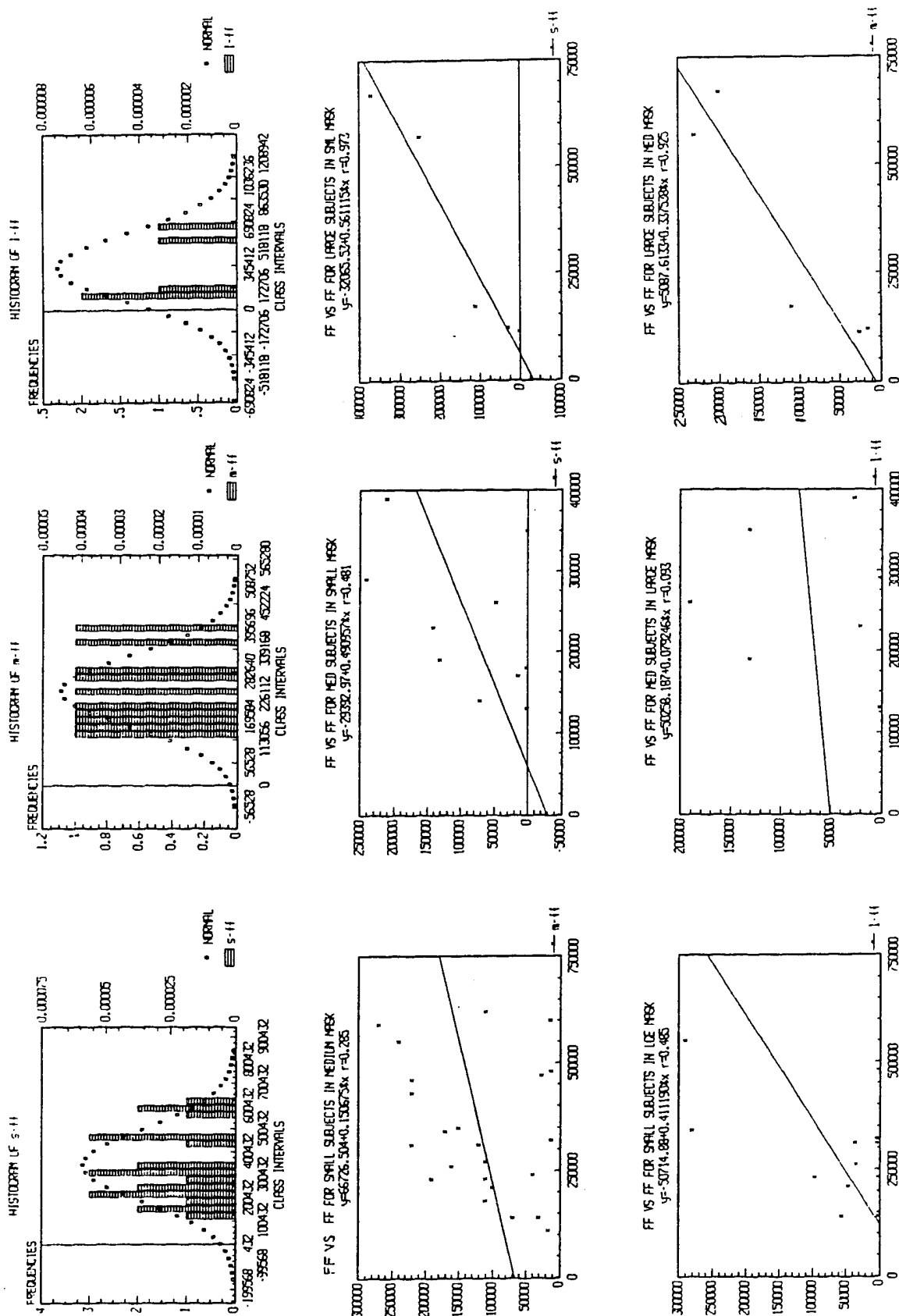


FIGURE A116

SMALL SUBJECTS IN SHALL MASK						
VAR NAME	MEAN	STD ERR	LOWER 95%	UPPER 95%	LOWER 99%	UPPER 99%
s-ff	340869.6	32509.73	273444.4	408294.8	249224.6	432514.5
s-bn	1343913	165283	1001116	1686710	877980.4	1809846
s-bd	699565.3	173946.8	338799.6	1060331	209209.1	1189921
s-ss	1118522	274557.2	547090.2	1685953	342545.1	1890499
s-ud	879565.2	148698.5	571164.4	1187966	460384	1298740
s-rp	182130.4	19398.09	141898.8	222362.1	127447.2	236813.6
s-fe	219043.5	25270.9	166631.6	271455.3	147804.8	290282.2

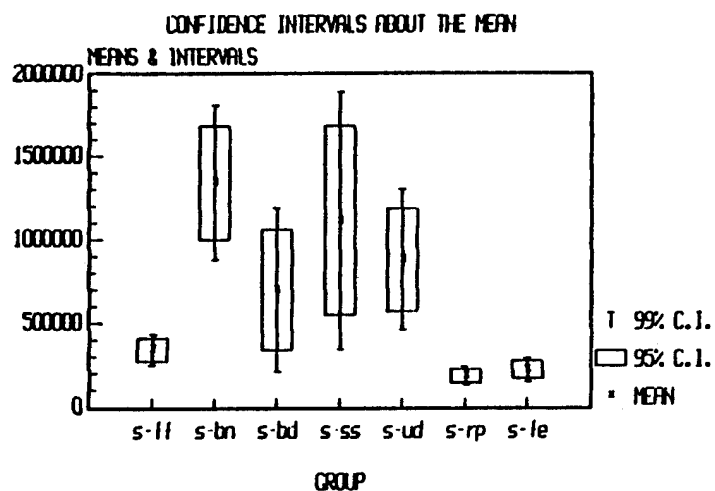


FIGURE A117

VAR NAME	MEAN	STD ERR	MED SUBJECTS IN MED MASK			
			LOWER 95%	UPPER 95%	LOWER 99%	UPPER 99%
m-ff	233000	27930.47	169821.3	296178.7	142226	323774
m-bn	586000	97001.71	366582.1	805417.9	270744.4	901255.6
m-bd	308600	72263.13	145140.8	472059.2	73744.84	543455.1
m-ss	529000	112984.3	273429.6	784570.4	161801.1	896198.9
m-ud	467000	82919.64	279435.8	654564.3	197511.2	736488.9
m-rp	168700	33803.37	92236.79	245163.3	58839.06	278561
m-fe	137500	18667.41	95274.31	179725.7	76830.91	198169.1

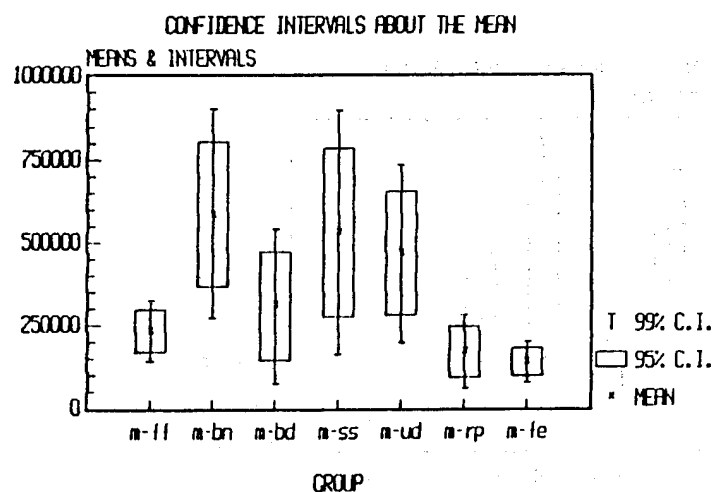


FIGURE A118

LARGE SUBJECTS IN LARGE MASK						
VAR NAME	MEAN	STD ERR	LOWER 95%	UPPER 95%	LOWER 99%	UPPER 99%
1-ff	328000	120681.4	-7011.562	663011.6	-227617.2	883617.2
1-bn	806000	317294.8	-74810.44	1686811	-654825.4	2266826
1-bd	769600	562112.2	-790823.5	2330024	-1818365	3357565
1-sa	797400	417687.4	-362100.3	1956900	-1125633	2720433
1-ud	686000	212922.5	94927.06	1277073	-294295.3	1666295
1-rp	199000	98101.48	-73329.69	471329.7	-252659.2	650659.3
1-fe	250000	66633.32	65025.91	434974.1	-56779.81	556779.8

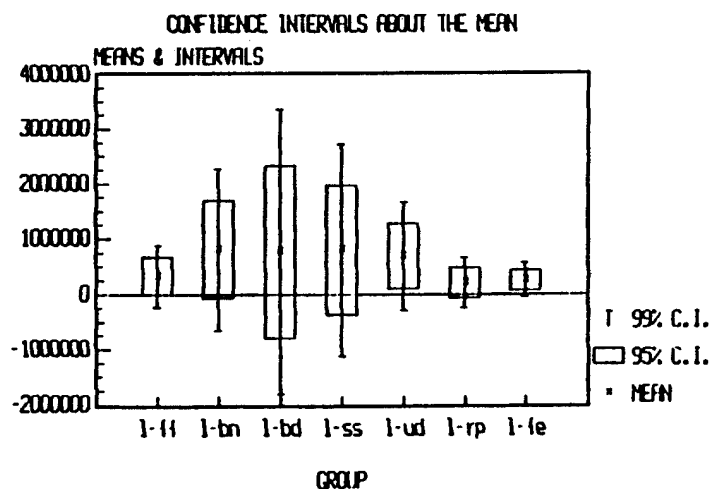


FIGURE A119

LARGE SUBJECTS IN MED. MASK						
VAR NAME	MEAN	STD ERR	LOWER 95%	UPPER 95%	LOWER 99%	UPPER 99%
m-ff	115800	44029.99	-6427.258	238027.3	-86914.09	318514.1
m-bn	392000	43977.27	269919.1	514080.9	189528.7	594471.3
m-bd	135060	52579.4	-10900.42	281020.4	-107015.6	377135.6
m-ss	226600	66862.25	40990.39	412209.6	-81233.81	534433.8
m-ud	243400	64043.41	65615.47	421184.5	-51455.91	538255.9
m-rp	94000	23073.79	29947.15	158052.8	-12231.74	200231.8
m-fe	87520	33645.96	-5881.179	180921.2	-67385.98	242426

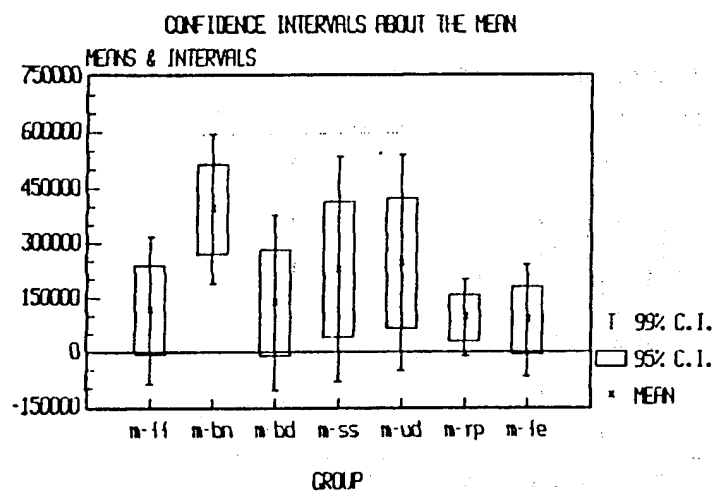


FIGURE A120

SMALL SUBJECTS					
VAR NAME	SIZE	MEAN	SAMPLE STD DEV	SAMPLE VARIANCE	COEF. OF VARIATION
----	----	----	-----	-----	-----
s-ff	23	340869.6	155911.2	2.43083E+10	.45739
m-ff	23	118087	82413.55	6.791993E+09	.69791
l-ff	12	69900.84	104562.3	1.093327E+10	1.49587
s-rp	23	182130.4	93029.95	8.654573E+09	.51079
m-rp	23	82595.65	62836.63	3.948442E+09	.76077
l-rp	12	115442.5	253116.8	6.40681E+10	2.19258

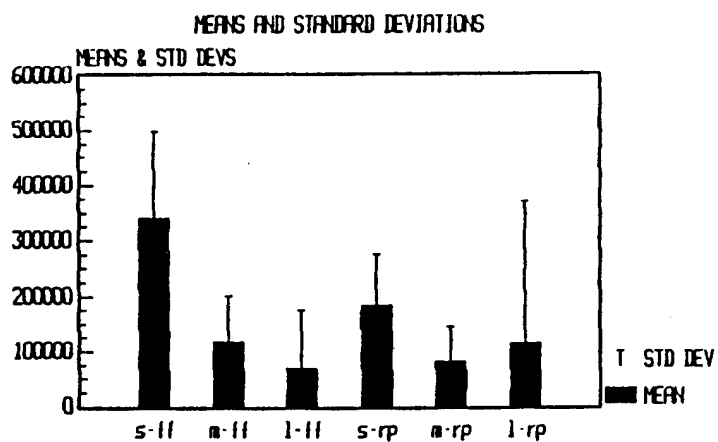


FIGURE A121

MEDIUM SUBJECTS					
E	SIZE	MEAN	SAMPLE STD DEV	SAMPLE VARIANCE	COEF. OF VARIATION
f	9	94455.58	90200.55	8.136139E+09	.95495
f	10	233000	88323.9	7.801111E+09	.37907
f	7	71088.57	77030.61	5.933715E+09	1.08359
p	9	102333.3	55025	3.02775E+09	.5377
p	10	168700	106895.6	1.142668E+10	.63364
p	7	50251.43	41311.94	1.706677E+09	.8221

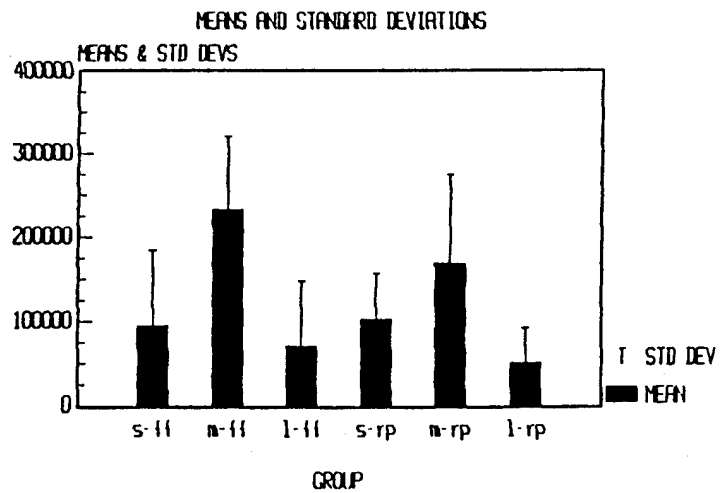


FIGURE A122

LARGE SUBJECTS					
VAR NAME	SIZE	MEAN	SAMPLE STD DEV	SAMPLE VARIANCE	COEF. OF VARIATION
s-ff	4	190000	150554.5	2.266667E+10	.79239
n-ff	5	115800	98454.06	9.6932E+09	.85021
l-ff	5	328000	269851.8	7.282E+10	.82272
s-rp	4	111500	76900.37	5.913667E+09	.68969
n-rp	5	94000.01	51594.57	2.662E+09	.54888
l-rp	5	199000	219361.6	4.81195E+10	1.10232

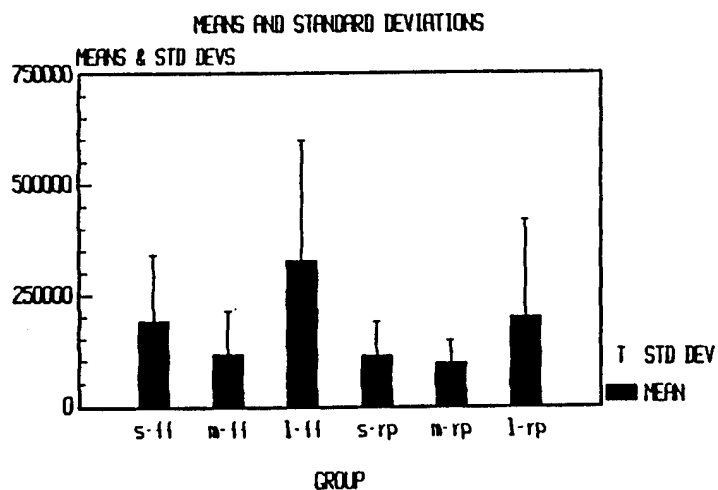


FIGURE A123

SMALL SUBJECTS							
n	VAR NAME	MEAN	STD ERR	LOWER 95%	UPPER 95%	LOWER 99%	UPPER 99%
23	a-ff	340869.6	32509.73	273444.4	408294.8	249224.6	432514.5
23	a-ll	118087	17184.41	82446.48	153727.4	69644.09	160529.8
12	l-ff	69900.83	30184.53	3464.695	136337	-23852.3	163654
23	a-rp	182130.4	19398.09	141898.8	222362.1	127447.2	236813.6
23	a-rp	82595.65	13102.34	55421.39	109789.9	45660.15	119531.2
12	l-rp	115442.5	73068.52	-45381.3	276266.3	-111508.3	342393.3
MEDIUM SUBJECTS							
n	VAR NAME	MEAN	STD ERR	LOWER 95%	UPPER 95%	LOWER 99%	UPPER 99%
9	a-ff	85000.09	28506.45	20518.5	149481.7	-7645.875	177646.1
10	a-ll	233000	27930.47	169821.3	296178.7	142226	323774
7	l-ff	71088.57	29114.83	-155.43	142332.6	-36840.12	179017.3
9	a-rp	92090.1	19340.56	48341.76	135838.4	29233.29	154946.9
10	a-rp	168700	33803.37	92236.79	245163.3	58839.06	278561
7	l-rp	50251.43	15614.45	12042.88	88459.98	-7631.324	108134.2
LARGE SUBJECTS							
n	VAR NAME	MEAN	STD ERR	LOWER 95%	UPPER 95%	LOWER 99%	UPPER 99%
4	a-ff	190000	75277.27	-49532.25	429532.3	-249694.5	829694.5
5	a-ll	115800	44029.99	-6427.258	238027.3	-86914.09	315114.1
5	l-ff	328000	120681.4	-7011.562	663011.6	-227617.2	883617.2
4	a-rp	111500	38450.18	-10646.48	233846.5	-113087.5	336087.5
5	a-rp	94000	23073.79	29947.15	158052.8	-12231.74	200231.8
5	l-rp	199000	98101.48	-73329.69	471329.7	-252659.2	850659.3

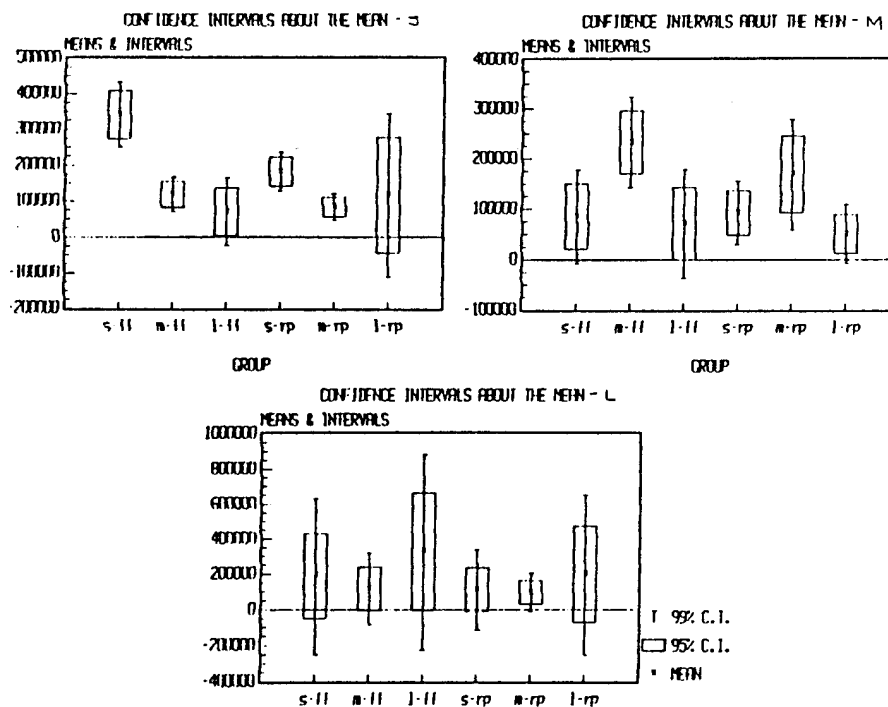


FIGURE A124

RHO, THETA AND PHI FOR MISFIT SUB13

	POINTS	RHO	THETA	PHI
1	R-TRAG	88.34	81.25	65.43
2	R-ZYG	80.07	86.15	78.86
3	R-GON	194.19	-4.86	79.88
4	R-ZGF	76.55	-53.52	98.77
5	R-IFO	60.86	-51.51	128.32
6	GLAB	74.22	.13	114.71
7	SELL	57.5	-1.13	132.24
8	PRON	81.16	-5.36	160.94
9	HENT	103.3	1.89	146.98
10	L-IFO	58.86	47.79	133.49
11	L-ZGF	74.07	56.53	100.15
12	L-ZYG	81.7	-89.82	80.93
13	L-GON	92.88	-41.15	96.73
14	L-TRAG	91.24	-81.97	67.22
15	1	94.68	0	90
16	2	95.6	16.95	85.57
17	3	95.95	32.86	81.02
18	4	89.59	52.14	78.03
19	5	79.97	71.9	79.67
20	6	78.11	-90	90
21	7	77.51	-72.11	101.65
22	8	82.23	-57.6	118.16
23	9	89.93	-42.72	130.87
24	10	99.48	-25.18	139.7
25	11	97.77	.41	140.03
26	12	98.34	25.97	137.59
27	13	91.13	42.03	128.12
28	14	83.08	57.04	116.47
29	15	77.33	71.25	101.12
30	16	76.2	-90	90
31	17	79.38	-71.52	79.2
32	18	87.91	-51.85	78.02
33	19	95.54	-35.2	82.82
34	20	93.99	-16.41	87.87

FIGURE A125

RHO, THETA AND PHI FOR MISFIT SUB40

	POINTS	RHO	THETA	PHI
1	R-TRAG	78.42	75.12	77.21
2	R-ZYG	73.64	88.39	86.88
3	R-GON	83.81	39.23	110.35
4	R-ZGF	72.76	-55.67	100.42
5	R-IFO	58.99	-42.51	129.05
6	GUAB	75.43	.39	109.42
7	SELL	67.94	2.23	118.93
8	PRON	85.85	2.59	147.73
9	HEJIT	99.07	-5.92	156.82
10	L-IFO	57.55	43.17	126.19
11	L-ZGF	70.93	53.61	98.18
12	L-ZYG	69.5	88.26	83.73
13	L-GON	79.75	-36.54	101.58
14	L-TRAG	74.75	-74.94	67.54
15	1	93.1	0	90
16	2	91.61	15.86	89.38
17	3	88.05	31.74	82.44
18	4	80.75	50.34	77.94
19	5	1000	1000	1000
20	6	68.24	-90	90
21	7	68.16	-72.68	102.7
22	8	76.3	-56.62	117.96
23	9	83.04	-41.69	132.07
24	10	86.98	-23.22	140.21
25	11	89.3	-.41	141.48
26	12	86.78	21.55	140.39
27	13	86.29	44.47	133.66
28	14	79.49	59.23	120.48
29	15	71.28	73	104.76
30	16	72.84	-90	90
31	17	1000	1000	1000
32	18	85.7	-48.55	80.73
33	19	91.34	-31.26	84.55
34	20	93.31	-15.51	89.42

APPENDIX B: TABLES

TABLE B-1

RAW DATA FOR COMPARISON OF HAND VS SCAN MEASUREMENT
FOR BIZYGOMATIC BREADTH

	BIZYBR	ZYGZYG	DELBZY
1	152	155.08	3.080002
2	149	155.08	6.080002
3	152	159.17	7.169998
4	128	134.59	6.589996
5	143	150.25	7.25
6	135	142.65	7.649994
7	130	141.07	11.07001
8	142	148.03	6.029999
9	130	139.91	9.910004
10	146	154.79	8.789993
11	137	146.72	9.720001
12	136	146.87	10.87
13	136	150.73	14.73
14	134	142.89	8.889999
15	130	138.93	8.929993
16	133	142.95	9.949997
17	134	141.59	7.589996
18	141	147.91	6.910004
19	135	141.81	6.809998
20	155	143.82	-11.17999
21	145	152.38	7.380005
22	148	156.72	8.720001
23	134	145.9	11.89999
24	122	133.6	11.60001
25	126	134.79	8.789993
26	142	151.4	9.399994
27	139	146.96	7.960007
28	135	145.08	10.08
29	135	143.85	8.850006
30	130	145.02	15.02
31	127	140.59	13.59
32	147	154.97	7.970001
33	139	147.91	8.910004
34	128	141.93	13.92999
35	131	144.27	13.27
36	135	145.94	10.94
37	142	150.75	8.75
38	129	135.78	6.779999
39	130	141.39	11.39
40	134	142.01	8.009995

TABLE B-2

RAW DATA FOR COMPARISON OF HAND VS SCAN MEASUREMENT
FOR BIGONIAL BREADTH

	BIGOBR	GONGON	DELBGN
1	125	124.1	-.9000015
2	118	120.67	2.669998
3	111	136.57	25.57001
4	104	107.92	3.919998
5	107	114.34	7.339996
6	91	97.11	6.110001
7	103	108.42	5.419998
8	116	121.25	5.25
9	101	105.54	4.540001
10	113	117.06	4.059998
11	102	110.52	8.519997
12	99	103.97	4.970001
13	96	100.66	4.660004
14	99	105.74	6.739998
15	100	106.42	6.419998
16	104	108.58	4.580002
17	101	105.94	4.940002
18	105	107.77	2.769997
19	107	116.89	9.889999
20	100	108.57	8.57
21	108	107.58	-.4199982
22	111	122.51	11.51
23	95	103.35	8.349999
24	87	100.5	13.5
25	90	96.75	6.75
26	115	120.25	5.25
27	101	108.19	7.190002
28	100	109.8	9.800003
29	100	110.31	10.31
30	103	107.84	4.839996
31	96	102.42	6.419998
32	110	113.89	3.889999
33	105	106.24	1.239998
34	104	111.93	7.93
35	105	116.43	11.43
36	111	121.49	10.49
37	101	111.87	10.87
38	98	101.79	3.790001
39	108	111	3
40	96	102.61	6.610001

TABLE B-3

RAW DATA FOR COMPARISON OF HAND VS SCAN MEASUREMENT
FOR MENTON SELLION LENGTH

	MENSEL	MNSELL	DELMNS
1	127	120.57	-6.43
2	116	117.24	1.239998
3	110	109.84	-.1600037
4	110	101.68	-8.32
5	115	115.76	.7600021
6	112	114.18	2.18
7	114	111.67	-2.330002
8	115	113.18	-1.82
9	117	116.61	-.3899994
10	122	122.55	.5500031
11	107	112.11	5.110001
12	124	120.96	-3.040001
13	117	115.82	-1.18
14	111	110.73	-.2699966
15	122	120.44	-1.559998
16	111	105.64	-5.360001
17	114	106.62	-7.379997
18	121	117.01	-3.989998
19	123	122.61	-.3899994
20	114	109.5	-4.5
21	123	112.44	-10.56
22	126	115.75	-10.25
23	122	111.32	-10.68
24	112	96.58	-15.42
25	110	103.67	-6.330002
26	118	114.67	-3.330002
27	118	116.3	-1.699997
28	108	101.66	-6.339996
29	106	101.97	-4.029999
30	107	108.78	1.779999
31	106	101.21	-4.790001
32	114	112.26	-1.739998
33	130	127.9	-2.099999
34	110	110.26	.2600021
35	114	110.72	-3.279999
36	109	106.58	-2.419998
37	120	113.08	-6.919998
38	110	100.94	-9.059998
39	106	105.08	-.9199982
40	115	110.42	-4.580002

TABLE B-4

DISTANCE DATA FROM HEAD SCANS, CONT.

	GONGON	BZG+BG	6+16	P1P11	GLBPT1
1	96.75	231.54	134	162	29.9
2	100.5	234.1	138	162	28.28
3	120.25	271.65	147	163	15.03999
4	107.84	252.86	142	167	34.56999
5	110.31	254.16	141	164	39.67001
6	105.94	247.53	140	167	28.68001
7	108.58	251.53	136	161	29.93999
8	107.77	255.68	136	169	16.36
9	108.57	252.39	137	160	22.35001
10	116.89	258.7	136	171	24.16
11	111.87	262.62	144	164	16.06
12	121.49	267.43	143	166	39.07
13	101.79	237.57	135	167	34.59
14	102.61	244.62	139	166	30.28
15	111	252.39	139	166	34.16
16	113.89	268.86	145	165	25.75
17	102.42	243.01	138	167	35.64999
18	106.24	254.15	134	162	10.39999
19	116.43	260.7	137	169	34.17999
20	111.93	253.86	141	174	38.58
21	108.42	249.49	136	165	31.25999
22	105.74	248.63	139	172	24.34999
23	106.42	245.35	136	161	9.349991
24	103.97	250.84	147	186	39.92
25	110.52	257.24	149	181	41.240001
26	108.19	255.15	147	184	35.37
27	122.51	279.23	156	187	27.38
28	117.06	271.85	149	190	41.73
29	107.92	242.51	141	179	42.01
30	120.67	275.75	149	183	41.42
31	105.54	245.45	140	177	37.70999
32	114.34	264.59	148	182	43.12
33	100.66	251.39	149	182	46.56
34	107.58	259.96	153	187	40.3
35	103.35	249.25	146	189	42.97
36	124.1	279.18	152	192	34.34
37	121.25	269.28	145	186	48.97
38	97.11	239.76	141	164	32.06
39	136.57	295.74	154	174	38.40999
40	109.8	254.88	143	163	26.22

TABLE B-5

DISTANCE DATA FROM HEAD SCANS, CONT.

	ZYGON	MNPT1	MNPT11	MNPT6	ZYGZYG
1	73	157.89	23.6	121.71	134.79
2	66.93	154.67	27.37	117.58	133.6
3	73.98	156.62	17.93	119.12	151.4
4	66.07	165.28	18.65	121.95	145.02
5	64.97	162.27	8.05	115.19	143.85
6	62.47	165.44	18.42	122.79	141.59
7	73.77	157.54	20.1	118.89	142.95
8	71.63	160.64	26.08	114.43	147.91
9	64.63	159.58	15.46	114.05	143.82
10	78.57	163.46	15.01	122.06	141.81
11	71.82	156.75	23	117.62	153.75
12	57.93	164.3	14.28	111.55	145.94
13	72.84	162.22	21.01	116.57	135.78
14	66.84	163.6	13	114.87	142.01
15	68.6	159.99	17.39	122.09	141.39
16	76.18	161.45	11.43	118.24	154.97
17	65.82	161.73	22.67	119.8	140.59
18	75.37	156.87	16.67	117.31	147.91
19	62.95	166.18	11.85	109.52	144.27
20	68.39	170.62	15.32	124.16	141.93
21	67.27	162.34	1515	112.83	141.07
22	71.36	154.84	27.33	118.64	142.89
23	70.85	159.31	19.64	121.46	138.93
24	76.69	182.17	26.94	141.7	146.87
25	69.13	174.5	25.25	136	146.72
26	70.94	175.72	28.17	132.44	146.96
27	72.52	169.38	36.83	131.67	156.72
28	75.15	184.83	18.56	139.41	154.79
29	64.71	167.67	26.64	134.84	134.59
30	66.48	174.97	29.4	126.71	155.08
31	70.6	172.51	38.98	132.61	139.91
32	72.46	176.89	19.5	134.28	150.25
33	80.05	179.63	17.54	130.73	150.73
34	69.53	179.31	31.54	132.56	152.38
35	68.55	187.72	27.93	135.95	145.9
36	69.69	183.44	26.02	128.42	155.08
37	72.73	178.42	26.65	133.48	148.03
38	72.61	160.33	27.3	118	142.65
39	75.85	174.04	13.46	130.63	159.17
40	56.21	160.64	20.08	120.36	145.08

TABLE B-6

DISTANCE DATA FROM HEAD SCANS
1-23=S, 24-32=M, 33-37=L, 38-40=MISFIT

	SUBJEC	MNSELL	MNGLAB	SELGON	XZYGON
1	89	103.67	127.99	123.75	134.61
2	88	96.58	126.39	114.99	132.06
3	90	114.67	141.58	132.73	155.04
4	94	108.78	130.71	120.01	141.52
5	93	101.97	122.6	124.55	142.31
6	70	106.62	136.76	121.29	139.15
7	68	105.64	127.6	134.55	142.88
8	72	117.01	144.28	137.42	146.26
9	74	109.5	137.23	128.32	139.45
10	73	122.61	139.3	136.2	148.27
11	108	113.08	140.69	130.53	150.86
12	107	106.58	125.23	123.62	145.3
13	109	100.94	127.63	123.69	139.14
14	113	110.42	133.32	130.67	136.81
15	112	105.08	125.83	130.41	143.9
16	101	112.26	135.7	134.82	153.58
17	96	101.21	126.08	126.87	137.23
18	103	127.9	146.47	139.64	148.16
19	106	110.72	132	127.96	145.22
20	105	110.26	132.04	125.5	144.55
21	41	111.67	131.08	129.67	137.89
22	63	110.73	130.49	127.21	140.36
23	64	120.44	149.96	124.82	141.21
24	60	120.96	142.25	137.71	144.18
25	56	112.11	133.26	131.45	143.58
26	91	116.3	140.35	138.44	145.19
27	81	115.75	142	130.41	156.7
28	53	122.55	143.1	143.35	155.03
29	22	101.68	125.66	122.13	136.99
30	10	117.24	133.55	135.49	153.21
31	53	116.61	134.8	125.95	139.68
32	23	115.76	133.77	133.66	148.87
33	62	115.82	133.07	137.97	148.05
34	76	112.44	139.01	132.28	147.2
35	87	111.32	144.75	115.37	141.71
36	5	120.57	149.1	133.33	156.43
37	50	113.18	129.45	130.63	155.94
38	40	114.18	128.27	131.03	139.33
39	13	109.84	135.63	130.78	201.98
40	92	101.66	134.42	118.68	136.03

TABLE B-7

DISTANCE DATA FROM DATASHEETS, CONT.

	MENSEL	HEIGHT	WEIGHT
1	13	80	210
2	11	71	145
3	11.4	71	195
4	10.7	63	125
5	10.6	63	125
6	11.4	71	155
7	10.6	66	130
8	11.5	65	125
9	11	66	132
10	10.9	68	135
11	12	62	140
12	10.6	65	140
13	11.1	68	150
14	11.4	64	120
15	12.2	64	132
16	11.4	65	119
17	11.1	65	145
18	12.1	71	175
19	11	62	105
20	11.8	68	176
21	11.2	62	120
22	12.3	73	160
23	11.4	64	130
24	12.4	74	165
25	10.7	66	140
26	11.8	73	137
27	12.6	67	145
28	12.2	73	175
29	11	65	135
30	11.6	69	155
31	11.7	69	130
32	11.5	69	150
33	11.7	73	155
34	12.3	69	140
35	12.2	68	155
36	12.7	75	192
37	11.5	68	165
38	11.2	67	130
39	11	66	135
40	13	70	140
41	10.8	62	120
42	11	73	158

TABLE B-8

DISTANCE DATA FROM DATASHEETS
1-23=S, 24-32=M, 33-37=L, 38-42=MISFIT

	SUBJECT	MENARC	SBMARC	BIZYBR	BIGOBR
1	103	34.3	31	13.9	10.5
2	105	29.2	28.4	12.8	10.4
3	101	32.5	29.8	14.7	11
4	94	30.2	26	13	10.3
5	96	29.7	26.8	12.7	9.6
6	106	31.2	29.2	13.1	10.5
7	112	29.8	28.5	13	10.8
8	113	29.7	26.6	13.4	9.6
9	109	28.3	27.7	12.9	9.8
10	107	30.4	27.3	13.5	11.1
11	108	31.2	29.2	14.2	10.1
12	93	29.5	27.5	13.5	10
13	68	30.9	29.2	13.3	10.4
14	70	29.3	27.6	13.4	10.1
15	64	30.9	28.9	13	10
16	41	27.5	28	13	10.3
17	63	29	29.1	13.4	9.9
18	72	31.9	29.6	14.1	10.5
19	89	29.2	26.3	12.6	9
20	90	31.5	29.5	14.2	11.5
21	88	29.5	25.9	12.2	8.7
22	73	32.4	30	13.5	10.7
23	74	29.6	26.2	15.5	10
24	60	31	28.3	13.6	9.9
25	56	28.5	27.3	13.7	10.2
26	91	31	28.3	13.9	10.1
27	81	31.4	30.1	14.8	11.1
28	53	34.3	31.9	14.6	11.3
29	22	29.8	27.3	12.8	10.4
30	10	32.2	30	14.9	11.8
31	51	30.6	28.9	13	10.1
32	23	32.1	29.2	14.3	10.7
33	62	33.1	29.9	13.6	9.6
34	76	31.7	29	14.5	10.8
35	87	30.4	27.5	13.4	9.5
36	5	33.6	32	15.2	12.5
37	50	33.3	30.8	14.2	11.6
38	40	29.1	25.9	13.5	9.1
39	100	29.2	26.7	12.7	9.7
40	14	34.1	28.7	14.3	11
41	92	29.8	26.6	13.5	10
42	13	33.6	31	15.2	11.1

APPENDIX C: DISTANCE DATA

DISTANCE DATA FROM HEAD SCANS
1-23=S, 24-32=M, 33-37=L, 38-40=MISFIT

	SUBJEC	MNSRL	MNGLAB	SELGON	XZYGON
1	89	103.67	127.99	123.75	134.61
2	88	96.58	126.39	114.99	132.06
3	90	114.67	141.58	132.73	155.04
4	94	108.78	130.71	120.01	141.52
5	93	101.97	122.6	124.55	142.31
6	70	106.82	136.76	121.29	139.15
7	68	105.64	127.6	134.55	142.88
8	72	117.01	144.28	137.42	146.26
9	74	109.5	137.23	128.32	139.45
10	73	122.61	139.3	136.2	148.27
11	108	113.08	140.69	130.53	150.86
12	107	106.58	125.23	123.62	145.3
13	109	100.94	127.63	123.69	139.14
14	113	110.42	133.32	130.67	136.81
15	112	105.08	125.83	130.41	143.9
16	101	112.26	135.7	134.82	153.58
17	96	101.21	126.08	126.87	137.23
18	103	127.9	146.47	139.64	148.16
19	106	110.72	132	127.96	145.22
20	105	110.26	132.04	125.5	144.55
21	41	111.67	131.08	129.67	137.89
22	63	110.73	130.49	127.21	140.36
23	64	120.44	149.96	124.82	141.21
24	60	120.96	142.25	137.71	144.18
25	56	112.11	133.26	131.45	143.58
26	91	116.3	140.35	138.44	145.19
27	81	115.75	142	130.41	156.7
28	53	122.55	143.1	143.35	155.03
29	22	101.68	125.66	122.13	136.99
30	10	117.24	133.55	135.49	153.21
31	51	116.61	134.8	125.95	139.68
32	23	115.76	133.77	133.66	148.87
33	62	115.82	133.07	137.97	148.05
34	76	112.44	139.01	132.28	147.2
35	87	111.32	144.75	115.37	141.71
36	5	120.57	149.1	133.33	156.43
37	50	113.18	129.45	130.63	155.94
38	40	114.18	128.27	131.03	139.33
39	13	109.84	135.63	130.78	201.98
40	92	101.66	134.42	118.68	136.03

DISTANCE DATA FROM HEAD SCANS, CONT.

	GONGON	BZG+BG	6+16	PIP11	GLBPT1
1	96.75	231.54	134	162	29.9
2	100.5	234.1	138	162	28.28
3	120.25	271.65	147	163	15.03999
4	107.84	252.86	142	167	34.56999
5	110.31	254.18	141	164	39.67001
6	105.94	247.53	140	167	28.68001
7	108.58	251.53	136	161	29.93999
8	107.77	255.68	136	169	16.36
9	108.57	252.39	137	160	22.35001
10	116.89	258.7	136	171	24.16
11	111.87	262.62	144	164	16.06
12	121.49	267.43	143	166	39.07
13	101.79	237.57	135	167	34.59
14	102.61	244.62	139	166	30.28
15	111	252.39	139	166	34.16
16	113.89	268.86	145	165	25.75
17	102.42	243.01	138	167	35.64999
18	106.24	254.15	134	162	10.39999
19	116.43	260.7	137	169	34.17999
20	111.93	253.86	141	174	38.58
21	108.42	249.49	136	165	31.25999
22	105.74	248.63	139	172	24.34999
23	106.42	245.35	136	161	9.349991
24	103.97	250.84	147	186	39.92
25	110.52	257.24	149	181	41.24001
26	108.19	255.15	147	184	35.37
27	122.51	279.23	156	187	27.38
28	117.06	271.85	149	190	41.73
29	107.92	242.51	141	179	42.01
30	120.67	275.75	149	183	41.42
31	105.54	245.45	140	177	37.70999
32	114.34	264.69	148	182	43.12
33	100.66	251.39	149	182	46.56
34	107.58	259.96	153	187	40.3
35	103.35	249.25	146	189	42.97
36	124.1	279.18	152	192	34.34
37	121.25	269.28	145	186	48.97
38	97.11	239.76	141	164	32.06
39	136.57	295.74	154	174	38.40999
40	109.8	254.88	143	163	26.22

DISTANCE DATA FROM HEAD SCANS, CONT.

	ZYGON	MNPT1	MNPT11	MNPT6	ZYGZYG
1	73	157.89	23.6	121.71	134.79
2	66.93	154.67	27.37	117.58	133.6
3	73.98	156.62	17.93	119.12	151.4
4	66.07	165.28	18.65	121.95	145.02
5	64.97	162.27	8.05	115.19	143.85
6	62.47	165.44	18.42	122.79	141.59
7	73.77	157.54	20.1	118.89	142.95
8	71.63	160.64	26.08	114.46	147.91
9	64.63	159.58	15.46	114.05	143.82
10	78.57	163.46	15.01	122.06	141.81
11	71.82	156.75	23	117.62	150.75
12	57.93	164.3	14.28	111.55	145.94
13	72.84	162.22	21.01	116.57	135.78
14	66.84	163.6	13	114.87	142.01
15	68.6	159.99	17.39	122.09	141.39
16	76.18	161.45	11.43	118.24	154.97
17	65.82	161.73	22.67	119.8	140.59
18	75.37	156.87	16.67	117.31	147.91
19	62.95	166.18	11.85	109.52	144.27
20	68.39	170.62	15.32	124.13	141.93
21	67.27	162.34	15	112.83	141.07
22	71.36	154.84	27.33	118.64	142.89
23	70.85	159.31	19.64	121.46	138.93
24	76.69	182.17	26.94	141.7	146.87
25	69.13	174.5	25.25	136	146.72
26	70.94	175.72	28.17	132.44	146.96
27	72.52	169.38	36.83	131.67	156.72
28	75.15	184.83	18.56	139.41	154.79
29	64.71	167.67	26.64	134.84	134.59
30	66.48	174.97	29.4	126.71	155.08
31	70.06	172.51	38.98	132.61	139.91
32	72.46	176.89	19.5	134.28	150.25
33	60.05	179.63	17.54	130.73	150.73
34	69.53	179.31	31.54	132.56	152.38
35	68.55	187.72	27.93	135.95	145.9
36	69.69	183.44	26.02	128.42	155.08
37	72.73	178.42	26.65	133.48	148.03
38	72.61	160.33	27.3	118	142.65
39	75.85	174.04	13.46	130.63	159.17
40	56.21	160.64	20.08	120.36	145.08

DISTANCE DATA FROM DATASHEETS
1-23-S, 24-32-M, 33-37-L, 38-42-MISFIT

	SUBJEC	MENARC	SBMARC	BIZYBR	BIGOBR
1	103	34.3	31	13.9	10.5
2	105	29.2	28.4	12.8	10.4
3	101	32.5	29.8	14.7	11
4	94	30.2	26	13	10.3
5	96	29.7	26.8	12.7	9.6
6	106	31.2	29.2	13.1	10.5
7	112	29.8	28.5	13	10.8
8	113	29.7	26.6	13.4	9.6
9	109	28.3	27.7	12.9	9.8
10	107	30.4	27.3	13.5	11.1
11	108	31.2	29.2	14.2	10.1
12	93	29.5	27.5	13.5	10
13	68	30.9	29.2	13.3	10.4
14	70	29.3	27.6	13.4	10.1
15	64	30.9	28.9	13	10
16	41	27.5	28	13	10.3
17	63	29	29.1	13.4	9.9
18	72	31.9	29.6	14.1	10.5
19	89	29.2	26.3	12.6	9
20	90	31.5	29.5	14.2	11.5
21	86	29.5	25.9	12.2	8.7
22	73	32.4	30	13.5	10.7
23	74	29.6	26.2	15.5	10
24	60	31	28.3	13.6	9.9
25	56	28.5	27.3	13.7	10.2
26	91	31	28.3	13.9	10.1
27	81	31.4	30.1	14.8	11.1
28	53	34.3	31.9	14.6	11.3
29	22	29.8	27.3	12.8	10.4
30	10	32.2	30	14.9	11.8
31	51	30.6	28.9	13	10.1
32	23	32.1	29.2	14.3	10.7
33	62	33.1	29.9	13.6	9.6
34	76	31.7	29	14.5	10.8
35	87	30.4	27.5	13.4	9.5
36	5	33.6	32	15.2	12.5
37	50	33.3	30.8	14.2	11.6
38	40	29.1	25.9	13.5	9.1
39	100	29.2	26.7	12.7	9.7
40	14	34.1	28.7	14.3	11
41	92	29.8	26.6	13.5	10
42	13	33.6	31	15.2	11.1

DISTANCE DATA FROM DATASHEETS, CONT.

	MENSEL	HEIGHT	WEIGHT
1	13	80	210
2	11	71	145
3	11.4	71	195
4	10.7	63	125
5	10.6	63	125
6	11.4	71	155
7	10.6	66	130
8	11.5	65	125
9	11	66	132
10	10.9	68	135
11	12	62	140
12	10.6	65	140
13	11.1	68	150
14	11.4	64	120
15	12.2	64	132
16	11.4	65	119
17	11.1	65	145
18	12.1	71	175
19	11	62	105
20	11.8	68	176
21	11.2	62	120
22	12.3	73	160
23	11.4	64	130
24	12.4	74	165
25	10.7	66	140
26	11.8	73	137
27	12.6	67	145
28	12.2	73	175
29	11	65	135
30	11.6	69	155
31	11.7	69	130
32	11.5	69	150
33	11.7	73	155
34	12.3	69	140
35	12.2	68	155
36	12.7	75	192
37	11.5	68	165
38	11.2	67	130
39	11	66	135
40	13	70	140
41	10.8	62	120
42	11	73	158